

2

NAVAL POSTGRADUATE SCHOOL

Monterey, California

AD-A220 109



SDTIC
ELECTE
APR 5 1990
B D

THESIS

A PC-BASED IMAGING SYSTEM
FOR THE NAVAL POSTGRADUATE SCHOOL
INFRARED SEARCH AND TARGET DESIGNATION
(NPS-IRSTD) SYSTEM

by

Raymond Charles Engel

September, 1989

Thesis Advisor:
Co-Advisor

Alfred W. Cooper
David D. Cleary

Approved for public release; distribution is unlimited.

00 04 04 089

Unclassified

SECURITY CLASSIFICATION OF THIS PAGE

REPORT DOCUMENTATION PAGE				
1a REPORT SECURITY CLASSIFICATION Unclassified			1b RESTRICTIVE MARKINGS	
2a SECURITY CLASSIFICATION AUTHORITY			3 DISTRIBUTION/AVAILABILITY OF REPORT Approved for public release; distribution is unlimited.	
2b DECLASSIFICATION/DOWNGRADING SCHEDULE				
4 PERFORMING ORGANIZATION REPORT NUMBER(S)			5 MONITORING ORGANIZATION REPORT NUMBER(S)	
6a NAME OF PERFORMING ORGANIZATION Naval Postgraduate School		6b OFFICE SYMBOL (If applicable) 55	7a NAME OF MONITORING ORGANIZATION Naval Postgraduate School	
6c ADDRESS (City, State, and ZIP Code) Monterey, CA 93943-5000			7b ADDRESS (City, State, and ZIP Code) Monterey, CA 93943-5000	
8a NAME OF FUNDING/SPONSORING ORGANIZATION		8b OFFICE SYMBOL (If applicable)	9 PROCUREMENT INSTRUMENT IDENTIFICATION NUMBER	
8c ADDRESS (City, State, and ZIP Code)			10 SOURCE OF FUNDING NUMBERS	
			Program Element No.	Project No.
			Task No.	Work Unit Allocation Number
11. TITLE (Include Security Classification) A PC-BASED IMAGING SYSTEM FOR THE NAVAL POSTGRADUATE SCHOOL INFRARED SEARCH AND TARGET DESIGNATION (NPS-IRSTD) SYSTEM				
12 PERSONAL AUTHOR(S) Raymond Charles Engel				
13a TYPE OF REPORT Master's Thesis		13b TIME COVERED From To	14 DATE OF REPORT (year, month, day) September 1989	15 PAGE COUNT 149
16 SUPPLEMENTARY NOTATION The views expressed in this thesis are those of the author and do not reflect the official policy or position of the Department of Defense or the U.S. Government.				
17 COSATI CODES			18 SUBJECT TERMS (continue on reverse if necessary and identify by block number)	
FIELD	GROUP	SUBGROUP	IRSTD, Framegrabber, Thermal Imaging	
19 ABSTRACT (continue on reverse if necessary and identify by block number)				
<p>A system to display images from data generated by the Naval Postgraduate School Infrared Search and Target Designation (NPS-IRSTD) System (modified AN/SAR-8 ADM) was developed using an Intel 80386 CPU based desktop computer as the base platform. This computer was enhanced with a Metrabyte PDMA-16 Input/Output board to facilitate data transfers and a Data Translation DT2861 framegrabber board for image processing. Images are displayed on a 512 by 480 pixel resolution color monitor.</p> <p>Digitized NPS-IRSTD data is stored on recording tape and accessed for imaging during playback at reduced speeds. Data is received into the 386 computer through the PDMA-16 using Direct Memory Access (DMA) transfers into the Random Access Memory (RAM). Data is sorted in RAM into the proper format for display, and then moved to a frame buffer in the DT2861. FORTRAN programs using Data Translation DT-IRIS subroutines were written to manage image and display processing.</p> <p>Images produced using the system showed clearly identifiable features from the scene observed by the IIRSTD. They also provided valuable insight into the IIRSTD operation. For example, the detector AC-coupling undershoot was clearly evident. Additionally, images showed the number of non-operational detectors to be larger than previously noted.</p> <p>Recommendations were made for system improvements to enhance speed and reliability, and for additional study of the imaging properties of the NPS-IRSTD.</p>				
20 DISTRIBUTION/AVAILABILITY OF ABSTRACT <input checked="" type="checkbox"/> UNCLASSIFIED/UNLIMITED <input type="checkbox"/> SAME AS REPORT <input type="checkbox"/> DTIC USERS			21 ABSTRACT SECURITY CLASSIFICATION Unclassified	
22a NAME OF RESPONSIBLE INDIVIDUAL Alfred W. Cooper			22b TELEPHONE (Include Area code) (408) 646-2452	22c OFFICE SYMBOL 61Cr

DD FORM 1473, 84 MAR

83 APR edition may be used until exhausted
All other editions are obsoleteSECURITY CLASSIFICATION OF THIS PAGE
Unclassified

Approved for public release; distribution is unlimited.

A PC-Based Imaging System
for the Naval Postgraduate School
Infrared Search and Target Designation (NPS-IRSTD) System

by

Raymond Charles Engel
Lieutenant, United States Coast Guard
B.S., U. S. Coast Guard Academy, 1982

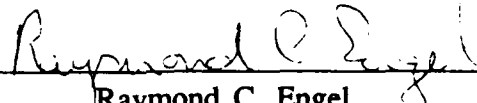
Submitted in partial fulfillment
of the requirements for the degree of

MASTER OF SCIENCE IN PHYSICS

from the

NAVAL POSTGRADUATE SCHOOL
September 1989

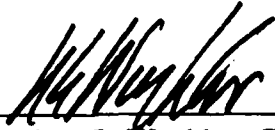
Author:


Raymond C. Engel

Approved by:


Alfred W. Cooper, Thesis Advisor


David D. Cleary, Co-Advisor


Karlheinz E. Woehler, Chairman
Department of Physics

ABSTRACT

A system to display images from data generated by the Naval Postgraduate School Infrared Search and Target Designation (NPS-IRSTD) system (modified AN/SAR-8 ADM) was developed using an Intel 80386 CPU based desktop computer as the base platform. This computer was enhanced with a Metrabyte PDMA-16 Input/Output board to facilitate data transfers and a Data Translation DT2861 framegrabber board for image processing. Images are displayed on a 512 by 480 pixel resolution color monitor.

Digitized NPS-IRSTD data is stored on recording tape, and accessed for imaging during playback at reduced speeds. Data is received into the 386 computer through the PDMA-16 using Direct Memory Access (DMA) transfers into Random Access Memory (RAM). Data is sorted in RAM into the proper format for display, and then moved to a frame buffer in the DT2861. FORTRAN programs using Data Translation DT-IRIS subroutines were written to manage image display and processing.

Images produced using the system showed clearly identifiable features from the scene observed by the IRSTD. They also provided valuable insight into the IRSTD operation. For example, the detector AC-coupling undershoot was clearly evident. Additionally, images showed the number of non-operational detectors to be larger than previously noted.

Recommendations are made for system improvements to enhance speed and reliability, and for additional study of the imaging properties of the NPS-IRSTD.



Accession For	
NTIS GRA&I	<input checked="checked" type="checkbox"/>
DTIC TAB	<input type="checkbox"/>
Unannounced	<input type="checkbox"/>
Justification	
By _____	
Distribution/	
Availability Codes	
Dist	Avail and/or Special
A-1	

TABLE OF CONTENTS

I. INTRODUCTION	1
II. THE NPS-IRSTD	5
A. PROGRAM HISTORY AND BACKGROUND	5
B. CURRENT SYSTEM HARDWARE CONFIGURATION	8
III. EXPERIMENTAL/ENGINEERING PROCEDURES	23
A. GENERAL	23
B. IMAGING SYSTEM HARDWARE AND SOFTWARE ENGINEERING	23
C. IMAGE DISPLAY AND PROCESSING	40
IV. RESULTS	48
A. GENERAL	48
B. DATA TRANSFERS	48
C. IMAGE PROCESSING PROGRAM PERFORMANCE	49
V. CONCLUSIONS AND RECOMMENDATIONS	84
A. CONCLUSIONS	84
B. RECOMMENDATIONS	86
APPENDIX A	88
APPENDIX B	95
APPENDIX C	105

APPENDIX D	132
LIST OF REFERENCES	135
INITIAL DISTRIBUTION LIST	137

LIST OF FIGURES

Figure 1.	Block Diagram of the NPS-IRSTD Imaging System	3
Figure 2.	Unmultiplexed Data from the NPS-IRSTD Showing the Dropout Characteristic	9
Figure 3.	Photograph of NPS-IRSTD Scanner, and the Buffer and Power Unit	11
Figure 4.	NPS-IRSTD Telescope and Detector Assembly	12
Figure 5.	Simplified Diagram of the NPS-IRSTD's Modified Detector Cooling Apparatus	15
Figure 6.	Multiplexing Arrangement for the Lead Detector Array	16
Figure 7.	Photograph of Spanagel Hall, Room 703, Electronics Racks	19
Figure 8.	Analog-To-Digital Converter Multiplexing	22
Figure 9.	Random Access Memory Organization for the 386 Computer	26
Figure 10.	PDMA-16 Input/Output Board Pin Assignments	28
Figure 11.	Flow Diagram of Possible Data Transfer Methods	34
Figure 12.	DMA Transfer and Sorting Sequence	38
Figure 13.	Output Lookup Table Assignments	45
Figure 14.	PDMA-16 Handshaking Protocol	50
Figure 15.	Image Resulting from a Bad DMA Transfer	51
Figure 16.	The Effect of Hamming on a Cosine Wave Signal	54
Figure 17.	NPS-IRSTD Image (3° Wide) of an Antenna on Spanagel Hall	59
Figure 18.	Photograph the Roof of Spanagel Hall Showing the Antenna in Figure 17 and the Crane in Figure 19	60
Figure 19.	NPS-IRSTD Image (3° Wide) Showing a Crane on Spanagel Hall	61
Figure 20.	NPS-IRSTD Image (6° Wide) Combining Figures 17 & 19	62
Figure 21.	NPS-IRSTD Image (6° Wide) Showing the Radar Lab Antenna on Spanagel Hall	63
Figure 22.	Photograph Showing the Radar Lab Antenna	64
Figure 23.	NPS-IRSTD Image (3° Wide) Part of the Roof of Hermann Hall is Visible in the Lower Right Corner	65
Figure 24.	NPS-IRSTD Image (3° Wide) Showing the Roof of Hermann Hall	66
Figure 25.	NPS-IRSTD Image (6° Wide) Combining Figures 23 & 24	67
Figure 26.	NPS-IRSTD Image (6° Wide) of the Bay Visible to the Right of Hermann Hall	68
Figure 27.	Photograph of the Roof of Hermann Hall	69
Figure 28.	Diagrams Representing a Point Source Imaged on the Focal Plane	70
Figure 29.	NPS-IRSTD Image (12° Wide) Showing the Roof of Hermann Hall	71
Figure 30.	NPS-IRSTD Image (3° Wide) with the Monotonically Increasing Lookup Table Active	72
Figure 31.	NPS-IRSTD Image (3° Wide) with the Monotonically Decreasing Lookup Table Active	73

Figure 32.	NPS-IRSTD Image (3° Wide) Corrected for Detector Response Differences	74
Figure 33.	NPS-IRSTD Image (3° Wide) with Rows for Bad Detectors Filled	75
Figure 34.	NPS-IRSTD Image (3° Wide) Corrected for X-direction Detector Shape MTF	76
Figure 35.	NPS-IRSTD Image (3° Wide) Corrected for X-direction Optical MTF	77
Figure 36.	NPS-IRSTD Image (3° Wide) with One-Detector-To-Five-Row Expansion Smoothing Employed	78
Figure 37.	NPS-IRSTD Image (3° Wide) with all Available Corrections Applied	79
Figure 38.	NPS-IRSTD Image Comparing a Corrected to an Uncorrected Image.	80
Figure 39.	NPS-IRSTD Image (12° Wide) of the Monterey Hillside with all Corrections Applied	81
Figure 40.	Photograph of the Monterey Hillside	82
Figure 41.	NPS-IRSTD Image (12° Wide) of the Monterey Hillside with no Corrections Applied	83
Figure 42.	Figures of Merit for Single Element Detectors	89
Figure 43.	InSb Detector Performance Data at 77 K	90
Figure 44.	Spectral Detectivities for Above Average Crystal Detectors at Frequency f_m	91
Figure 45.	Simple AC-coupling Circuit	92
Figure 46.	AC-coupling Effects on Detector Output Signals	94
Figure 47.	Imaging of a Point Source at Infinity with a Circular Lens	97
Figure 48.	Point Spread Function for a Circular Aperture	99
Figure 49.	Two Dimensional Fourier Pairs	100
Figure 50.	Modulation of Point Source Distributions at Infinity Imaged onto the Image Plane	102
Figure 51.	MTFs for the ADM and the NPS-IRSTD	104

LIST OF ABBREVIATIONS/ACRONYMS

ADM	Advanced Development Model
BLKMAT	PC Tools FORTRAN subroutine for moving word (16-bit) sized data around RAM using absolute addresses
BLKMOV	PC Tools FORTRAN subroutine for moving byte (8-bit) sized data around RAM using absolute addresses
DMA	Direct Memory Access
BNU	Background Normalizer Unit
DOS	Disk Operating System
DT2861	Data Translation Framegrabber Board
DT-IRIS	Data Translation Image Processing Subroutine Library
EOR	End-of-rotation
IRSTD	InfraRed Search and Target Designation
I/O	Input and Output
ISGETP	DT-IRIS subroutine to retrieve byte value data from framegrabber RAM
ISPUTP	DT-IRIS subroutine to write byte value data to framegrabber RAM
KB	Kilobyte, 1,024 bytes of computer storage
LUT	Look-up Table
MB	Megabyte, 1,048,576 bytes of computer storage
NPS	Naval Postgraduate School
RAM	Random Access Memory
386	Everex Step 386/20 Computer

ACKNOWLEDGEMENTS

Completion of this project would not have been possible a great deal of support and assistance. I wish to offer my thanks to everyone involved.

First, I wish to thank God for allowing me the chance to attend the Naval Postgraduate School where I have been exposed to many new and fascinating insights into His creation. I also wish to thank Him for providing the many people at NPS and in the local community who offered the often needed help and encouragement. In addition, I am convinced that this project has been completed only through His kindness and benevolence many times throughout its duration.

Second, I need to thank my wife Denise, and Daniel and Audrey, our two kids, for their patience as they waited for me to remember that they are more important than any job or project.

Next I wish to express my gratitude to my advisors, Prof. Alfred. W. Cooper and Prof. David D. Cleary, for their guidance and encouragement. Completion of this project would not have been possible without their pointing out the path on many occasions.

Finally, I wish to thank Prof. Edmund A. Milne, Mr. W. J. "Jerry" Lentz, Ms. Ludy Oppel-Block and Mr. Eric Moore for each of their efforts on my behalf.

This thesis is prepared in conjunction with research funded in part by the Naval Sea Systems Command, PMS-421, and funded by the Naval Postgraduate School.

I. INTRODUCTION

The AN/SAR-8 is a passive, scanning, infrared detection system originally designed to detect the presence of targets of military interest in a maritime environment, designate and track detected targets, and display pertinent track information on a video monitor. Data was collected and processed to efficiently detect the presence of infrared emission sources while strongly discriminating against background clutter. Such design parameters led to a system where essentially all data underwent some form of processing prior to display. The video displays provided information on targets meeting certain criteria while suppressing all other scene information.

The original prototype AN/SAR-8 IRSTD (InfraRed Search and Target Designation), the Advanced Development Model (ADM), was obtained by the Naval Postgraduate School (NPS) in January, 1985 after testing and evaluation periods both afloat and ashore. At NPS the ADM was placed under the control of the Naval Academic Center for Infrared Technology (NACIT) to be used for research and student instruction. When it arrived at NPS, the ADM was largely in a state of disrepair. As part of returning the system to an operational condition some modifications have been performed to enhance its research potential. The most significant of these modifications was the bypassing of the background suppression hardware on one of the two focal plane infrared detector arrays to allow access to unprocessed data. As the result of these modifications the system is no longer truly an AN/SAR-8, and thus except for historical discussions will be referred to throughout this thesis as the NPS-IRSTD.

The goal of this thesis project was to develop a method whereby the infrared scene data generated by the NPS-IRSTD can be displayed on a video monitor, and then by applying various image processing techniques, to enhance the images produced. The imaging system is now available for a number of useful applications including:

- rapid visual data searches for locating data on interesting scene compositions desirable for testing background suppression algorithms.
- visual analysis of image after clutter rejection algorithms have been applied.
- continued research in imaging properties of the system and infrared image processing techniques.
- evaluation of image data collection and processing techniques applied for possible wider IRST program applications, specifically examining the viability of framegrabber technology for shipboard IRSTD system video.
- instructional demonstrations on infrared sensing and imaging characteristics.

In the course of working through this project, a number of decisions were made that restricted the focus in an attempt to scale it to a reasonable size given the time available, and thereby hopefully provide a sufficient percentage of that time to be used to study the physics of the imaging process. The most notable of these choices came regarding the rate at which the system should be able to produce an image. Because of the high data rate output by the NPS-IRSTD and the potential for engineering complications arising from hardware idiosyncracies (known and unknown), it was decided not to attempt implementation of an imaging system relying on data generated at normal system speeds. Instead the image would be produced using data recorded on a tape recorder at normal speeds and then played back at a much slower rate.

The hardware used to receive the data from the tape recorder and produce the image was an IBM compatible computer based around the Intel 80386 microprocessor chip. This computer was enhanced with a large 320 MB ESDI hard disk, an eight megabyte memory expansion, a high speed digital input/output board, a VGA display adapter connected to an 800X600 pixel resolution multisync monitor, and a Data Translation high speed image processing board possessing four megabytes of on board video image storage memory which outputs to a dedicated video display monitor. The Data Translation DT2861 board will be referred to as the framegrabber. Figure 1 is a block diagram of the NPS-IRSTD PC based imaging system.

To form an image from the data recorded on tape a direct memory access (DMA) transfer is employed to move data into the standard random access memory

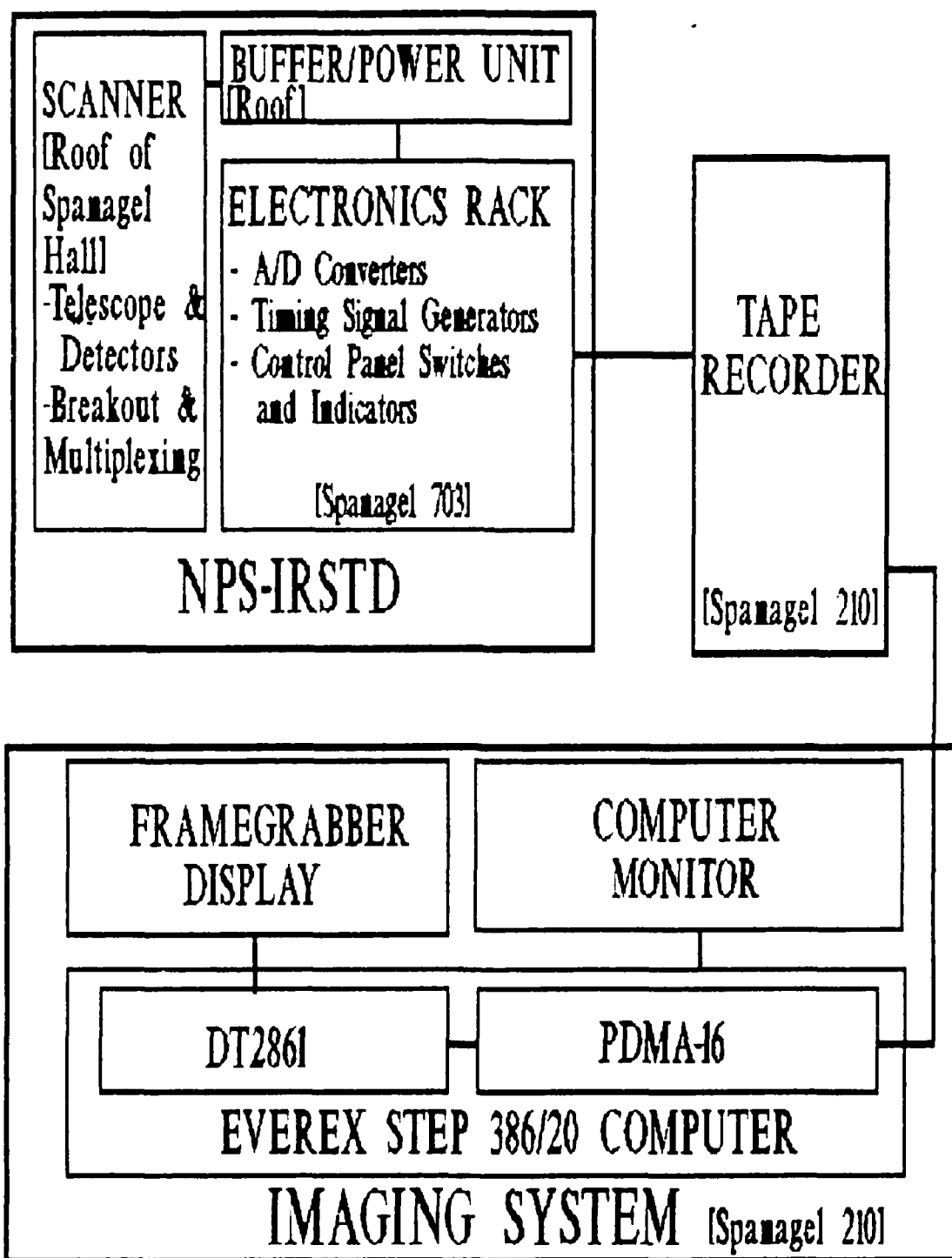


Figure 1 Block Diagram of the NPS-IRSTD Imaging System

area of the 386 computer. This data is arranged in a format incompatible with the display characteristics of the framegrabber, so it is unscrambled into a correctly formatted block and then moved into framegrabber frame store memory. Running Fortran programs based around Data Translations DT-IRIS subroutines allows image data written to frame storage memory to be processed and displayed on the dedicated video monitor.

The image processing and video display functions have been divided into two programs, BEGIN and IMAGE, each of which fills a distinct role. BEGIN is designed for use prior to viewing images to build tables which define display color characteristics. IMAGE is used to control processing and display for specific images.

The remainder of this report is organized as follows:

- Chapter II provides additional information on the history of the IRST program and the AN/SAR-8 ADM as well as a description of the system hardware as it exists at this time.
- Chapter III comprises the body of the report. The details of the imaging process are spelled out, including information on engineering approaches that failed to produce acceptable results. This is followed by a description of the image processing techniques employed while attempting to enhance the image.
- Chapter IV presents the results achieved with the imaging system and discusses the pertinent features of these results. It also discusses the performance results of the imaging system, noting items which require attention in order to increase its performance and reliability.
- Chapter V draws conclusions based on the findings, and then makes recommendations regarding areas for future investigation which became evident during the course of this project.
- Appendix A discusses the operation of infrared detectors, with special emphasis on the semi-conductor photovoltaic type used in the NPS-IRSTD.
- Appendix B discusses the imaging properties of the NPS-IRSTD using the concepts of linear systems filter theory.
- Appendix C is a collection of the computer program listings used in generating and enhancing the video images.
- Appendix D provides detector calibration data.

II. THE NPS-IRSTD

A. PROGRAM HISTORY AND BACKGROUND

The AN/SAR-8 IRSTD system, including the extensive research and development program conducted to bring it into existence and support its continued evolution, is the result of the Navy's recognition of the desirability of a modern, effective, passive detection system on board its ships. A passive system can be developed by exploiting the fact that all objects at temperatures above absolute zero (0 K) emit electromagnetic radiation characteristic of the exposed surface temperature and emissive properties. Such a passive infrared detection system employed on a ship would complement the ship's other detectors and consequently increase the overall flexibility, reliability and effectiveness of the composite detection package. It could be operated independently during a period when emission control measures (EMCON) are in effect, or it could be operated concurrently to provide an additional source of information to verify information received from other sources, or for cuing of other detection assets.

Electromagnetic radiation emitted from an object by virtue of its surface temperature and emissivity is a phenomenon that is not dependent on an illuminating light source. For targets of interest such as aircraft, missiles, surface ships, etc., temperatures range from ambient atmospheric for some external surfaces to 1000 °C for the jet exhaust. All objects in this temperature range radiate strongly in the infrared region of the electromagnetic spectrum.

Motivated by the desirability of such a system, the AN/SAR-8 IRSTD was developed to detect, evaluate and track sources of infrared radiation. The following is a summary of the major milestones, taken from the thesis by Ayers [Ref. 1], in the history of the AN/SAR-8 ADM which is now located at NPS:

- In 1960, the U.S. Navy sponsored the development and testing of the first Infrared Electronic Warfare System (IREWS).

- IRST (first test version on the IRSTD) prototype testing took place by SPAR in 1969.
- In 1974, the Canadian Navy sponsored the development and testing of the Shipboard Passive Surveillance and Detection System (SPSDS).
- The U. S. Navy posted the operational requirement for a passive IRST system in 1975.
- A U.S.-Canadian Memorandum of Understanding and a Joint Project agreement was signed in 1976 which resulted in the actual contracting and construction of the Advanced Development Model(ADM) of the IRST system.
- May of 1978 the IRST system was tested in Halifax, Nova Scotia.
- In June of 1978 the IRST went aboard HMCS ALGONQUIN for at-sea shake down and further testing.
- In April of 1979 the ADM was moved to Key West, Florida for further testing and program validation.
- Upon completion of the Key West testing, OPTEVFOR recommended full scale engineering development of the IRST/IRSTD. The system was then transferred to the USS Kinkaid, in September of 1979, for continued testing and developmental considerations.
- After the trial the ADM was sent to the Naval Surface Weapons Center (NSWC) at Dahlgren, Virginia.
- Full scale engineering development was approved in June of 1981.
- In 1983 a subsequent Joint Agreement was signed by the U.S. and Canada for engineering development of the IRSTD system.
- The prime contract was signed with SPAR and General Electric in August, 1984.
- In January of 1985, the ADM was transferred to NACIT at NPS Monterey, California to be used in research.
- In 1986 the cryogenic cooling engine was replaced by a system which uses liquid nitrogen. One germanium window was removed from the optical path to accomplish the alteration.
- Thesis by Parker December, 1986 recommends realignment of optical system to compensate for window removal. [Ref. 2]
- Subsequent to completion of recommended optical realignment, a thesis by Ayers September, 1987 studies calibration of detectors. [Ref. 1]
- Bypassing Background Normalizer Unit (BNU) and initial installation of signal transmission lines to Spanagel 210 was completed in 1988.

- January, 1989 six detector data recorded. Problems with data quality discovered.
- August, 1989 data quality problems corrected, full multiplexed data recorded.

As can be noted from this list, there have been some changes made to the system since at its arrival at NPS. The reasons for change were twofold. First, when the AN/SAR-8 ADM arrived after its numerous trials, transfers, and storage periods it was found to be in an obvious state of disrepair. Second, its usefulness for research in its original configuration would have been limited by the background normalizing hardware.

The first major item modified was the detector cooling system. The original cooling system was driven by a Cryogenic Technologies cryogenic engine operating on a Gifford-McMahon cycle. This engine was complicated, expensive to repair, and had a limited operational lifetime. Additionally, a leak was discovered at the top of the inner germanium window which was allowing water to condense on the detectors. For these reasons it was decided to replace the original system by using a pool of liquid nitrogen as the coolant. [Ref. 3]

In evaluating the optical system after the cooling system was modified Parker analyzed the effects of the removal of the inner germanium window, which changed the optical path by removing approximately 4 mm of refractive material near the focal plane of the system. Using the Super-Oslo optical design software developed by Sinclair Optics, INC. he found that a focal shift of the dewar sub-assembly of approximately 0.133 ± 0.030 " toward the reflecting mirror would restore the optical performance by reducing the spot size of a point source to less than the characteristic size of the individual detectors (0.02"). The corrected configuration spot size would be twice the original spot size, but well within the detector size. The MTF of the optical system would also be slightly affected; a reduction in modulation of approximately 6% from the original configuration can be expected at a spatial frequency of 250 lines/inch. [Ref. 2]

Following the corrections made to the system verifying Parker's analytical work, Ayers and Crittenden [Ref. 1] performed calibrations of detector responses.

This work was used in making first order corrections to the data used for imaging. A summary of the detector calibration results is included as Appendix D.

The task of restoring the NPS-IRSTD has required a great deal of effort by many people; students, staff and faculty. Special recognition is due Mr. W. J. Lentz for his work on the system's electronics. The major modifications were complete and the first sets of data were taken in January-February, 1989. While taking these initial data sets the detector multiplexer clock was disconnected so that only six detectors on each array were sampled. This data showed intermittent, unpredictable instabilities when retrieved from the tape recorder for analysis. Subsequent data sets taken in March through July, 1989 showed similar characteristics. Figure 2 is a plot showing the data irregularities. After numerous diagnostic checks and fine tuning modifications, which revealed a variety of problems ranging from crosstalk in the data lines in several locations to a bad channel in the tape recorder, the system was made fully functional in August, 1989. The data used in the video imaging processes for this thesis was collected August 12, 1989.

B. CURRENT SYSTEM HARDWARE CONFIGURATION

The following description of the NPS-IRSTD ADM is intended to give the reader a complete overview of how the system works as it is presently configured. The emphasis is on the role of each major component and how those components interact.

The NPS-IRSTD is presently installed on the seventh and eighth floors of Spanagel Hall at NPS. The scanner assembly and buffer power unit are located on the eighth floor, the highest location on NPS grounds , with a 360° view of Monterey Bay and the surrounding hills. The analog-to-digital converters and system control panels are located in Spanagel 703. The signals generated by the NPS-IRSTD are transmitted to Spanagel 210 for tape recorder storage and computer analysis.

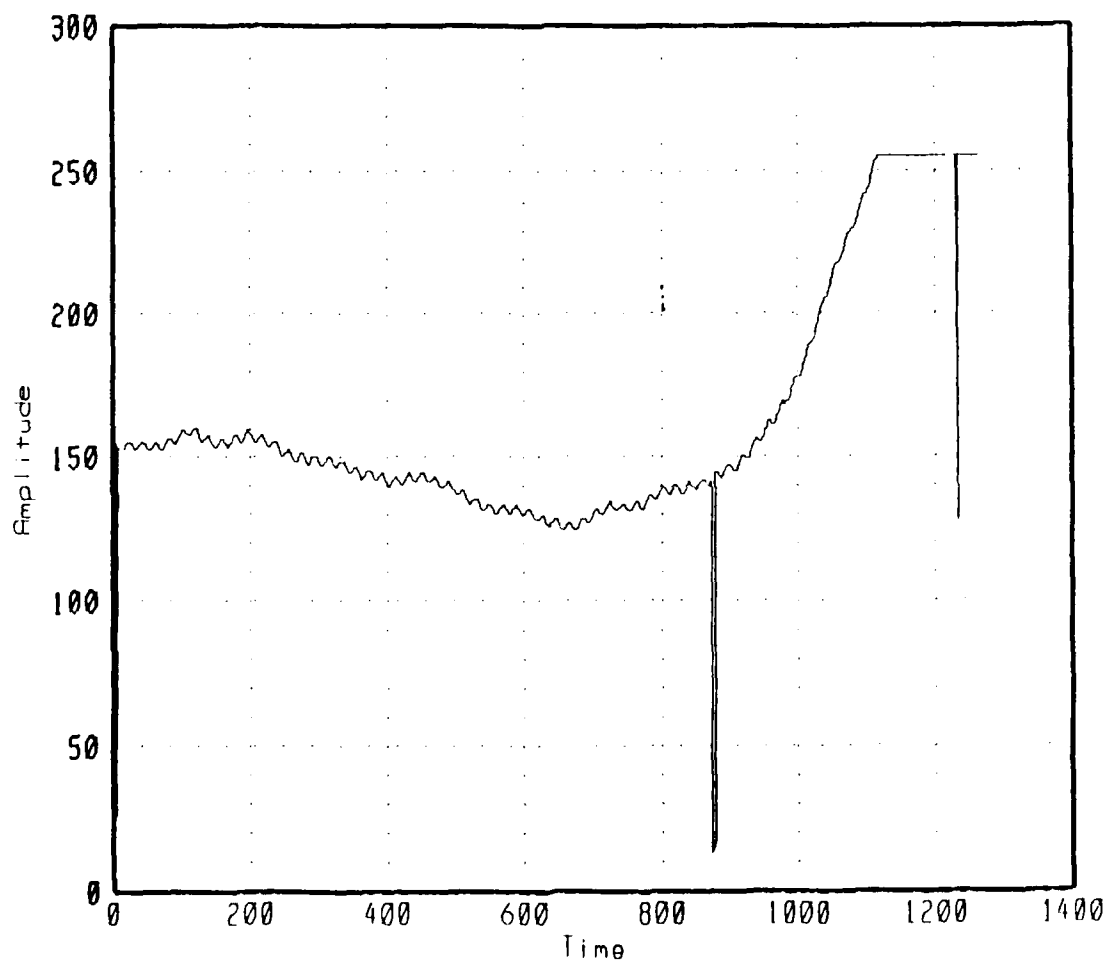


Figure 2 Unmultiplexed Data from the NPS-IRSTD Showing the Dropout Characteristic

1. Scanner Assembly

The scanner assembly contains the hardware necessary to collect infrared radiation in a 360° field of view from 1/2° below the horizon to 10° above, and convert this radiation to an electrical signal that can be transmitted to other parts of the system for analysis. The scanner assembly houses:

- Schmidt F/1 catadioptric telescope.
- Two vertical 90 detector arrays operating in the 3-5 μm range. These are mounted side-by-side with approximately 1/2° horizontal separation and are referred to as the lead and lag arrays.
- A detector cooling system that uses a pool of liquid nitrogen as the coolant.
- Pre-amplifier bandpass filters.
- Background Normalizer Units, one for each array. The one for the operational array has been bypassed.
- Detector signal breakout and multiplexing hardware.
- Slip-ring assemblies for passing the data signal from the rotating head to the fixed base.
- Position-in-rotation signal generating hardware.

Figure 3 shows the scanner assembly and the buffer power unit mounted on the roof of Spanagel Hall.

a. The Telescope

The Schmidt catadioptric F/1 telescope receives infrared radiation through a 10" corrector plate. The corrector plate is made of germanium which transmits well in the infrared and has the necessary material properties required of lenses. The light is focussed onto the detector assembly by reflection from a 16" diameter spherical mirror at the back of the telescope. The detector assembly consists of two focal plane detector arrays on a cooling finger enclosed in an insulated cylinder. Light reaches the detectors through a germanium window mounted in the cylinder wall. The two detector arrays are also covered by separate filters which selectively pass different portions of the 3-5 μm infrared band. Figure 4 shows the telescope and detector arrangement.



Figure 3 Photograph of NPS-IRSTD Scanner, and the Buffer and Power Unit

SCHEMATIC OF THE NPS-IRSTD OPTICAL SYSTEM

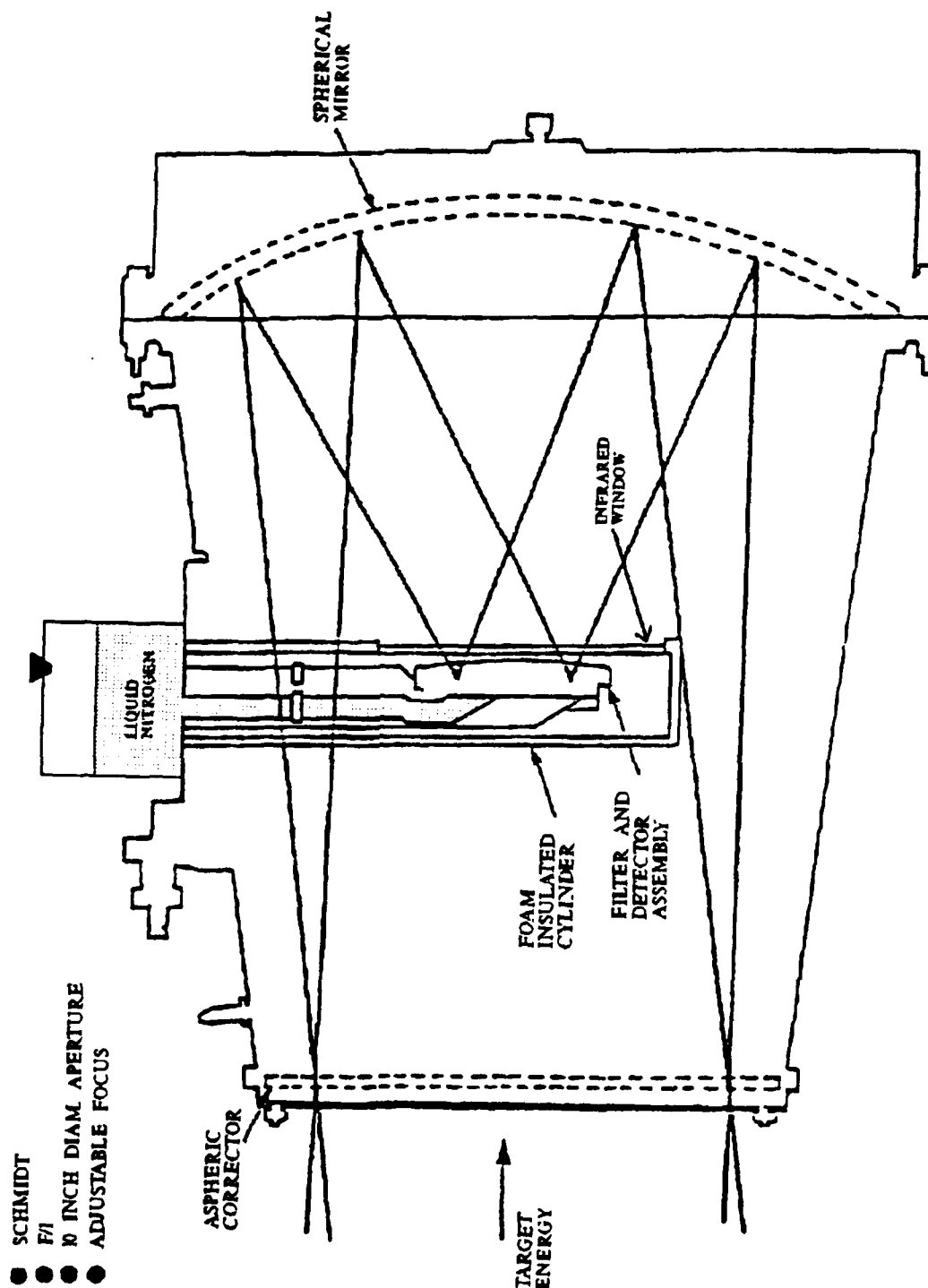


Figure 4 NPS-IRSTD Telescope and Detector Assembly

b. Detectors and Detector Noise Reduction

The NPS-IRSTD's detectors are Indium Antimonide semi-conductor photodiodes, and they function as quantum detectors. That is, they work by counting individual incident photons which have energies similar to the band gap energy of the semiconductor material. Photon energies are determined by the relationship $E=hc/\lambda$. Detector output is a voltage signal related to the number of photons received. Of relevant interest to this thesis is the fact that production of a television type video image was not a principal concern in development of the ADM. Consequently detector size, type, scan pattern and other imaging properties were designed to specifications more conducive to effective detection, categorization, and tracking of targets with certain defined infrared signatures, than to detecting differentiations in the full range of scene elements. Appendix A provides additional information on the workings of the indium antimonide detectors.

Because of the small band gap energy of the semiconductor material there is sufficient thermal energy at normal atmospheric temperatures to excite electrons within the material. This produces a background noise voltage level capable of masking the detectors' ability to register the arrival of an infrared photon. This thermally generated noise is controlled by cooling the detectors to near 85 K with liquid nitrogen.

The ability to detect incident radiation is also affected by "1/f" noise, a category including a number of mechanisms for which the fluctuation amplitude varies approximately reciprocally with frequency. The frequency here is not that of the radiation, but is the frequency of the electronic signal. Each of the 180 detectors is coupled to an electronic channel. The effect of 1/f noise is limited by connecting each channel to a pre-amplifier band pass filter to eliminate the low frequency components of the voltage signals coming out of the detectors.

c. Detector Cooling System

The modified detector cooling system uses liquid nitrogen filling the detector support stalk from a reservoir to cool the detectors to approximately 85 K. This arrangement is shown in Figure 5. Other items of interest in this figure are:

- the regions of foam insulation which restrict thermal transfer between the stalk and surrounding areas. This increases the time it takes to boil off the supply of liquid nitrogen, thus increasing operating time between refills, and also reduces the degree of cooling experienced by surrounding areas diminishing the risk of condensation of moisture on easily damaged surfaces.
- the heating elements surrounding the germanium window. These are designed to prevent condensation on the window surface that would block the infrared radiation and could possibly damage the window.
- the vent tubes which serve to direct the evaporating nitrogen into the area around the detectors and eventually into the telescope enclosure to assist in maintaining a moisture free atmosphere.

d. Signal Multiplexing Hardware

On the operational (lead) array the signal coming out of the pre-amplifier bandpass filter has been re-routed. Instead of connecting to the Background Normalizer Unit, where all data except that which contains patterns meeting criteria indicative of the presence of a pre-defined target type is suppressed, each detector channel is brought into a breakout box to provide direct access to the signal. This breakout box contains 90 connection points, one for each detector in the array, with the continuously varying detector output voltage at each point.

To reduce the number of cables running from the scanner to Spanagel 703, and to reduce the number of electronic components required to handle the data, the 90 detector output channels are connected to six multiplexers, fifteen channels to each multiplexer. Each multiplexer selects one of its 15 input lines for output. At any time, the six multiplexer outputs are for detectors physically separated by 14 detectors. Detector multiplexing is shown in Figure 6.

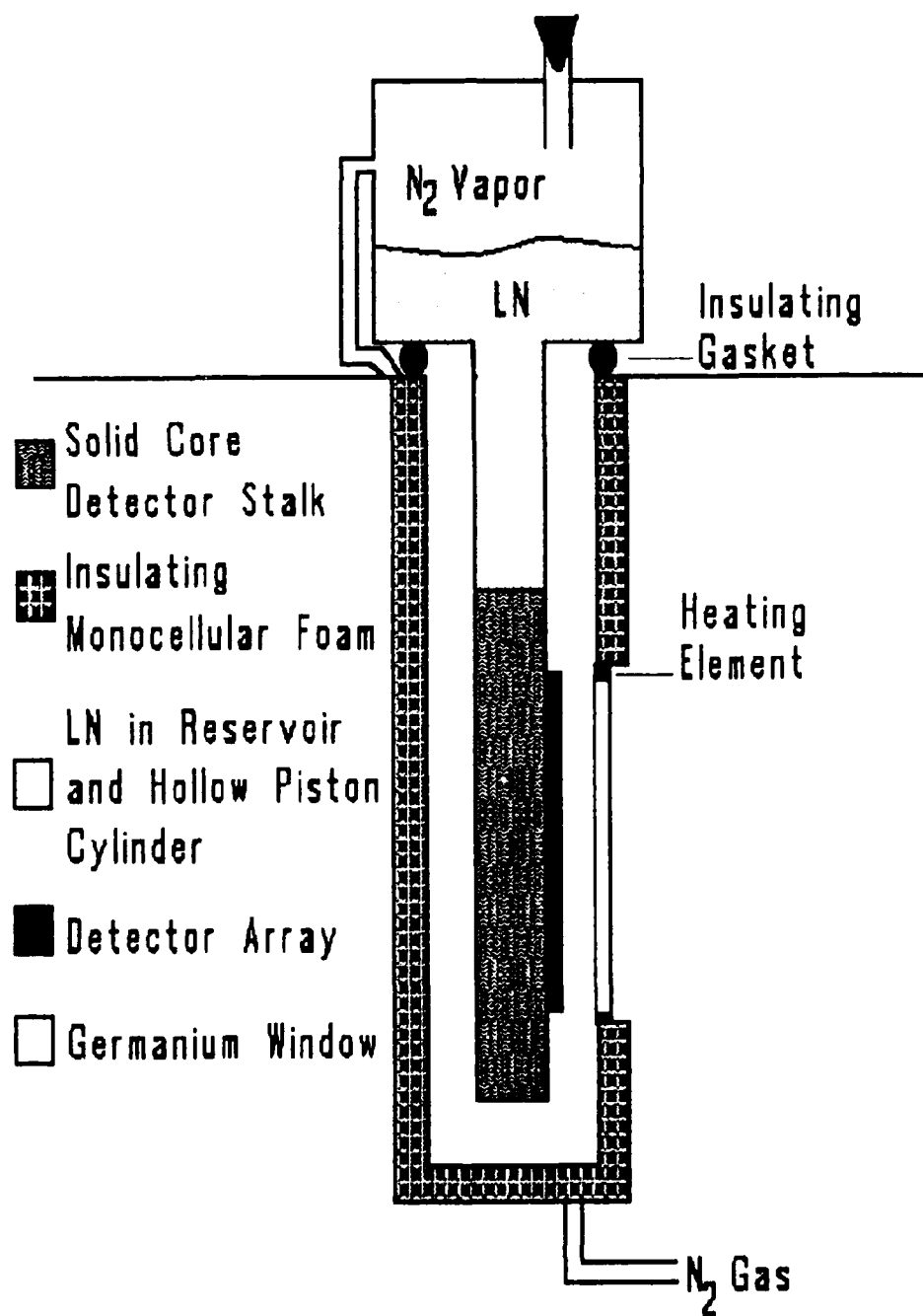


Figure 5 Simplified Diagram of the NPS-IRSTD's Modified Detector Cooling Apparatus

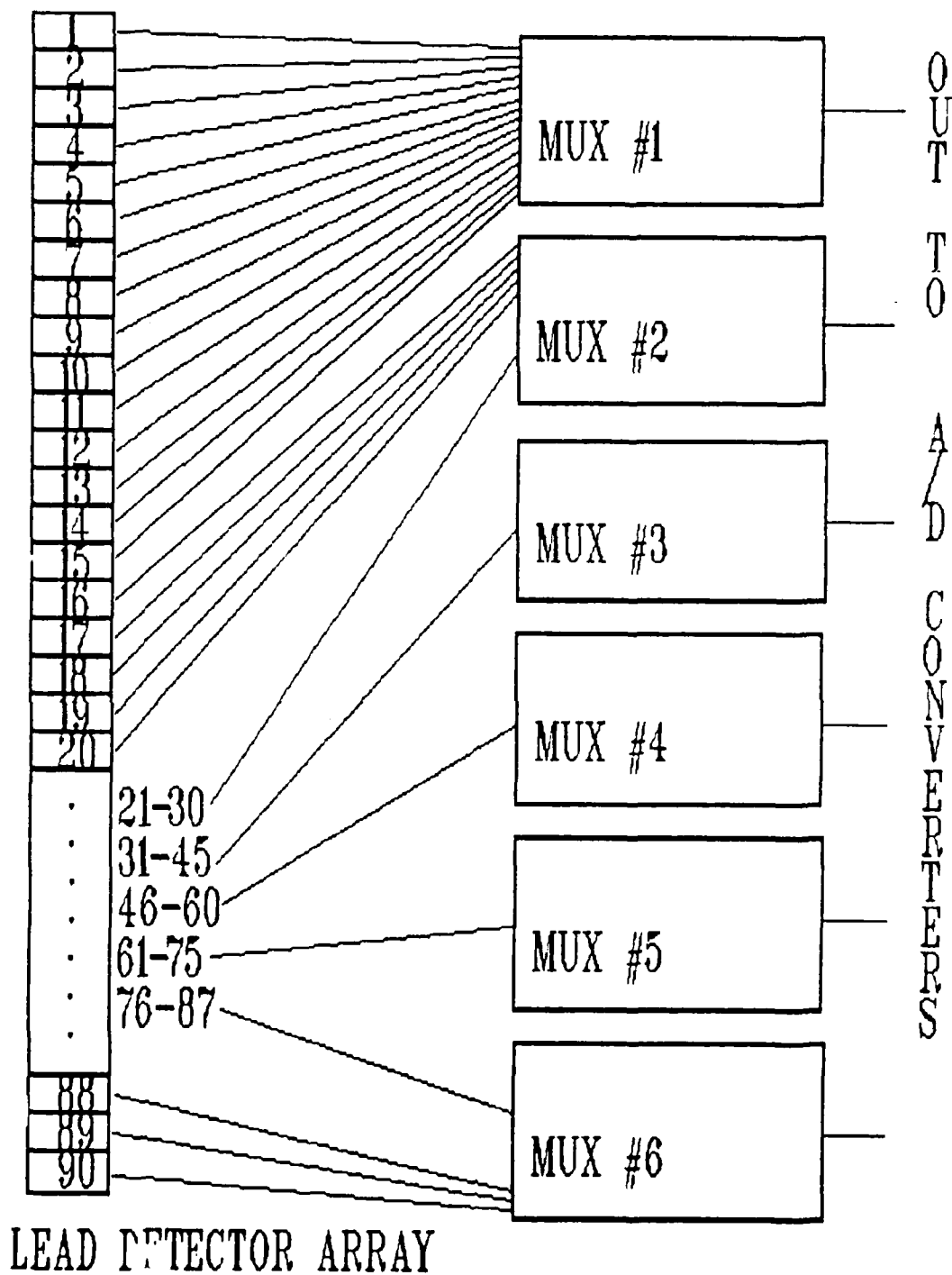


Figure 6 Multiplexing Arrangement for the Lead Detector Array

e. Slip-ring Assembly

To get the electrical signals from the continuously rotating head to the fixed base a set of slip rings is employed. There is one slip ring for each multiplexer channel, 12 in all, and several others for synchronization/timing signals. Each slip-ring assembly consists of a continuous, circular copper contact strip on the bottom side of the rotating head. Attached to the fixed base is a contact brush which rests in constant contact with the rotating ring. An area currently being studied for possible improvement of the NPS-IRSTD is to replace the slip-rings with an air-gap coupled fiber optic system.

f. Position-in-Rotation Signals

The NPS-IRSTD generates the signals necessary for correlating scene data with its corresponding azimuthal position. This is done using gear driven signal generators which produce a certain number of pulses based on gear ratios during each revolution of the scan head. Presently there are two position-in-rotation signals available for use. The first is 1/60 (changeable to 1/120) of a revolution which divides the scan into 6° elements referred to as sectors. The second is 1/1000 of a sector. The rotation time of the head is usually set as close to 2 seconds as possible so the 1/1000 signal equates to approximately 60 KHz and is generally referred to by that frequency. A single, fixed position pulse has been superimposed on the channel carrying the sector pulses to give an end-of-rotation mark. This is not generated by a gear driven wheel, but rather by passing a metallic tab affixed to the scanner through a notch attached to the base, thereby interrupting a circuit in the notch once each rotation.

3. Buffer and Power Unit

The Buffer and Power Unit acts as an intermediary between the scanner assembly and the electronic processing hardware in Spanagel 703. Because of the large separation, approximately 150' of cable run, between the scanner and the equipment in room 703 it is necessary to boost voltage levels and otherwise modify the transmitted signals to match the characteristics required at each end. The Buffer and Power Unit can be seen in Figure 3 to the right of the scanner assembly.

4. Spanagel 703 Electronics

The electronic equipment located in Spanagel 703 includes the electronic power supplies, the power control switches and associated status indicators, system timing and synchronization signal generators and data signal analog-to-digital converters and multiplexers, which can be seen in Figure 7. The original ADM data processing and display units which interfaced with the existing equipment for system testing and evaluation were not suitable for research applications and were not installed.

The components in room 703 for which a functional understanding is essential for processing the data generated by the NPS-IRSTD include the system timing and synchronization signal generators and the data signal Analog-to-Digital (A/D) converters and multiplexer. The fundamental clock frequency for data produced by the NPS-IRSTD is 5.4 MHz; that is 5.4×10^6 detector digitizations are performed each second. All frequencies driving components involved in data digitization are derived from this rate. There are twelve eight bit A/D converters, two sets of six, with one set for each detector array. The twelve A/D converters all connect to eight multiplexers, one for each data bit. It is the output from these multiplexers, along with the synchronization and rotation signals, that is transmitted to the tape recorder in Spanagel 210.

5. Ampex Tape Recorder

The tape recorder used in this project is an Ampex HBR 3000i which can record twelve independent channels of data simultaneously. Tape recorder operation may be driven by either an internal or an external clock, and tape speed is selectable from seven possible choices ranging from 1 7/8 inches per second (ips) to 120 ips. Data is recorded at 120 ips using the 5.4 MHz IRSTD clock, and played back for imaging at 1 7/8 ips using the internal tape recorder clock set to 4.32 MHz.

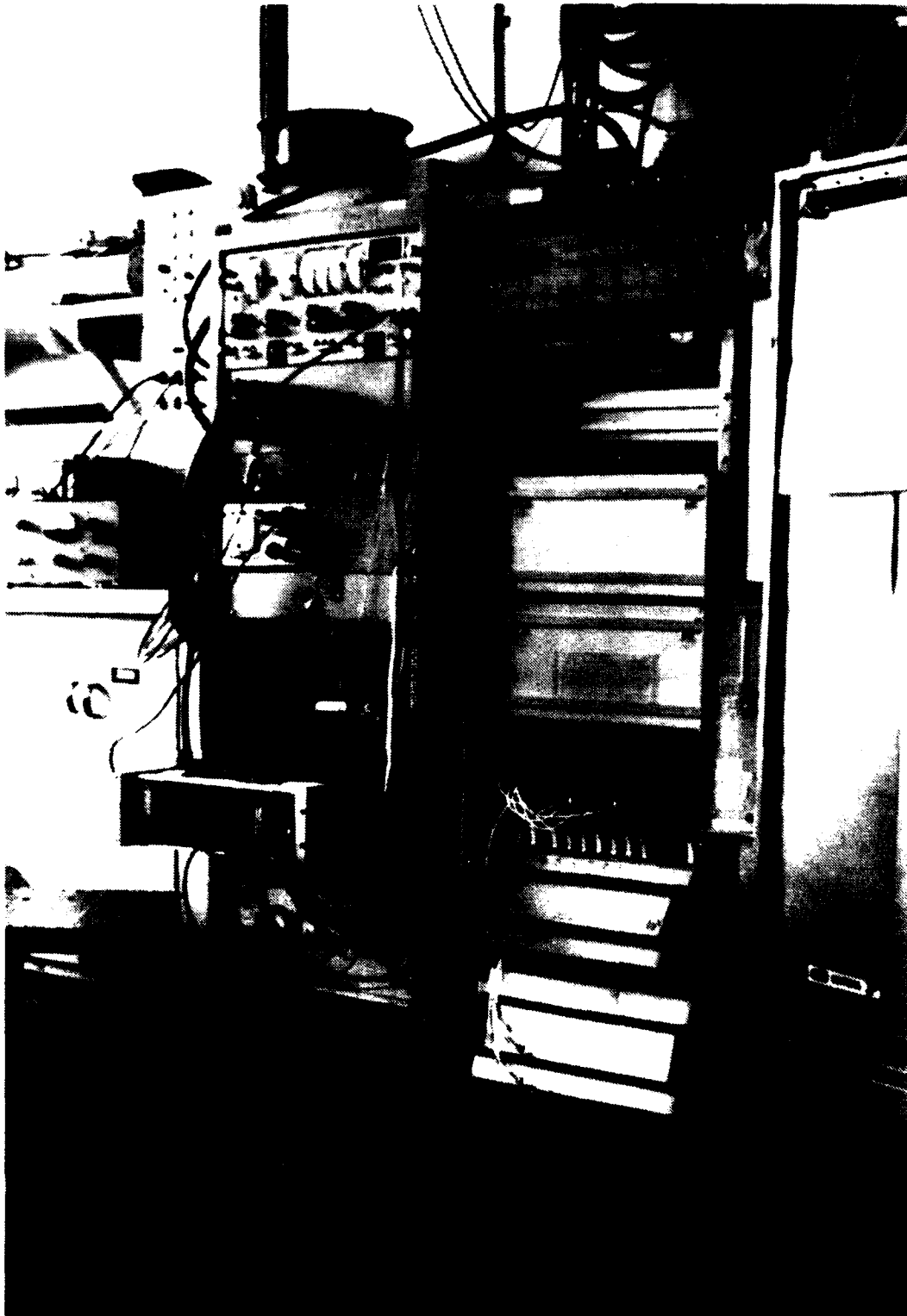


Figure 7 Photograph of Spanagel Hall, Room 703, Electronics Racks

6. Data and Timing Signal Interrelationships

This section steps somewhat beyond the stated framework of an overview but this is necessary to develop an adequate understanding of the system. The NPS-IRSTD 5.4 MHz digitization rate includes all 180 detectors in each period of a 30 KHz clock, (this 30 KHz is not in any way related to or synchronized with the 30 KHz rotation signal). Therefore, on the transmission line to the tape recorder a digitized data byte from a given detector will be followed by the next byte from the same detector 33.3 μ s later, with information from the other 179 detector's transmitted in between the two. However, because of signal multiplexing, the order in which the detectors are digitized is not sequential from top to bottom.

To relate the detector digitization sequence these conventions will be followed: The detectors on the lead array are numbered 1-90 with #1 on top and #90 on the bottom; the detectors on the lag array are numbered 91-180 with #91 on top and #180 on the bottom. Starting at a point in the cycle where the top detector on the lead array, #1, is being digitized, the sequence continues as follows:

- 1,16,31,46,61,76,91,106,121,136,151,166,2,17,32,47,62,77,92,107,122,137,152,167,3,18,33,48,63,78,93,108,123,138,153,168,4,19,34,49,64,79,94,109,124,139,154,169,5,20,35,50,65,80,95,110,125,140,155,170,6,21,36,51,66,81,96,111,126,128,143,158,173,9,24,39,54,69,84,99,114,129,144,159,174,10,25,40,55,70,85,100,115,130,145,160,175,11,26,41,56,71,86,101,116,131,146,161,176,12,27,42,57,72,87,102,117,132,147,162,177,13,28,43,58,73,88,103,118,133,148,163,178,14,29,44,59,74,89,104,119,134,149,164,179,15,30,45,60,75,90,105,120,135,150,165,180.

Notice that blocks of six detectors from the lead array (e.g. 1,16,31,46,61, and 76) alternate with blocks of six detectors from the lag array (e.g. 91,106,121,136,151, and 176).

To decipher how this sequence is generated, start by looking at the 15-to-1 multiplexed channels in the scanner. By setting the multiplexer input address lines for line zero, the data from detectors 1,16,31,46,61,76,91,106,121,136,151,166 is presented on the multiplexer outputs. These analog data signals are connected to the inputs of the A/D converters, which generate digitized 8-bit bytes. Cycling through the 12-to-1 multiplexer attached to the A/D converters sequentially introduces the digitized data for detectors 1,16,31,46,61,76,91,106,121,136,151,166 onto the line leading to the tape recorder. The sequence for detectors

2,17,32,47,62,77,92,107,122,137,152,167 is generated by setting the input address lines for line one. This process is repeated until the input address lines reach line fourteen, after which they are reset to zero and then the process starts again. Figure 8 shows the digitization multiplexing scheme.

The next complication arises from the signal timing for the various parts of the system. All clock signals originate in room 703; however, they do not all propagate the same distance to the various devices which require synchronization. For example, the rising edge of the 30 KHz digitization signal is used to set the scanner multiplexers output selector bits to zero. But to do this, the signal must propagate from room 703 to the scanner and reset the multiplexer. The data signal on the multiplexer output line must then propagate back down to the A/D converters. Assuming signals propagate at the speed of light in both directions, given the approximately 300' of wiring in a round trip and the 5.4 MHz digitization rate, nearly two digitization periods will have passed before the signals reach the A/D converters. Added to this are the delays encountered in propagation through the electronic circuitry. Since all these delays are subject to fluctuations based on temperature and on the condition of the wiring, circuit components and connections, it is clear that the precise synchronization of signals is a complex issue.

Having given a flavor of the intricacies of the timing signals, the issue is to find a way of sorting out the relationships between these signals to make them useful for data analysis. The first step towards making signals usable involves synchronizing them in phase-lock-loops where a feedback process constantly adjusts the timing to establish fixed phase relationships. Once the signals have stable phase relationships it is possible to determine the actual relationships between different signals as they are transmitted to the tape recorder by displaying them on an oscilloscope.

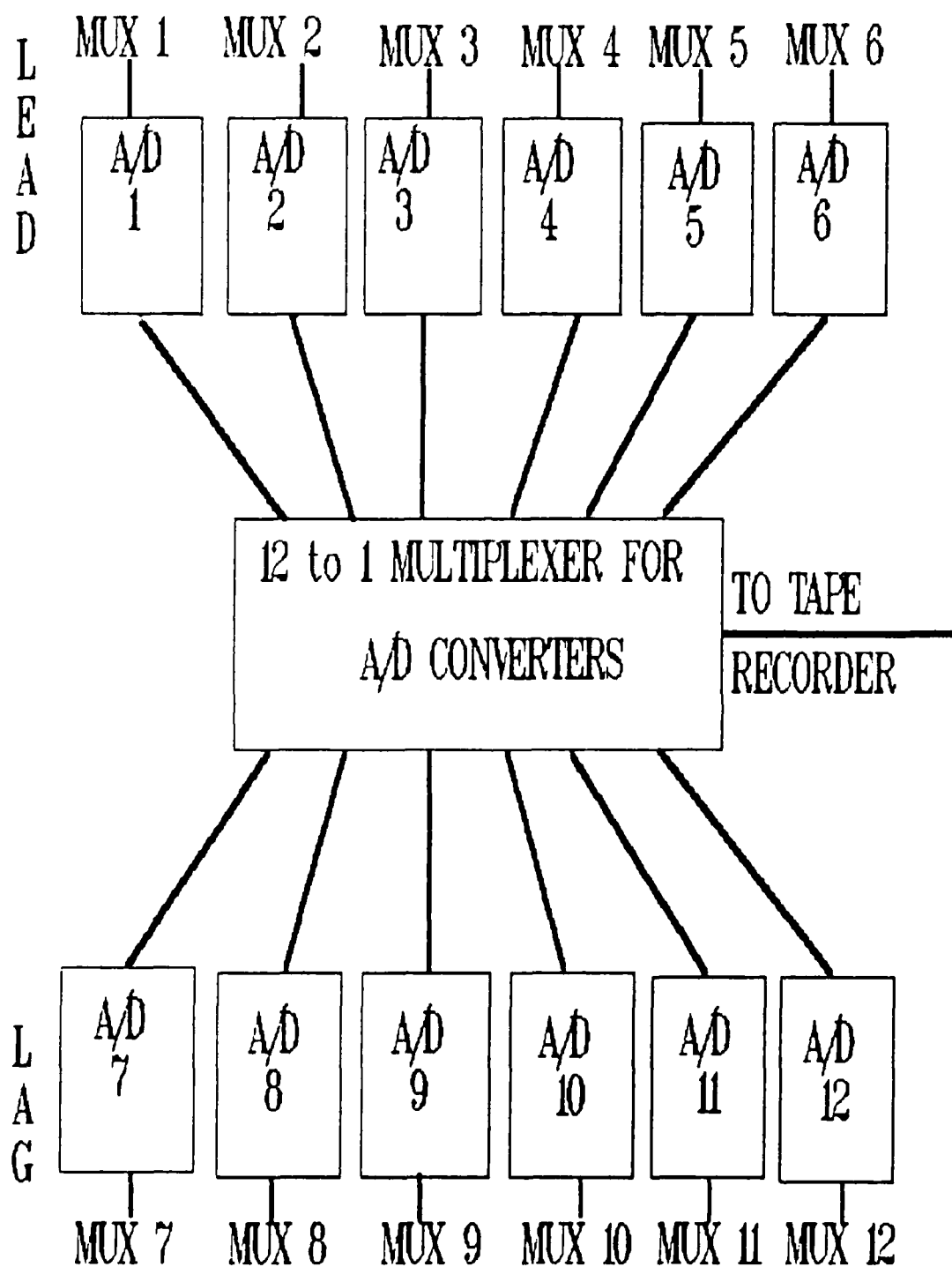


Figure 8 Analog-To-Digital Converter Multiplexing

III. EXPERIMENTAL/ENGINEERING PROCEDURES

A. GENERAL

Given the desired goal of producing video images of the scene being observed by the NPS-IRSTD, this project naturally divided itself into two distinct parts. The first task was to develop a method by which the digitized data could be manipulated into a form conducive to display on some type of computer video monitor. Once this method was fully developed and verified, the next task was to acquire real image data and to perform various image processing techniques to produce the best possible image.

B. IMAGING SYSTEM HARDWARE AND SOFTWARE ENGINEERING

1. Introduction

Before commencing with the development of the data transfer and manipulation processes, several fundamental choices had to be made. The first issue related to the speed at which the system should be designed to operate. It would be desirable eventually to have a display capable of producing images at the same rate as the NPS-IRSTD scans (referred to locally as 'real time'). Considering the large amount of data to be handled and the high 5.4 MHz digitization rate of the NPS-IRSTD, the goal of real time operation was beyond the scope of this project. Instead of trying to handle data in real time, the imaging process would be accomplished using data recorded on a high speed tape recorder and played back at much slower rates.

The next issue was the choice of the computer to serve as the first stage receiver of data from the tape recorder. The choice here was between two completely different computers, a MASSCOMP (a minicomputer built around a Motorola 86000 CPU) and an IBM compatible 80386 based microcomputer running at 20 MHz (Everex Step 386/20). While the MASSCOMP possessed a number of desirable features, including a proven interface with the tape recorder and a large

library of sophisticated data analysis software, its use also carried definite drawbacks. Because the MASSCOMP video display is limited in capability when compared with the two displays available with the 386, a second transfer from the MASSCOMP to the 386 would be necessary to take advantage of the 386's superior video monitors. In addition to the obvious awkwardness and slow operation of such an arrangement there was the secondary consideration of needing to learn two completely different sets of computer operating systems and software applications packages before really beginning to work effectively. Consequently, the decision was made to commit to finding a valid method of passing the data directly from the tape recorder to the 386.

The final fundamental task was to select one of the two monitors available to the 386 as the principle video display for the NPS-IRSTD data. Here the choice was between the standard computer video display, an 800 column by 600 row resolution multisync VGA monitor, and a specialized video display system add-on consisting of a Data translation framegrabber board and dedicated display monitor. The framegrabber system is specially designed for high speed image processing, and thus was the more desirable choice if it could be effectively employed.

2. The Everex 80386 Computer System and Associated Components

Before getting to the description of the image display process at its current stage of maturity, I believe it necessary and beneficial to include a reasonably detailed description of the 386 computer system which includes all the relevant add-on components. This description is intended to provide a clear understanding of the operation of each major component, and how they all interact.

a. Base 386 Computer, Memory/Mass Storage, DMA controller

The Everex Step 386/20 is a fully IBM PC compatible desktop computer based on the Intel 80386 Central Processing Unit with a maximum system clock speed of 20 MHz. In addition to the digital input/output board and the image processing board discussed in the following sections, the computer used for this project was equipped with:

- One megabyte (MB) of system RAM. RAM, Random Access Memory, is the workspace used by the computer to run application programs. A standard ASCII character requires one byte of memory, and codes employed by programs to execute functions or perform manipulations normally require one to several bytes per single operation. One megabyte equals 1,048,576 bytes=(1024 bytes)x(1024 bytes). The low 640 kilobytes (KB) is used for the Disk Operating System (DOS) and programs. DOS acts as a translator between the operator and the computer to allow programs to be executed, files to be accessed, and printers and other peripherals controlled. The RAM above 640 KB is used for specialized functions such as video display memory. Figure 9 shows the system RAM apportionment along with the expanded memory and image processor board memory. Note that addresses are given in Hexadecimal format.
- Eight megabytes of expanded RAM managed by the Quarterdeck Expanded Memory Manager system. Many programs operated by themselves can't take advantage of expanded memory because they have been designed to be compatible with earlier computers. Special handlers, such as Microsoft Windows or DESQview must be used to take advantage of the extra space. Unfortunately, these programs often remap addresses to assign programs to the space available and then keep track of them. This remapping conflicts with efforts to access specific memory locations directly.
- 350 MB hard drive. Each image stored in a data file requires 1/4 of a megabyte.
- 40 MB tape backup system. This allows fast, regular backup of both data and programs stored in case the hard disk system fails.
- VGA adapter and multisync monitor with 800 column by 600 row maximum resolution. This display, along with Ontar Corporation's PC-IMG software, allows limited image analysis and processing, in addition to that done on the image processing board.
- Intel 8237 D.M.A. controller. This is a specialized circuit, commonly available on many computers, but hardly ever used. The DMA controller can take over the memory address lines to perform external read/writes directly to or from the lower 640 KB of system ram. It is controlled by writing to input/output registers 8H (the command register), BH (the mode register), AH and FH (mask registers), 2H or 6H (address registers), 3H or 7H (the byte count registers), 81H or 82H or 83H (the page register). The data written to these registers determines all the characteristics of the transfer to take place; the channel used, input or output, increasing addresses or decreasing, number of transfers, etc. To function properly the DMA controller must interface with a device which sends and receives timing signals in a certain pattern, called a handshaking protocol. The input/output board Metrabyte PDMA-16 serves this purpose. The PDMA-16 manual provides a detailed description of the DMA controller. [Ref. 4]

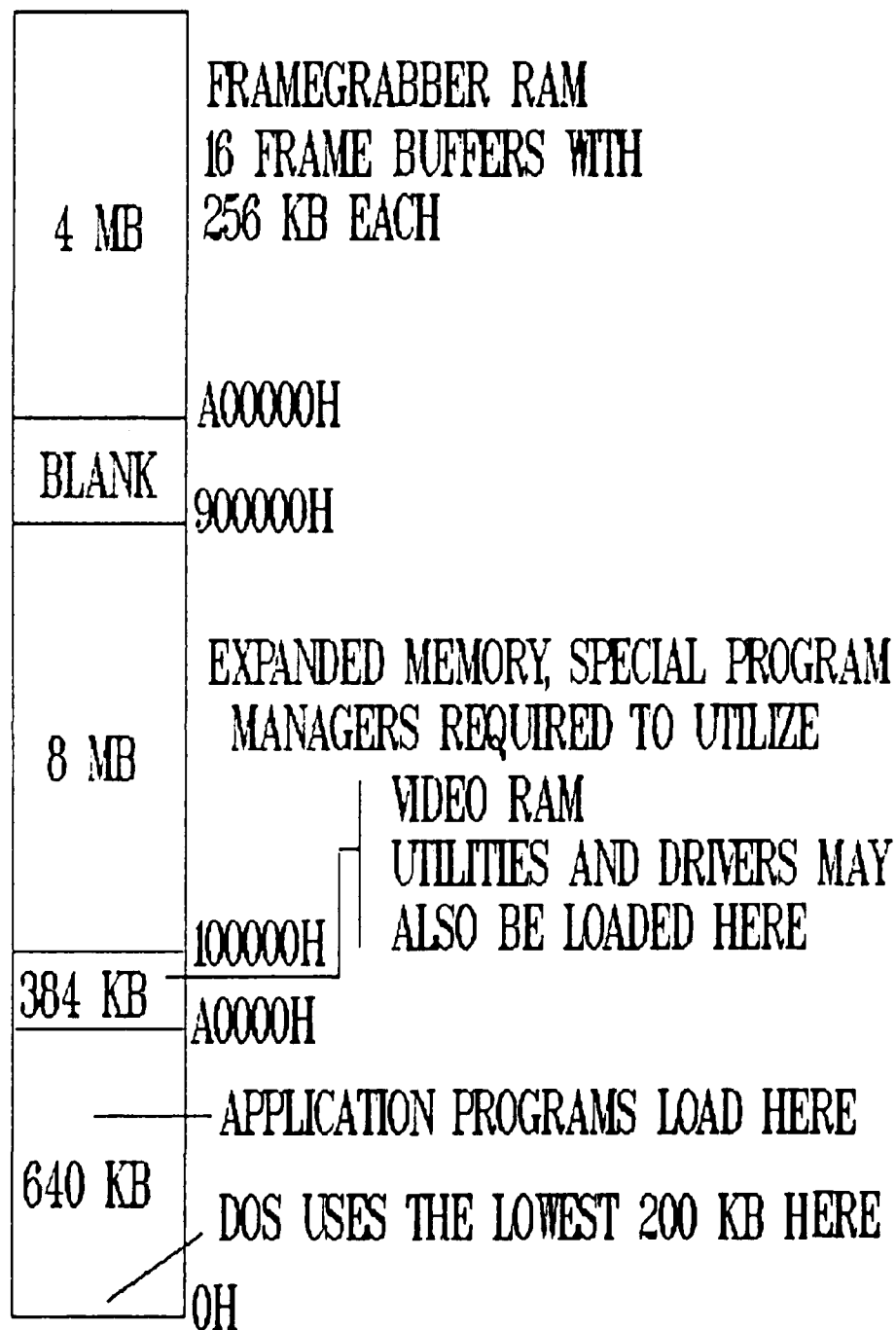


Figure 9 Random Access Memory Organization for the 386 Computer

- Various input/output ports and registers to interface with peripheral devices such as printers, modems, mice, video displays, and disk drives. Certain port addresses are to specific types of devices by industry standards, while others are left open for use by add-on boards or devices. When installing boards or devices, it is often necessary to set a number of switches and run an installation program to tell the computer that the board exists at a certain location and tell the board to respond to commands addressed to that location. To access the devices attached to a port the computer writes command bytes to the register/s associated with that particular port. Table 1 shows the assignment of ports in the Everex 386.

TABLE 1
I/O PORT ASSIGNMENTS FOR 386 COMPUTER

<u>Address (hex)</u>	<u>Device</u>	<u>Address (hex)</u>	<u>Device</u>
000-1FF	Internal System	378-37F	LPT1:
200-20F	Game	380-38C	SDLC comm.
210-217	Expansion Unit	380-389	Binary comm. 2
220-24F	Reserved	3A0-3A9	Binary comm. 1
250-26F	DT2861	3B0-3BF	Mono dsp/LPT1:
278-27F	Reserved	3C0-3CF	Reserved
2F0-2F7	PDMA-16	3D0-3DF	Color Graphics
2F8-2FF	COM2:	3F0-3F7	Floppy Disk
300-31F	Prototype Card	3F8-3FF	COM1:
320-32F	Hard Disk		

b. Digital Input-Output Board

The digital input-output (I/O) board serves as the interface between the timing and data signals coming from the tape recorder and the computer. The I/O board used for this project was the PDMA-16 which is capable of two basic types of input-output modes, programmed I/O and Direct Memory Access (DMA) transfers. The PDMA-16 uses a standard 37-pin connector. 16 Data lines are divided into two eight bit input-output ports, A and B, and the remaining lines are for control and timing signals. Figure 10 shows the pin assignments for the PDMA-16. The functions of the pins are as follows:

- A0-A7; Port A data (input/output)
- B0-B7; Port B data (input/output)
- A DIR; Port A direction (output only). 0 = Port A is set for input, 1 = Port A is set for output.
- B DIR; Port B direction (output only). 0 = Port B is set for input, 1 = Port B is set for output.
- XFER.REQ.; A positive edge on this input initiates a DMA transfer as long as all other settings necessary for transfer are correct.

REAR VIEW OF PDMA-16 I/O CONNECTOR

PORT A DATA IN/OUT	A0	19	37	A DIR. OUT
	A1	18	36	GND
	A2	17	35	GND
	A3	16	34	GND
	A4	15	33	GND
	A5	14	32	GND
	A6	13	31	GND
	A7	12	30	GND
PORT B DATA IN/OUT	B0	11	29	B DIR. OUT
	B1	10	28	GND
	B2	9	27	GND
	B3	8	26	AUX 3 OUT
	B4	7	25	AUX 2 OUT
	B5	6	24	AUX 1 OUT
	B6	5	23	TIMER GATE IN
	B7	4	22	TIMER OUT
XFER. ACK. OUT		3	21	+5v
XFER. REQ. IN		2	20	+5v
INTERRUPT IN		1		Power from computer

Figure 10 PDMA-16 Input/Output Board Pin Assignments

- XFER. ACK.; On receipt of the XFER. REQ. the XFER. ACK. goes low. After the transfer is complete, XFER. ACK. returns high indicating valid data is on the port in output mode, or that the port is ready to receive new data in input mode.
- TIMER OUT; A positive pulse or square wave output from the timer.
- TIMER GATE; this provides a means of inhibiting external and internal pulses from the timer. Pulses inhibited when pin is low.
- INTERRUPT; A positive or negative edge triggered interrupt input selected by the interrupt control register.
- AUX1-AUX3; General purpose control output lines corresponding to spare bits in the DMA and interrupt control registers.
- +5V; Logic supply from the computer. While it can potentially be used to power external peripherals, because it comes directly from the computer power supply there is a risk of damaging the computer if used. For this reason the lines in the connecting cable for these pins were cut.
- GND; Logic and power return ground.

Programmed I/O involves reading the data present at the port using a software call and writing the data into a variable in the program that is running. The data is then available for treatment as would be any other variable used by the program. It could be stored, printed, or used in mathematical operations. Programmed I/O is generally much slower than DMA transfers.

DMA writes the data into the standard RAM of the computer according to an absolute address. The RAM is divided into 64 KB blocks, called pages in the language of the DMA Controller. Starting at 0H, page boundaries are set every 10000H up to the A0000H address. The DMA controller can address only within a page, thus the maximum number of transfers that can be done at one time is 64 KB, and this only when the starting address for the transfer is the lower boundary of the page. The timing of a DMA transfer can be controlled by a counter on board the PDMA-16, or by timing signals generated external to the computer system.

Setup and control for the various functions performed by the PDMA-16 is done through eight addressable registers accessed starting at a base address of 2F0H. The addresses are mapped as shown in Table 2. The first four addresses correspond to the digital I/O and control, and the last four addresses

correspond to the 8254 timer. The 8254 timer is available on the PDMA-16 to control the speed of input-output operations, time delays, and interrupts as necessary. It was not used during this project.

TABLE 2
PDMA-16 REGISTER ADDRESSES

<u>Address</u>	<u>Function</u>	<u>Type</u>
2F0H	A port	Read/Write
2F1H	B port	Read/Write
2F2H	DMA Control	Read/Write
2F3H	Interrupt Control	Read/Write
2F4H	Counter 0	Read/Write
2F5H	Counter 1	Read/Write
2F6H	Counter 2	Read/Write
2F7H	Control	Write
	Status	Read

Because of the variety of operations performed by the PDMA-16, a complete overview on its use is not appropriate here. The PDMA-16 comes with a manual [Ref. 4] which should be referred to for specifics beyond that provided here. Any functions used to transfer data for imaging are thoroughly explained in section III.B.4, or in the program documentation in Appendix C. Additionally, Metrabyte included a set of basic language routines with the PDMA-16 which can be used to learn the capabilities of the board.

c. Image Processing Board and Display

The image processing board used in this project was the Data Translation DT2861-60Hz Arithmetic Framegrabber. The DT2861 has four megabytes of RAM dedicated to video image storage, a variety of input-output methods to handle different video formats, and specialized hardware for high speed application of numerous image processing routines. The board can be controlled by using one of these methods:

- Data Translations' IRIS-tutor, an interactive, command line driven software package. [Ref. 5]
- Data Translations' DT-IRIS FORTRAN callable routines. [Ref. 6]
- Direct program writes to various addressable process control registers. [Ref. 7]

The memory is divided into sixteen frame buffers, 256 KB each, for images of 512 rows by 512 columns. However the last 32 rows are not displayed,

giving a resolution of 512 X 480. Data is stored in memory sequentially by row. The base address of each frame buffer stores the data for pixel 0,0 (the upper left corner) and the next 511 bytes are row 1 data in order. The address $\text{base} + (512 * n)$ is for the left most pixel in the $n-1$ row. The data in any one of the frame buffers may be output to the video display at a given time. Switching the display between one frame buffer and another is done in 1/30 of a second. [Ref. 7]

The DT2861-60Hz is designed to accept standard video input signals including RS-170, RS-330, and NTSC as well as certain non-standard inputs in a slow scan mode. These are all analog signals, which are digitized internally for frame storage in memory. With an undetermined amount of effort on an interface design, it can also be made to accept previously digitized signals. For several reasons none of these input methods proved satisfactory for receiving data directly from the tape recorder. A more precise explanation of why this was so, and a thorough description of how data does get to frame storage is provided in section III.B.3. [Ref. 7]

The DT2861 displays a color or gray level in each pixel on the monitor based on the value of the corresponding data byte in memory. The 8-bit byte means data values range from 0 to 255. Each value 0 to 255 is assigned a specific color or gray level determined by eight bit values set in three separate look-up tables; red, green, and blue. For each pixel there are separate red, green and blue phosphor spots. The color on the display as seen by the eye is the result of mixing the three brightness levels. Table 3 shows examples of output colors. Note that gray levels are obtained when all three look-up table values are equal. [Ref. 6]

In addition to those already described, the DT2861 framegrabber board and Data Translation software has the following capabilities:

- Create windows, areas within a given frame that can be operated on independently.
- Perform a variety of arithmetic functions including setting all values in an active region to a constant, adding/subtracting one frame buffer to/from another, and multiplying or dividing all values in an active region by a constant.

- Perform logical operations including AND, OR and XOR of all values in a given frame with a constant and AND, OR, and XOR of one frame with another.
- Apply resultant look-up-tables to the results of frame addition to map each data value, which range from 0-511, to any new value 0-255 before writing the result in the frame buffer.
- Calculate the numerical sum of all the individual data bytes in a frame or create an array for a histogram of the distribution of data values.
- Perform convolutions on the images, or apply various types of filters to enhance edges, or other characteristics.
- Zoom, Pan and Scroll to inspect details of an image.
- Create graphic overlays to label, annotate and dress up the image displayed on the monitor.

TABLE 3
SAMPLE OUTPUT LOOKUP TABLE ASSIGNMENTS

For selected values of an all color display:

<u>Data Value</u>	<u>RED</u>	<u>GREEN</u>	<u>BLUE</u>	<u>Output Color</u>
50	0	0	255	Blue
100	0	200	200	Aqua
150	0	255	0	Green
200	200	200	0	Yellow
250	255	0	0	Red

For selected values of gray scale display:

<u>Data Value</u>	<u>RED</u>	<u>GREEN</u>	<u>BLUE</u>	<u>Output Color</u>
50	0	0	0	Black
100	64	64	64	Dark Gray
150	128	128	128	Medium Gray
200	196	196	196	Light Gray
250	255	255	255	White

3. Imaging System Development

At the outset of the project it appeared as though there were a relatively large number of ways to attack the basic problem of displaying an image from the data generated by the NPS-IRSTD. However, as is evident from the descriptions of the various components given in the previous sections, limitations in component capabilities significantly restrict the number of acceptable solutions. After sorting through the options, determining hardware-imposed restrictions and limitations, and then looking for a path through or around them, it became apparent that there was only one truly acceptable solution without resorting to design and construction of additional external hardware interfacing.

This section provides the information necessary to keep anyone working to improve the system from wasting time on processes already found unsuitable. The flow chart in Figure 11 provides a way of summarizing the possible data transfer methods. The following paragraphs discuss the issues relevant to the options shown in Figure 11 for transferring data from the tape recorder to the frame buffers for display.

There appears to be only one method with even the potential for real time image acquisition. The DT2861 can transfer data at a 10 MHz rate through an external port designed to interface with the DT2858 Auxiliary Frame Processor. It may be possible to use this port to transfer data directly from the tape recorder to the DT2861 frame store memory. This is probably not a trivial task. Experimenting directly with the internal interface of the DT2861 would cause notable anxiety for a novice because serious damage could be done to such an expensive board in the event of error.

There are a couple of other points worth making regarding the DT2861 and real time display. When reading the DT2861 documentation, the 12 MHz maximum transfer for the slow scan rate appears appealing. But slow scan is only for analog signals. To use slow scan, the data would have to be reconverted to analog signals identical to those digitized by the A/D converters in room 703. Even if these problems are solved, the data must still be sorted into the proper format which is an inherently slow operation because it requires a minimum of 45 KB of data that must be individually moved.

The factors involving the choice of the Everex 386 computer for receiving the data from the tape recorder were discussed previously in section III.B.1. While choosing the specific device in the 386 which would interface with the tape recorder initially held out the form of offering alternatives, such was not the case. The drawbacks weighing against the DT2861 just discussed still apply here, and thus need not be repeated.

Because of the large disparity in projected maximum transfer speeds between DMA and programmed I/O (120,000 bytes/second for DMA vs. 5,000 to 10,000 bytes/second for programmed I/O on a 4.77 MHz PC), a great deal of effort

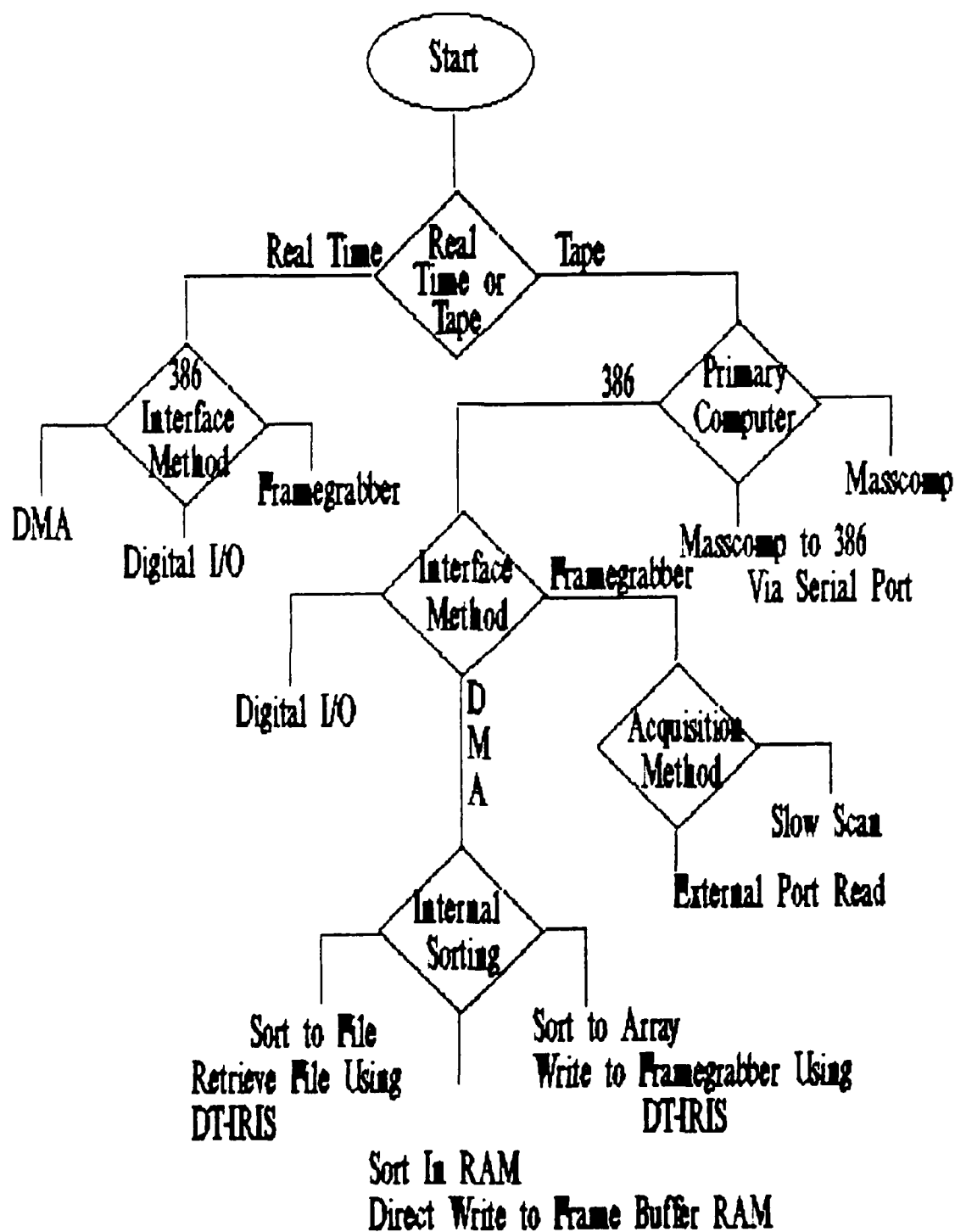


Figure 11 Flow Diagram of Possible Data Transfer Methods

and time was spent trying to understand and implement DMA transfers. Speeds are quoted for the 4.77 MHz PC because the PDMA-16 is not engineered to take advantage of the AT bus [Ref. 4]. Before the operation of the PDMA-16 was well understood, it appeared the only way to implement a DMA transfer started by rotation timing signals was to design a simple Transistor-to-Transistor Logic (TTL) circuit to count the sectors. The TTL circuits proved beneficial in investigating PDMA-16 operations using artificial signals generated on the breadboard. In this manner it was found that DMA transfer rates of 100 KHz were easily handled. Additionally, Port A and Port B were found to be capable of independent operation, allowing Port B to be used instead of the TTL circuits for sampling rotation and timing signals.

Progression from this point did not go smoothly. Two independent problems appeared and persisted in disrupting attempts to read data from the tape recorder. One was an apparent loss of data. Transfers set up for 64 KB resulted in only 12 KB of data appearing in RAM. Suspicions, which finally proved to be true, pointed to the DESQview multitasking environment's remapping of system memory as the cause of data loss. Operating outside Desqview solved this problem but brought on the appearance of the second problem: regular system crashes.

After innumerable crashes and reboot sequences, it was discovered that if the data levels on the DMA port are not stable, a parity error is generated in RAM at the location to which the particular byte is assigned. If that space in memory is not accessed, the problem can go unnoticed. It is only when sequential passes through RAM are made for data sorting that the system will invariably crash. An error check property of Desqview apparently had the ability to prevent the crashes, but the unlocatable data could not be used.

This seemingly left programmed I/O as the only remaining option. Experimentation with this method quickly showed that programmed I/O can't be done at high enough speeds to work with even the lowest tape recorder playback speed. Using PC-TOOLS' read-from-data-port command IPORTB by itself in a one step loop while the tape recorder played back at its slowest speed resulted in nearly, but not exactly, matching data rates. Looking at the data received one could trace

out the cyclic pattern of the twelve A/D converters and while at times there were twelve bytes before the pattern repeated, at other times there were eleven or thirteen. These nearly matched rates occurring with the computer reading as fast as possible leave no time to search the timing signals and use them to queue the execution of IPORTB calls.

At this point necessity forced a second, even more thorough look at the DMA process. Following many frustrating days of investigation, it was discovered that cutting the tape speed to 1/80 of real time and reversing the phase of the digitization clock produced successful transfers.

The initial work on sorting the data into proper format consisted of implementing the BASIC functions of PEEK and POKE. PEEK was used to read the DATA from RAM and then POKE was used to write it to a file according to DT2861 data file format specifications. This proved far too slow because BASIC (even compiled BASIC) is inherently slow and because writing to a disk file is one of the slowest operations possible. It required two minutes to unscramble and write a file representing an image of 512 columns by 90 rows.

The only branch on Figure 11 not tested is that which represents sorting data written by a DMA transfer into an array. Initially there was no known way to directly access RAM from inside a FORTRAN program as is required to use DT-IRIS to move the array into a frame buffer. Then, when PC-TOOLS routines were used to access memory directly using FORTRAN, the arrays could not be used because the version of PC-TOOLS available could only be compiled with Ryan-McFarlan FORTRAN while DT-IRIS required Microsoft FORTRAN for compilation. There are other factors which appear to make sorting to an array undesirable in current application, including maximum array size allowed by DT-IRIS and doubling the memory required by putting a byte in an Integer*2 space. However, for certain types of data processing it may be beneficial to switch to a system of sorting into arrays immediately after the DMA and then processing the arrays prior to moving the data to the frame buffer.

Having described many things that didn't work, it now remains to cover those which did. This is covered in the next section. Before beginning that it is

worth restating the point that while it appears data transfer rates may be increased somewhat by correcting certain recognized problems, it will probably require externally constructed hardware interfaces to achieve significant increases in performance. One possibility already discussed was the external port on the DT2861. Another would be to build a buffer memory bank in hardware in which the data is received in a scrambled format using one clock, and read out to the computer in the proper format using a separate clock.

4. Current System Operation

a. Data Transfer Timing

The process of timing the start of a set of DMA transfers to select a particular region of the 360° scan proved to be more difficult than anticipated. The original concept was to build external circuitry utilizing the End-of-Rotation and sector pulse data line to keep track of the position in rotation. Further investigation of the capabilities of the PDMA-16 board indicated it was feasible and potentially more convenient to track rotation by reading the state of the EOR and sector pulse line at the I/O port through software programming.

Counting the sector pulses at the I/O port proved to be unreliable. Noise on this data line provides false "sector pulses" which throw off the counting process. Checking this line with an oscilloscope seems to indicate the noise may not be just crosstalk from the data lines. For this reason, a method was developed to keep track of the position in rotation by timing the process using the internal clock in the 386 computer. Unfortunately, the rotation speed of the scanner assembly fluctuates enough to make this method ineffective in repeatedly pinpointing particular positions. Such a capability is essential in accomplishing frame to frame subtractions to look at time varying changes in a scene.

b. Data Transfer Process

Image data is moved from the tape recorder to the image processing board frame buffer in a three step process:

- DMA transfers into standard computer RAM.
- A byte sorting move to a separate location in standard RAM.

- Large blocks of sorted data moved into a frame buffer.

This process is shown in Figure 12. Once in a frame buffer, the data will remain there until it is overwritten, cleared by a software operation, or the system power is turned off. Frame display is controlled by software and will be discussed shortly.

The DMA transfer results in data from all 180 detectors being written into RAM in a column oriented format, where 180 contiguous RAM addresses contain data from single vertical scans down the two arrays in a pattern described in section III.B.2. The DMA one time transfer limit of 64 KB contains space for only 364 successive scans of the operational array. Three DMA transfers, (starting at 70000H, 80000H, and 90000H), are performed to provide sufficient data to construct two 512 column wide images, each representing 3° of horizontal scan. Since the DMA transfer takes several software operations to set up, one vertical scan of the detectors must be skipped moving between pages of RAM.

The next step, sorting the data into the correct format is done completely within standard RAM using BLKMOV, a subroutine from ONTAR Corporation's PC-TOOLS library. It would be desirable to be able to treat all RAM equally and sort directly to the frame buffer, but most software is limited to addressing the first megabyte of RAM in one way, and any extra memory another. In PC-TOOLS, the routine BLKMOV will move bytes (up to 64 KB) between any two locations in the first megabyte of RAM. This restriction to the first megabyte, not noted in the documentation, was verified by a phone call to ONTAR. [Ref. 8]

A second routine, BLKMAT, allows addressing above the first megabyte, but the smallest addressable unit is the 16-bit word. Since any two consecutive bytes written by the DMA transfer are moved to widely separated addresses during the sort, this routine is useless for unscrambling the data. It is also much slower than BLKMOV, requiring approximately 1 ms to complete compared with 1 μ s.

BLKMAT is used to move the correctly formatted image into a frame buffer. BLKMAT is limited to moving 32 Kilowords (64 KB) per transfer making it necessary to do four calls to the BLKMAT routine to transfer the full image. With sufficient data available for two 3° scans, two separate sets of sort

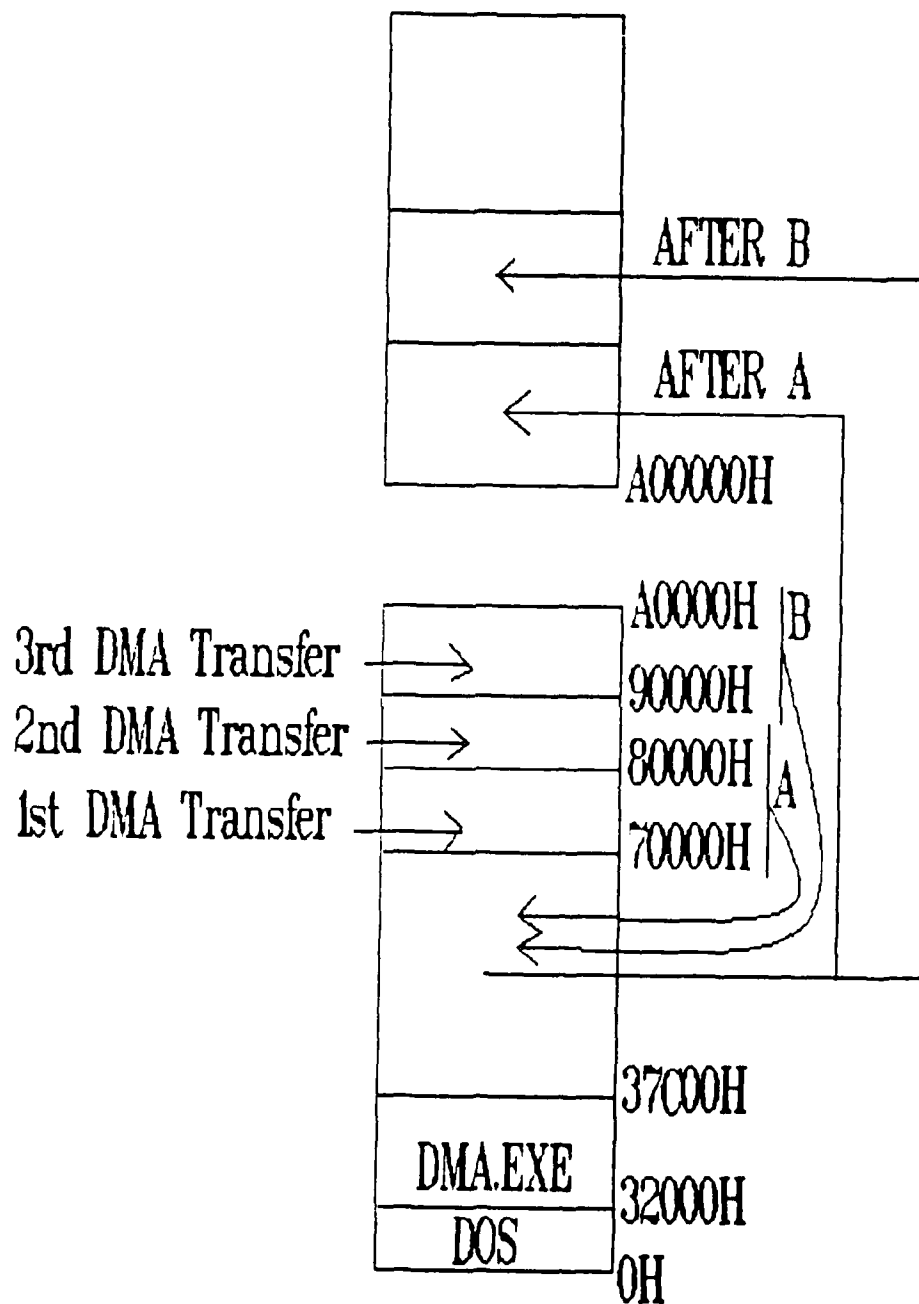


Figure 12 DMA Transfer and Sorting Sequence

and block transfers are necessary. The first 3° is placed in frame buffer 0 (base address = A00000H), the second in frame buffer 1 (base address = A40000H).

To utilize as much of the full display as practical and make each individual detector more apparent, each detector is represented by five consecutive rows of pixels on the display. Thus a full image requires 225 KB of RAM. The 225 KB immediately below the DMA region, starting at 37C00H, is used to build the correctly formatted image. Table 4 is a printout of selected portions of RAM showing how the data looks before and after sorting.

C. IMAGE DISPLAY AND PROCESSING

1. Objectives

The previous sections have illustrated the mechanisms involved in transforming the scene information incident on the detectors into digitized data stored in frame buffers in the correct format for display and processing. Once this task is complete, there exist several possible approaches to processing the data, dependent on the perspective of a particular researcher or system user. Working from the premise that anIRSTD is primarily a target detection and tracking device, many common data processing methods, such as the AN/SAR-8 ADM's BNU, are designed to identify regions or values within the data which exceed some predetermined background threshold. In the academic applications envisioned for the NPS-IRSTD, the evaluation of background clutter and noise rejection algorithms is only one of the possible avenues of research. Other areas of interest include:

- Evaluation of the infrared background scene characteristics
- Testing of advanced hardware modifications
- Use as an instructional platform for study of generalIRSTD characteristics, such as optical performance, detector performance, and hardware operations

With these applications in mind, a major objective guiding the development of the imaging system was to create a framework which allows study of the modifications introduced into the data by the system. Implied here is the desirability of eventually removing the system effects to restore the data to the closest possible representation of the actual thermal distribution present in the scene.

TABLE 4

SELECTED RAM LOCATIONS AFTER DMA TRANSFERS AND SORTING

<u>BASE></u> <u>(OFFSET)</u>	<u>SORTED</u>			<u>UNSORTED</u>		
	<u>40000H</u>	<u>50000H</u>	<u>60000H</u>	<u>70000H</u>	<u>80000H</u>	<u>90000H</u>
0	126	130	124	127	126	134
1	126	130	127	0	0	0
2	126	130	127	0	0	0
3	126	130	123	0	0	0
4	127	129	121	0	0	0
5	126	130	124	0	0	0
6	126	130	126	0	0	0
7	126	129	125	126	126	126
8	126	128	124	128	126	127
9	126	128	124	129	130	130
10	126	129	125	126	126	125
11	126	129	125	127	125	126
12	127	129	124	125	125	125
13	127	129	125	0	0	0
14	126	130	127	0	0	0
15	126	131	125	0	0	0
16	126	129	124	0	0	0
17	126	128	126	0	0	0
18	126	128	127	0	0	0
19	126	129	125	126	126	126
20	126	130	124	126	126	126
21	126	129	125	130	130	130
22	126	130	127	126	126	126
23	126	130	126	126	126	126
24	126	131	124	116	114	124
25	126	130	124	0	0	0
26	126	129	126	0	0	0
27	126	129	126	0	0	0
28	126	129	124	0	0	0
29	127	129	124	0	0	0
30	126	129	126	0	0	0
31	126	130	127	127	126	126
32	126	129	125	126	126	126
33	126	128	125	130	130	131
34	126	129	127	126	128	127
35	126	130	128	126	125	126
36	126	131	126	0	0	0
37	127	130	124	0	0	0
38	127	129	127	0	0	0
39	126	129	128	0	0	0
40	126	129	127	0	0	0
41	126	130	126	0	0	0
42	127	129	127	0	0	0

Essential to success in achieving this goal is the effective presentation on the display of the features determined to be of particular interest.

Satisfactory accomplishment of these tasks will allow pursuit of other aspects of the analysis with greater confidence in the nature and reliability of the data. Removing the system's influence would render the data, and any results obtained from its analysis, more valuable to researchers working on other studies related to thermal imaging or detection processes.

2. Techniques and Applications

Once the task of filling the frame buffers with data is complete, display of the data stored in a frame buffer on the video monitor is controlled by values written to various read/write registers on the DT2861 which are addressed through I/O locations. However, the register level operations are transparent to the system user when DT-IRIS subroutines are used. These subroutines use standard FORTRAN parameter format to pass arguments between the main program and the subroutine. DT-IRIS documentation for each subroutine lists the required and optional parameters with the appropriate data type and value range to make application in programming generally straightforward.

Two programs have been written, BEGIN and IMAGE, which utilize the DT-IRIS subroutines to provide control over a variety of image processing functions. The commented source code for these programs is provided as Appendix C. The remainder of this section is intended to amplify some of the more significant features designed into these programs.

BEGIN was principally designed for use in setting display color characteristics controlled through output lookup tables. The program begins by setting the DT2861 into display mode and selecting frame buffer 0 as the buffer for display. Additional operations are selected from a menu which includes:

- Create color scales for frame buffers 0 and 1
- Change output lookup tables 2-7 (Gaussian)
- Change output lookup tables 2-7 (Linear)
- Clear a designated frame buffer

- View a designated frame buffer .

Since the 90 individual detector channels, expanded to five rows each, utilize only 450 of the 480 rows displayed on the screen, the remaining 30 rows are used to form an on-screen, full-time color/gray scale reference. These rows are filled, in two column pairs, with increasing values from left to right, such that columns 0 and 1 contain the value 0 while columns 510 and 511 contain the value of 255. The values in a given region are then identified using DT-IRIS graphic overlay capability to print the corresponding numeric value onto the screen. The intent of this scheme is to provide an instant reference of the value represented by any pixel in the display.

As introduced in section III.B.2.c, the color displayed by any given pixel is the result of mixing the relative brightness of the red, green, and blue values assigned in the active output lookup table for the data value represented by the pixel. The DT2861 has eight output lookup tables numbered from 0 to 7, all of which are initialized automatically the first time a DT-IRIS program is run. However, any of these buffers may be modified in any manner by the user using DT-IRIS subroutines. The two choices on the menu in BEGIN provide two different methods for reassigning the characteristics of any of the two output lookup tables 2-7. A strong factor in the design of the output lookup table changing routines was the desirability of being able to define all the values in the table with a minimum number of parameters. Output lookup tables 0 and 1 are purposely excluded from changes because of their general applicability as monotonically increasing and decreasing gray scales respectively.

Two terms are important when discussing assignment of values to lookup tables: the index and the value. The index refers to the data value the pixel will be representing, while the value is the relative brightness to be associated with that index. In the "Gaussian" option, values are assigned relative to their relationship to a designated mean index. The mean index is assigned a brightness value of 255, and values fall off to either side according to the input standard deviation. In the "Linear" option, each color scale is computed from two lines connecting three points designated by index and value. Figure 13 shows the resulting lookup table

assignments for the case of a gaussian with red(mean=255,standard deviation=80), green(mean=128, standard deviation=80) and blue(mean=40, standard deviation=60). Figure 13 also shows a linear set with red(low index=100, low value=0, middle index=255, middle value= 255, high index=255, high value=255), green(low index=90, low value=0, middle index=130, middle value= 255, high index=170, high value=0), and blue(low index=0, low value=30, middle index=100, middle value= 255, high index=150, high value=0).

The majority of the control over image display and processing has been built into the IMAGE program. The routines in this program are those which directly apply to the display and processing on a particular image. Again, when this program is run the user is provided with a menu of options, which in this case include:

- Select the frame buffer to display
- Select the desired output lookup table
- Make a 6° image in buffer 2
- Correct an image for detector responsivity differences
- Fill in the lines on the display corresponding to bad detectors
- Apply MTF corrections
- Smooth out the vertical 1 detector to 5 row expansion
- Store a frame to a file
- Retrieve a frame from a file
- copy one frame from another
- Subtract one frame from another

The first two choices here simply allow the user to view any of the sixteen frame buffers using any of the output lookup tables.

a. Make a 6° Image in Buffer 2

The third option, make a 6° image in buffer 2, horizontally compresses the data which has been written into buffers 0 and 1, which after a normal DMA transfer sequence will consist of two adjacent 3° images, into a single image and places the result into buffer 2. This is accomplished using the

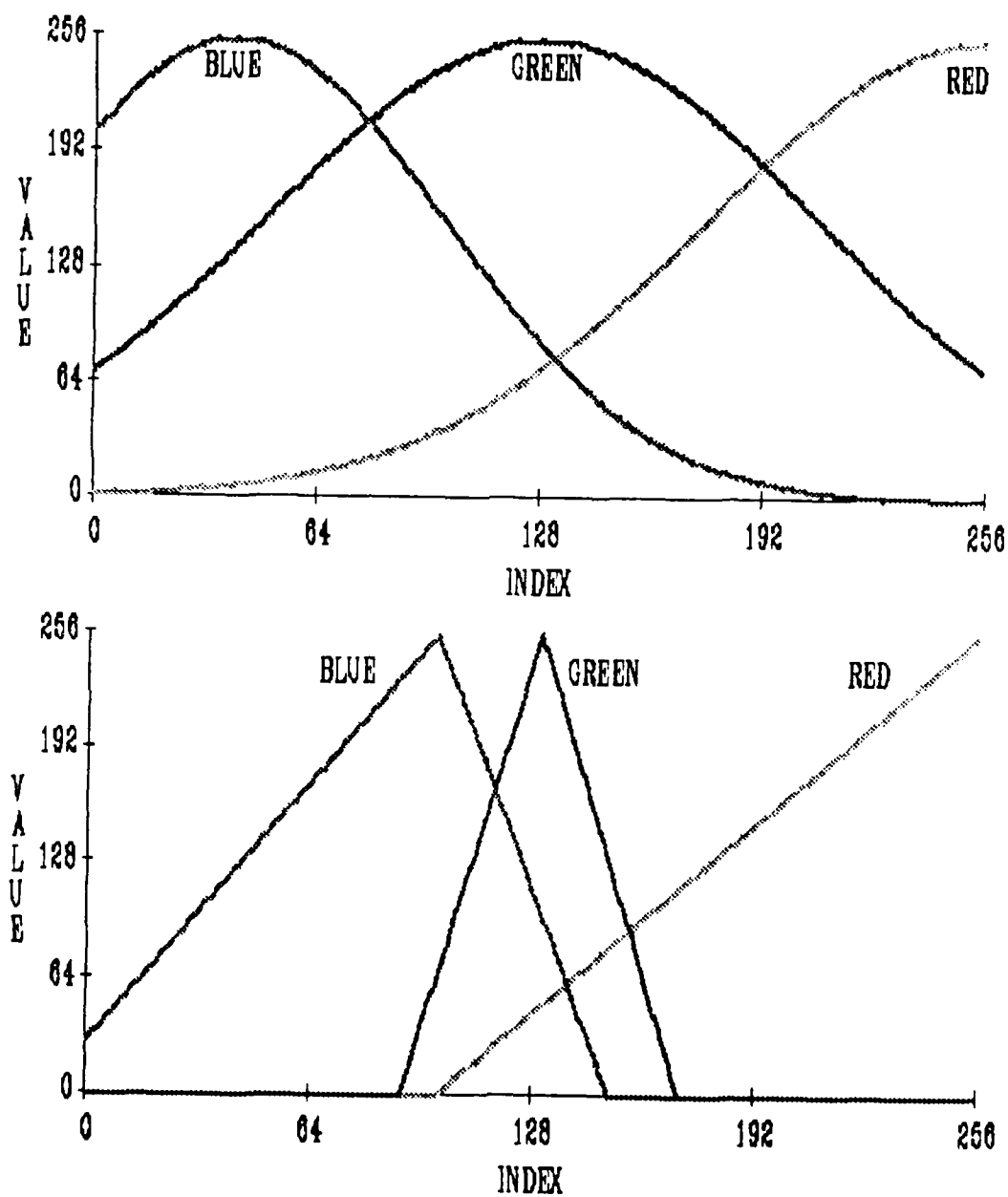


Figure 13 Output Lookup Table Assignments. (Top) Gaussian.
(Bottom) Linear.

characteristic array processing features of the DT2861 by dividing all the values in frame 0 by 2 and placing the result in frame 2 and dividing all the values in frame 1 by 2 and placing the result in frame 3 using a single call to the DT-IRIS routine ISDIVC for each frame. Then within each row each adjacent even/odd column pair are added together to form a row of 128 data values. The resulting row of 128 from buffer 2 is written to the left side of buffer 2, while the row of 128 from buffer 3 is written to the right side.

b. Responsivity Correction and Row Filling

In thermal imaging or thermal detection systems variations in the response characteristics of the detectors are expected, including a percentage of detectors which fail completely. The fourth and fifth choices on the IMAGE menu address these deficiencies for the output of the characteristics of the NPS-IRSTD. Using the calibration values determined by Ayers [Ref. 1], all detector values are adjusted based on the given deviation of the response values from the mean response of the detector array. To prevent dead detectors from biasing this process, they are assigned a response value equal to the mean response value. The dead detectors may be masked by using the routine called by the fifth menu choice which simply fills the corresponding rows with values interpolated between the row above and the row below the dead detector.

c. MTF Corrections

The MTF routines are designed to operate on the data in such a way as to remove particular aspects of the system transfer functions from the image. Specific routines have been developed for the x-direction detector scan deconvolution, the x-direction optical effects and the y-direction optical effects. No y-direction detector array function was included because the first zero of this function lies at a spatial frequency approximately equal to the minimum spatial frequency in the image. Additionally, most of the other frequencies in the y-direction detector function are so close to zero that dividing by them for deconvolution would unreasonably amplify small fluctuations in the scene.

The corrections are accomplished through application of the convolution theorem, which allows the system function to be simply divided out from the data in spatial frequency coordinates. The frequency spectrum of the image is computed by extracting a row (or column) of data, and applying the FFT using FORTRAN subroutines which were written by NPS Professor E. A. Milne. According to LLoyd [Ref. 9] and others, the x-direction detector function may be computed from the Fourier transform of the function representing the detector shape, which in the one-dimensional analysis of a rectangular detector produces a transfer function of $\text{Sinc}(\alpha f_x)$, where α is the width of the detector. The x-direction and y-direction optical functions are derived from Gaussian approximations to the MTF curves shown in Parker's thesis [Ref. 2]. Thus,

$$MTF = e^{-f^2 / 2\sigma^2}$$

where f is the spatial frequency, and σ^2 is the variance. The curve fit was established by calculating the variance such that the modulation value computed with the resulting Gaussian equation for the highest frequency present in the transfer array matched the corresponding modulation value from the curves.

Here again, the program design is aimed toward investigating the effects of changes in simple system parameters without major system changes. To look at other system functions, the MTF array may be changed by changing the defining parameter in the given equation, changing the form of the equation completely, or with a bit more effort by assigning the transfer properties of each spatial frequency specifically in a data array.

IV. RESULTS

A. GENERAL

This project provided a unique overall performance measure in the form of the images it produces. Measured by this standard the system provides good results; it correctly and efficiently receives and sorts the data and displays images which distinctly show recognizable and identifiable features present in the scanned scene. In addition, the value of the image processing capabilities which can enhance features deemed to be of particular interest or which can be used to study general operational characteristics of the NPS-IRSTD may be readily appreciated from the results of the preliminary usage accomplished to date.

Having overviewed the positive accomplishments, it seems best now to turn attention towards those aspects which did not fully meet all the standards or capabilities envisioned for the system while it was in the design stage. This section is intended to provide the basis for making the modifications which will undoubtedly improve the systems performance and utility. These topics can be divided into the following categories:

- Data transfers
- Image processing program performance
- Output image quality and usefulness

B. DATA TRANSFERS

As detailed in section III.B.3, the DMA transfer provided the most direct and efficient method of making data available for display without engineering a completely new interface device. The DMA process does effectively accomplish the role it was envisioned to fulfill, however it does so at a maximum rate that is inexplicably slow. The current DMA transfer rate is only 67,500 bytes/sec. Attempts to play back the data at twice this rate (135,000 bytes/sec) result in the corruption of the computer RAM in the region where the DMA transfers are

assigned. The subsequent use of the sorting routine to read data and move it about results in the computer processor detecting this corruption and crashing the system.

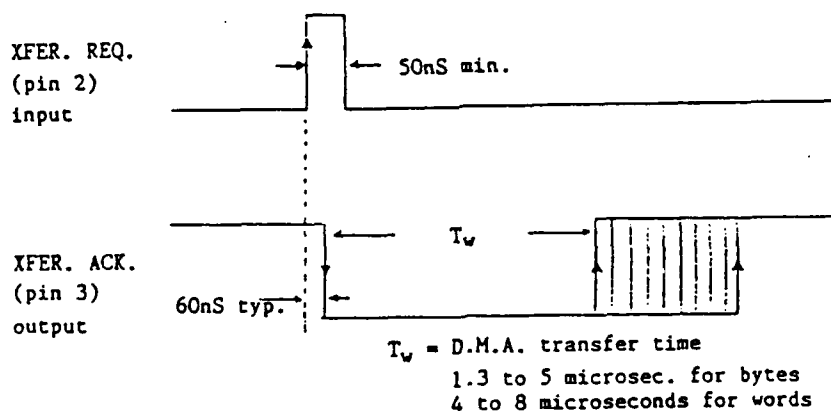
One additional idiosyncrasy superimposed onto this scenario is the apparent discrepancy between the I/O board documentation's description of the handshaking protocol expected by the DMA controller and the arrangement which works in practice. The top diagram in Figure 14 shows the handshake as depicted in the PDMA-16 manual. From this one would expect to find optimal performance with the data changes furthest away from the rising edge of the clock pulse as represented by the center diagram of Figure 14. However, trying to operate the system in this manner causes the type of crashes previously described to occur. Operating the system as depicted by the bottom diagram of Figure 14, where data signal changes take place immediately after clock changes, is the only way found to make the system work.

Another characteristic feature of the transfer process is the intermittent introduction of an extra byte into the data stream such that one cycle through the A/D converters contains thirteen bytes instead of the necessary twelve. This has the unfortunate effect of fouling the sorting process for all the subsequent bytes in that transfer. Such an event produces a blank band in the image and shifts the remaining parts of the image out of position as seen in Figure 15.

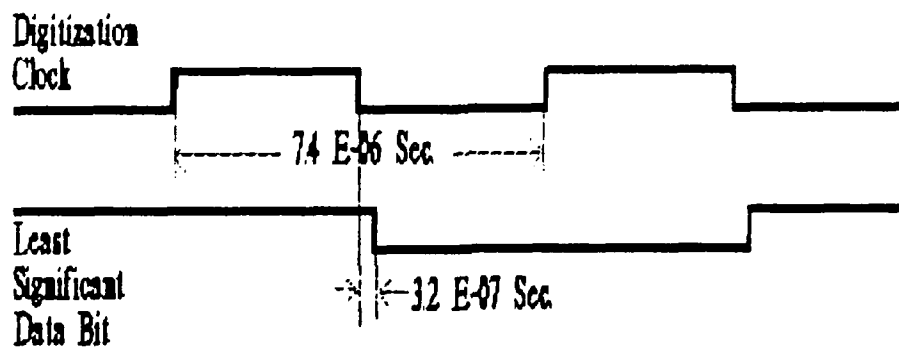
This type of image corruption takes place frequently enough to be annoying, but not so often as to render the system unusable. The cause may be as simple as noise being introduced on the clock line by signals propagating in the data lines of the ribbon cable connected to the PDMA-16. Cutting the length of this ribbon cable which connects to the I/O board seemed to reduce the error rate noticeably, and changing to a shielded coaxial cable may solve the problem altogether.

C. IMAGE PROCESSING PROGRAM PERFORMANCE

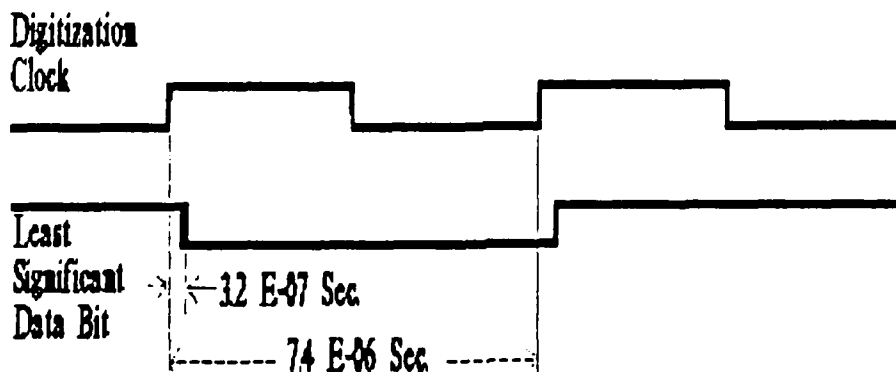
Because the majority of the routines in the image processing programs BEGIN and IMAGE are direct applications of the DT-IRIS subroutines, the overall performance can be summed up by saying that almost everything works as designed.



PDMA-16 HANDSHAKING PROTOCOL



EXPECTED PHASE RELATIONSHIP



FUNCTIONAL PHASE RELATIONSHIP

Figure 14 PDMA-16 Handshaking Protocol.
(Top) PDMA-16. (Center) Expected Synchronization.
(Bottom) Functional Synchronization.

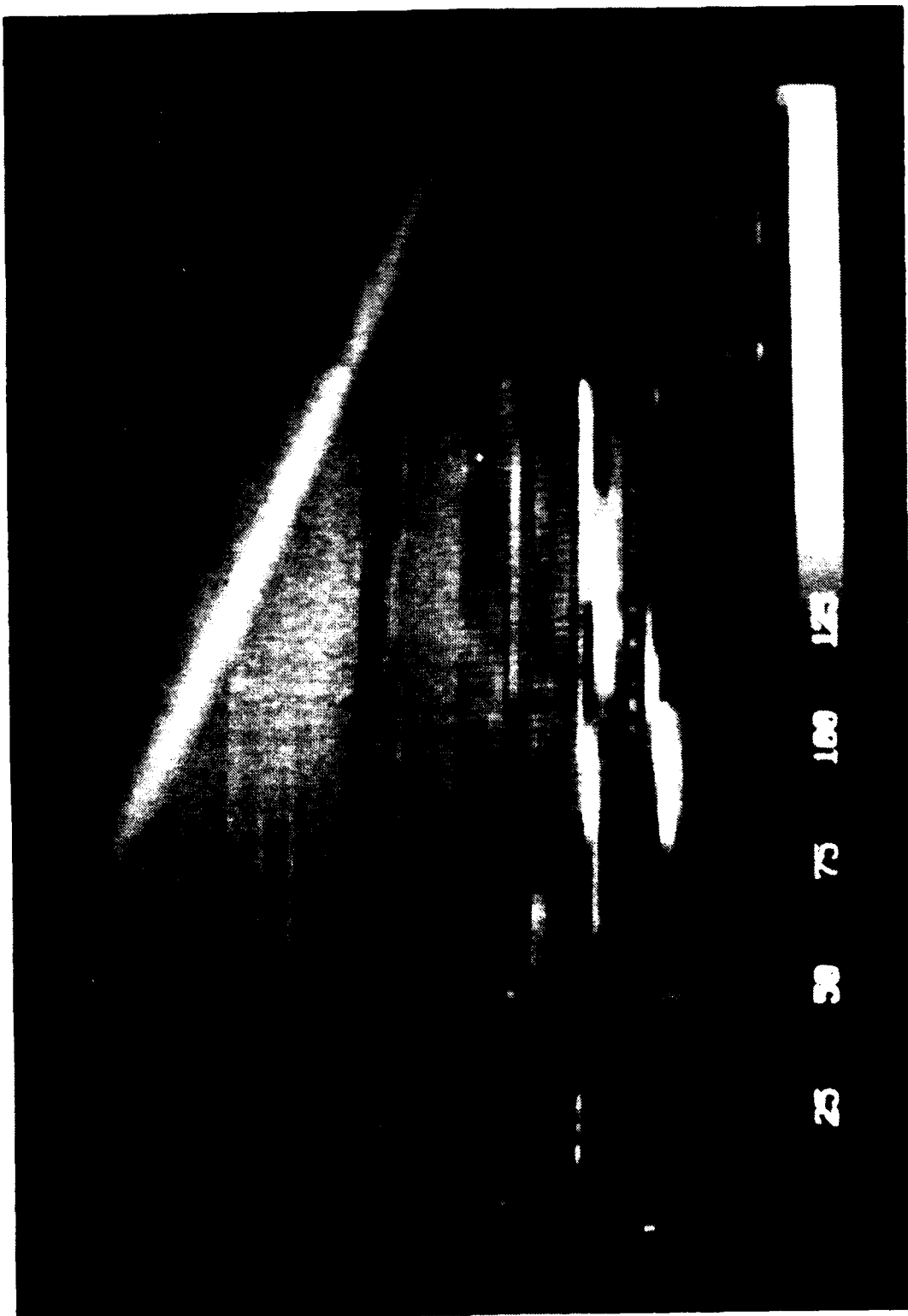


Figure 15 Image Resulting from a Bad DMA Transfer

However, there are several problems which were not anticipated which diminish the overall quality of the final product.

First and most irritating of the problems resulted from an unnoticed design characteristic built into the DT2861. While the DT2861 has 16 frame buffers, its address bus is only designed to address any two at a time. Thus when certain types of operations are performed in the IMAGE program, such as reading an image from a data file, upon completion of this process the address bus remains pointed to this particular buffer. If the IMAGE program is terminated at this point and the DMA transfer program is run, the transfer will proceed to write the data to the last used buffer instead of buffer 0 as designed. When such a problem occurs, the quickest and most reliable method of resetting the bus to direct DMA transfers correctly to frame buffers 0 and 1 is to use the BEGIN program routine to rewrite the color scales on the bottom of these buffers.

The other problem which relates to the DT-IRIS functions is an apparent flaw in the operation of the ISPUTP subroutine, the routine which is used to write data values directly to one or more consecutive pixels in a designated frame buffer. When ISPUTP is used to write more than one pixel, it seems to write meaningless values to the next two consecutive data locations. This only becomes a problem when a program, such as the smoothing routine in IMAGE, needs to read and use values from locations just written to by ISPUTP.

The remaining program performance comments relate to the MTF routines in the IMAGE program. These programs are not inherent functions of the DT2861, DT-IRIS system but instead only use DT-IRIS to access the data present in the image. As presently designed the MTF routines are subject to:

- Execution times which are noticeably longer than the other processing procedures
- Effects at the edges of the image due to the continuous data assumption of the FFT subroutine
- Modulation effects which raise the data values in regions containing high spatial frequency components above the maximum allowed value of 255 in an 8-bit byte storage location

The speed of execution issue is not unexpected considering the number of mathematical calculations and data transfers which must be performed. In fact, anyone familiar with performing transform calculations on older, slower computers may be initially impressed by how rapidly the entire process can be accomplished. X-direction MTFs complete in approximately a minute, but Y-direction MTFs take around fifteen minutes. The reason for the difference is twofold. The first reason is that there are only 90 rows to be processed in the X-direction case, while there are 512 columns in the Y-direction. Secondly, the routine to extract data ISGETP can be used to retrieve a full row with a single call, while 90 calls are necessary to get the data for a column. One positive aspect worth mentioning at this point is that at the current speeds of operation, the user can see the results of the transform process as it works its way through the image.

The edge effects noted in item two of the list pose one of the most interesting problems to anyone trying to remove the system's influence from the data. A common approach to dealing with this artificial discontinuity is to apply a data conditioning algorithm to either partially or completely remove it. Two examples of this type of processing, Hamming and Hanning, are contained in the last two subroutines on the IMAGE listing in Appendix C. When considering whether or not to implement one of these routines the issue arises on whether or not the cost of modifications done on the data by the conditioning algorithm is covered by the benefits gained through reducing the artificial high frequency characteristics of the edges.

A preliminary application of the Hamming routine while the data was in its original form, unscaled and with no "DC offset" removal, damped out all the image data except for the center third of the screen. This effect is demonstrated in Figure 16 where the original signal is a cosine wave with a period of 51.2 points (10 cycles/ 512 points), while the lower shows the signal after modification by the HAMMING routine.

The last issue listed, modulation effects at high frequency content edges, is the result of the limitations imposed by the 8-bit byte storage format. Often in the images, the edge between a "hot" object and the background is quite sharp. This

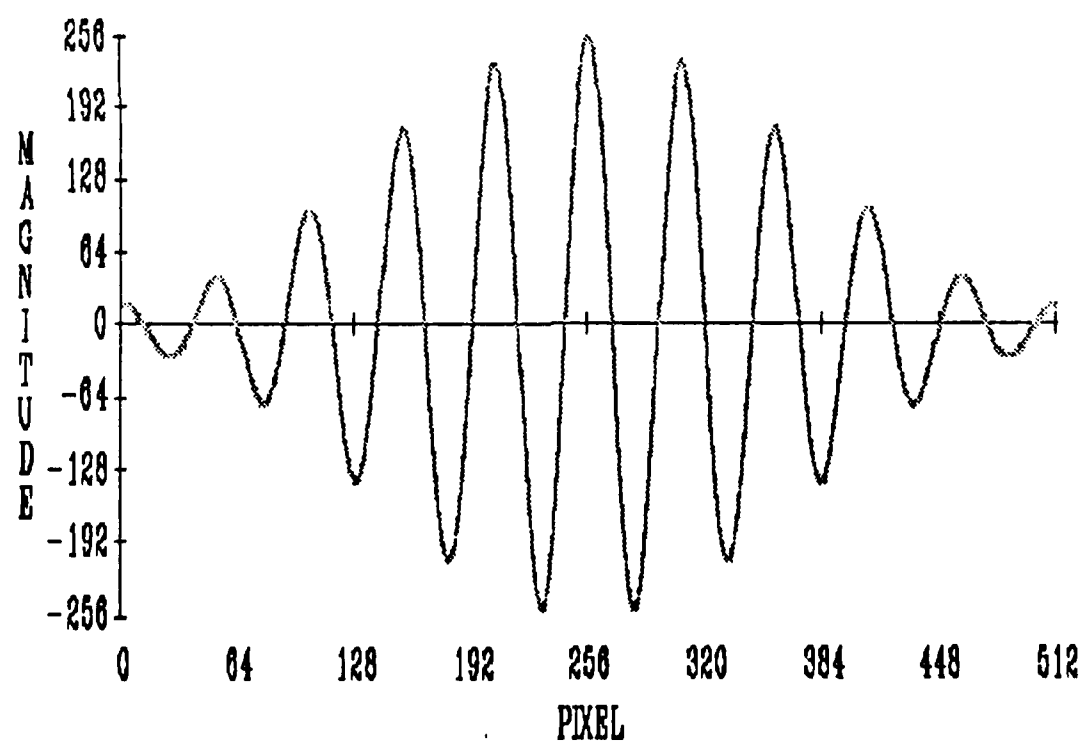
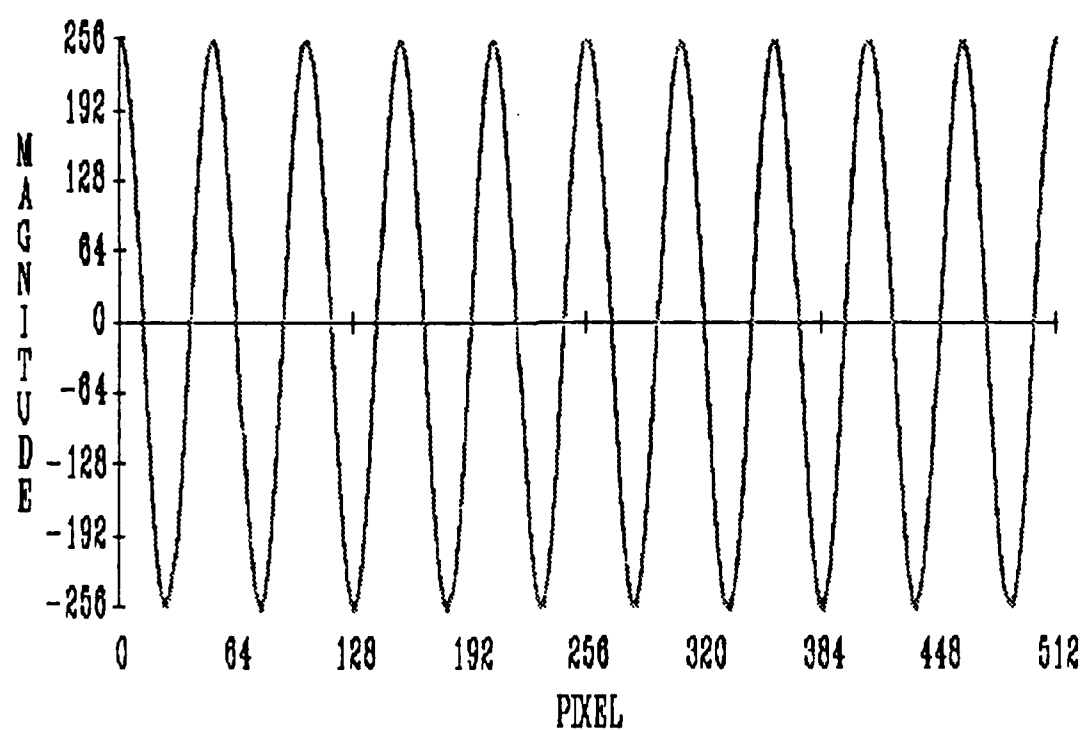


Figure 16 The Effect of Hamming on a Cosine Wave Signal

region of rapid transition to values which peak (and periodically clip) at 255 is also the type of region which will be most strongly affected by removing the system function because the process involves division by the small fractional values associated with the higher spatial frequencies. The question then arises whether to develop a method to normalize the entire scene based on the maximum value after the deconvolution or to simply assign 255 to all data which exceed this value as the result of processing.

The final topic of this chapter, image quality and usefulness, is best addressed by showing images and explaining what aspect of system performance each portrays. The images in Figures 17 through 35 are photographs of the framegrabber display taken with a 35 mm camera with a standard 50 mm lens at about two feet distance, using a 1/60 second shutter speed and an f/# 2 setting for ASA 125 black and white film. The diagonal streaks in the images are artifacts of the photographic process; probably reflections off the display face.

For the display of all infrared scenes the framegrabber was controlled by an output lookup table designed to show more detail in the 100 to 150 value range than the standard monotonically increasing scale, unless otherwise noted. The scale was created using the linear color table routine in the BEGIN program setting all colors with the set of points (80,0), (180,255), (255,255).

The following list contains the important data concerning each of the images and describes the features worth noting:

- Figure 17 is a 3° wide image showing an antenna which is located near the southwest corner of the roof area supporting the scanner assembly. This antenna is labelled "A" in the photograph displayed in Figure 18. This antenna does not have the double armed feature that it appears to have in this image. This object doubling is evident in a number of the other images and the exact cause has prompted much speculation.
- Figure 19 is the adjacent 3° region to the one shown in Figure 17 and was created as the second frame in the same DMA transfer set. The prominent object in this image is the crane which is labelled "B" in Figure 18.
- Figure 20 is the result of using the routine to combine the two 3° images into one 6° image within the IMAGE program. Note the difference in appearance as the horizontal dimension is now less distorted in scale relative to the vertical dimension.

- Figure 21 is another 6° image, this one for the area adjacent to that shown in Figure 20. The prominent object here is an antenna (also seen in Figure 22, labelled with an "A") used by the Electrical and Computer Engineering department in basic radar laboratory work. The double image is again apparent. Also, the broad vertical band structure seen in all the images so far is the image of four tall poles attached to a pallet that was sitting in the middle of the roof area close enough to the scanner assembly to be badly out of focus. These poles can also be seen in Figure 18.
- Figures 23 through 26 are a set of images similar in format to the set of images 17, 19, 21 and 22. The area of view for this set is around the highest part of the roof of Hermann Hall above its main entrance. Figure 27 is a photograph of this area provided for comparison. Figures 23 and 24 are 3° images, while Figures 25 and 26 are 6° . An observation worth noting at this point is the doubling of images regarding the antennas on the top of the roof. There are only two antennas, not the four apparent in the image. At this point it is worth suspending the listing to discuss the image doubling feature briefly.

Careful observation of the doubling feature shows it to be range dependent. Of the three objects where image doubling is most evident, the antenna in Figure 17 is the closest object to the scanner, the antenna in Figure 21 is slightly more distant, and the roof of Hermann Hall is significantly farther away than either of these. Measuring the distance between the object and its double (being careful to remember that Figure 21 is a 6° image) shows that the separation decreases with range. One of the leading contenders among possible explanations of this phenomenon is the telescope focus, and can be understood by referencing the diagrams in Figure 28 which have been taken from [Refs. 1, 2 and 4]. The two diagrams at the top of this figure are energy distribution representations of a point source imaged onto the focal plane. The size of these spots as calculated by the Super-Oslo software is less than the detector size of 0.02" by 0.003". The figure at the bottom is representative of the findings when the telescope is out of focus. Note the relationship of the spot size to the detector size, and how the detector support stalk shadow produces two horizontally separated regions of the spot image. It is possible, if the out of focus condition exists, that the image doubling results from the splitting of a single point into the two sides of its corresponding spot in the image plane.

Now to return to the description of the images:

- Figure 29 is the result of bringing the images seen in Figures 25 and 26 into a 12° image. The intent of this image is to give a perspective on how things look when the horizontal and vertical dimensions are brought into proper scale.
- Figures 30 and 31 are the same image as seen in Figure 21, displayed using different output lookup tables. Figure 30 uses the standard monotonically increasing gray scale while Figure 31 uses a monotonically decreasing gray scale. The intent here is to attempt to give the reader an impression of the significance of the choice of output lookup tables. It is unfortunate that presentation of some color output lookup tables is not possible in the thesis format, because the effect color adds is quite striking. I believe it is a reasonable assessment to say that proper design of output lookup tables is the most significant factor in optimizing the display to bring out particular scene features or characteristics.

The remaining figures all attempt to relate the effect of some particular type of image processing. A number of the images may appear to be essentially identical, because of the minimal effect of the image processing operation through which they have passed. Reproduction of the photographs in the printing process may even degrade image quality to the point where there is no discernable difference between certain images which do show slight differences on the display. This points out the fact that certain processing operations may prove to be of little or no real value after they have been thoroughly evaluated. Again resuming the description of the images:

- Figure 32, the same basic image as Figure 19, has been corrected only for variations in response between detectors. Application of this routine actually seems to make the presence of the individual detectors slightly more noticeable, instead of balancing them as was hoped. This may be due to any number of factors including the time elapsed since the calibration data has been taken or possibly the fact that installation on the roof and the passing of the data all the way through the system creates effects not present when the detector outputs were measured directly from a breakout box.
- Figure 33 is the result obtained when the bad detector lines have been filled in by linear interpolation. Note that the simplistic gradient calculation produces some truly undesirable effects at the edges of tilted or horizontal objects, such as has occurred to the crane in this image.
- Figure 34 is the result of performing the deconvolution only for the detector shape in the x-direction. The most noticeable effects from this routine were apparently the result of the discontinuity at the outside edges of the image, which are not real or desired.

- Figure 35 is the result of only deconvolving the x-direction optical effects. Here again this particular process had little impact on image appearance.
- Figure 36 shows the appearance after just the smoothing routine has been performed.
- Figure 37 shows the image after all the various processes have been performed.
- Figure 38 shows a side by side comparison of images, the left side after being processed with all the possible routines and the right with no processing done, put together by the combining routine in IMAGE.
- Figure 39 is also an image on which all the various processes have been performed. This is a 12° image of the Monterey hillside which has the Sheraton Hotel at the bottom and the Presidio at the top. No positive identification of an object has been made, however the prominent vertical line in the center may be Franklin street, which can also be seen in the photograph in Figure 40.
- Figure 41 is the same image without any processing. There is distinctly a difference between the two, but it appears debatable as to which is the better.

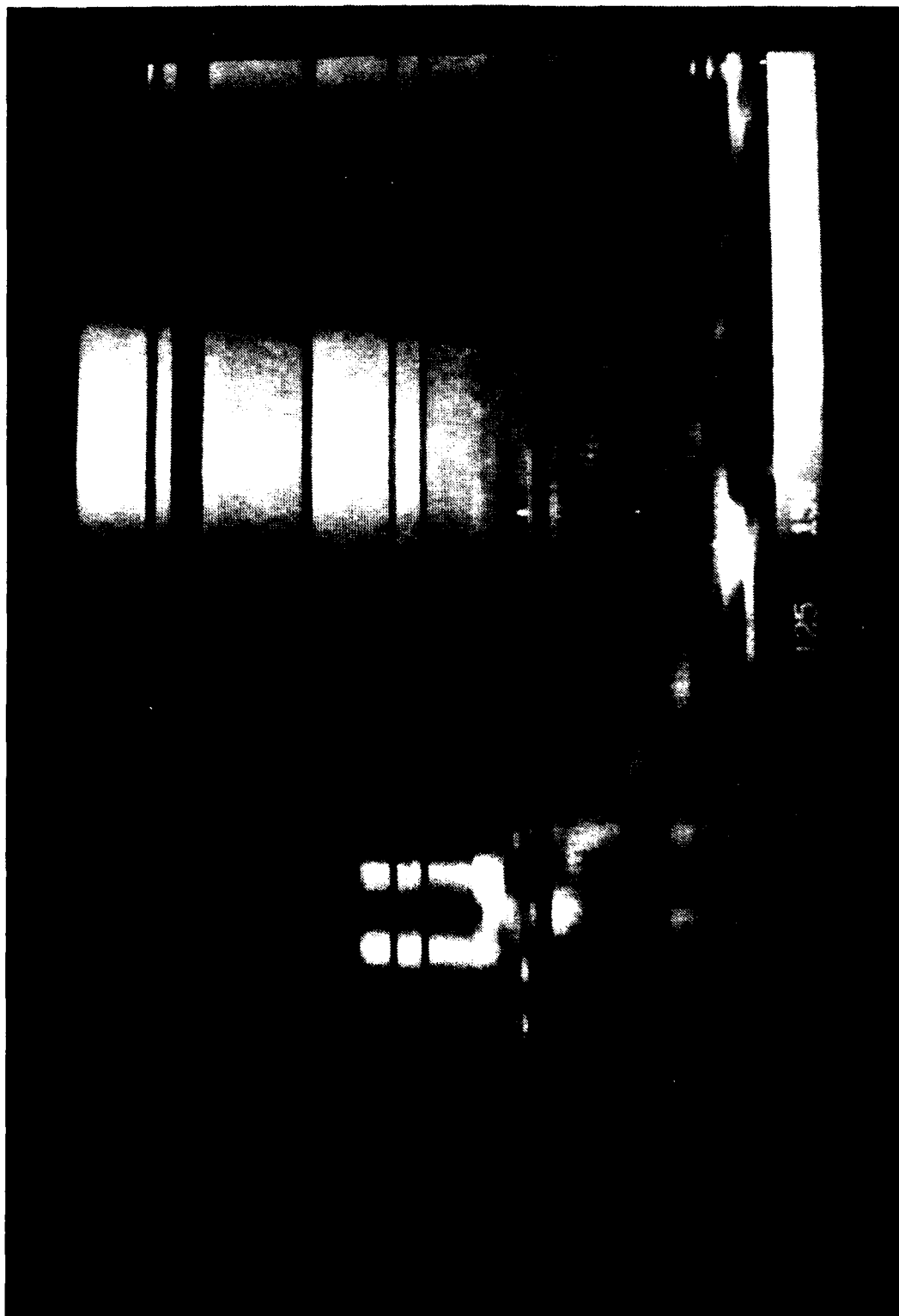


Figure 17 NPS-IRSTD Image (3° Wide) of an Antenna on Spanagel Hall



Figure 18 Photograph the Roof of Spanagel Hall Showing the Antenna
in Figure 17 and the Crane in Figure 19



Figure 19 NPS-IRSTD Image (3° Wide) Showing a Crane on Spanagel Hall

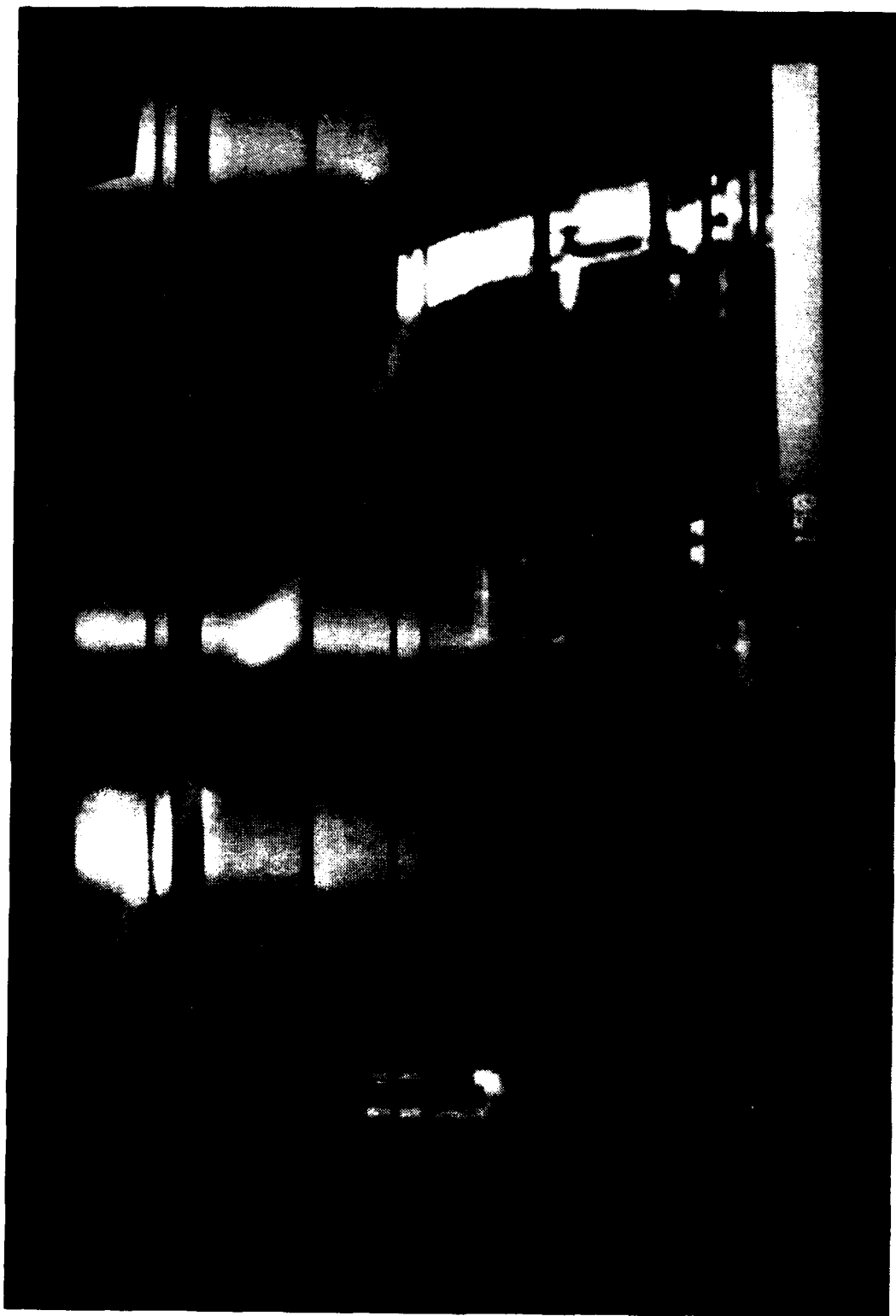


Figure 20 NPS-IRSTD Image (6° Wide) Combining Figures 17 & 19



Figure 21 NPS-IRSTD Image (6° Wide) Showing the Radar Lab Antenna on Spanagel Hall

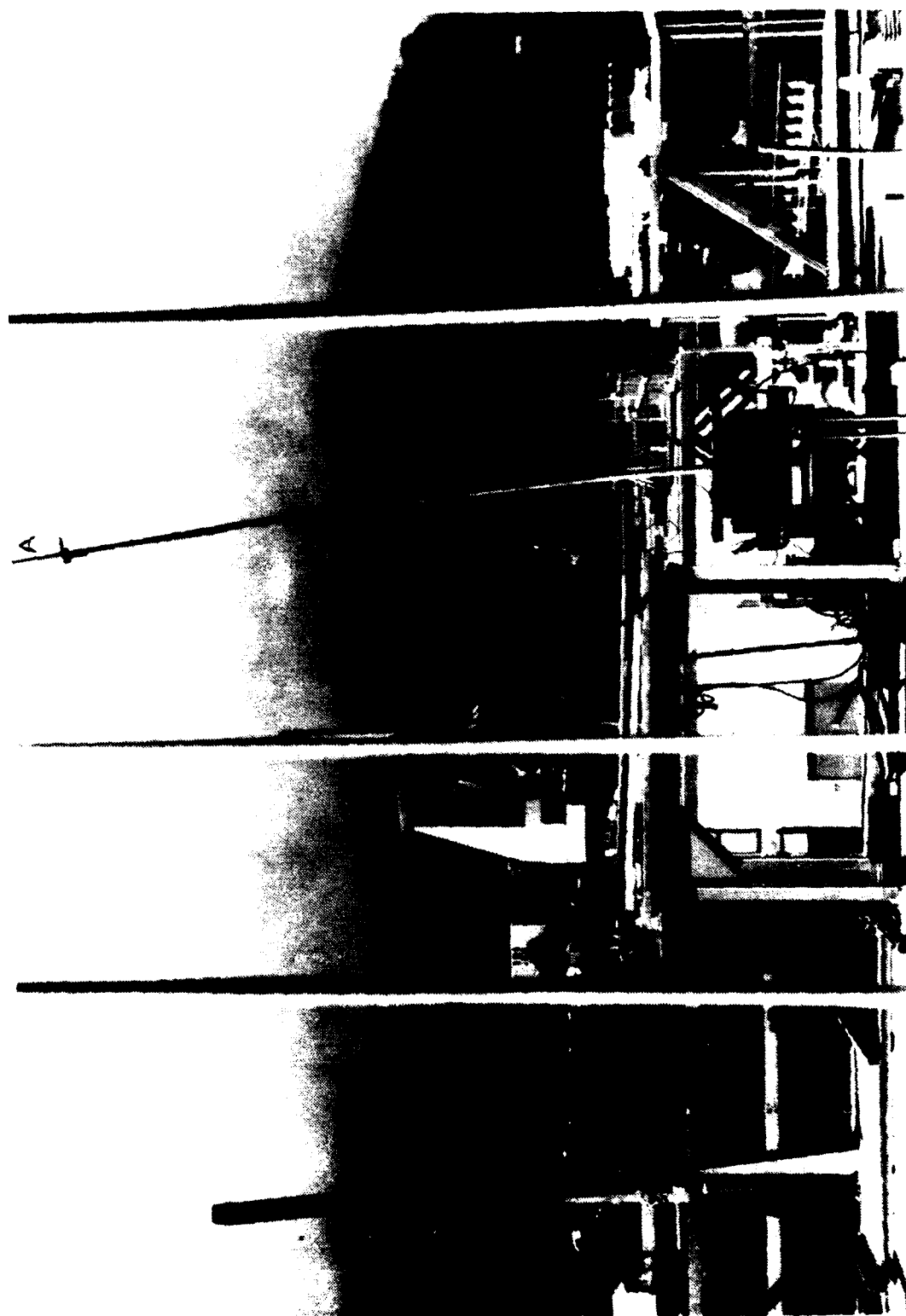


Figure 22 Photograph Showing the Radar Lab Antenna

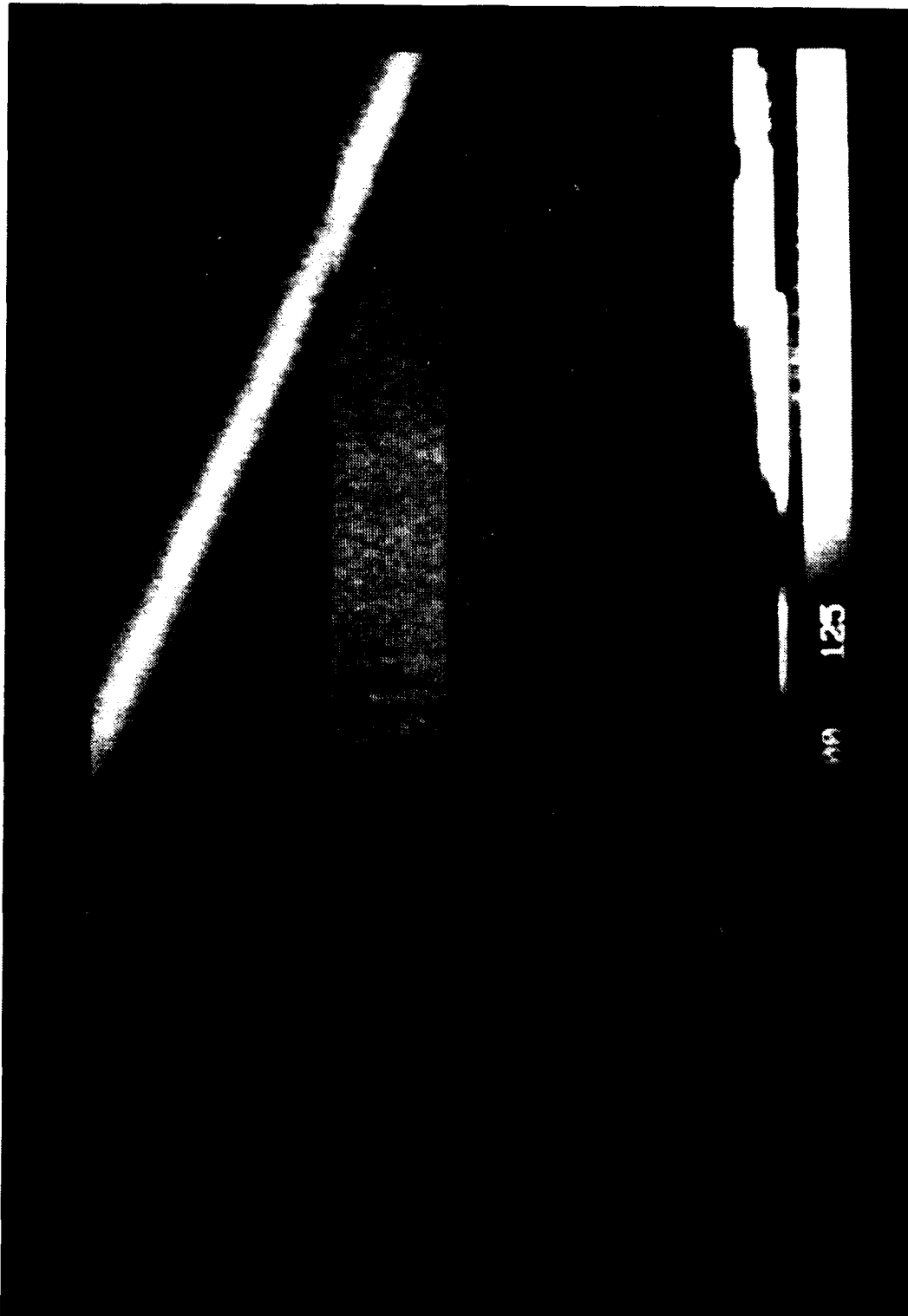


Figure 23 NPS-IRSTD Image (3° Wide) Part of the Roof of Hermann Hall is Visible in the Lower Right Corner

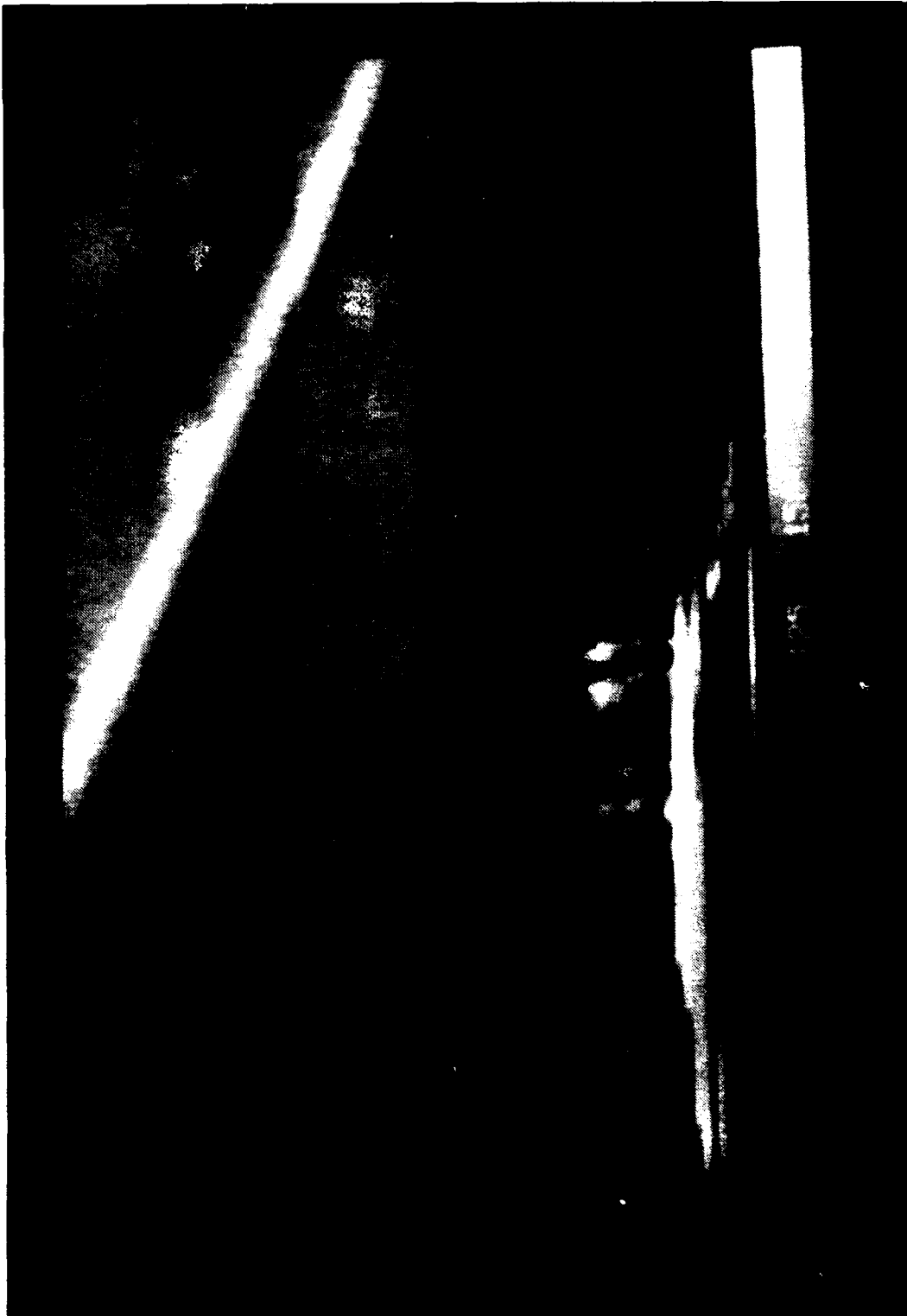


Figure 24 NPS-IRSTD Image (3° Wide) Showing the Roof of Hermann Hall



Figure 25 NPS-IRSTD Image (6° Wide) Combining Figures 23 & 24

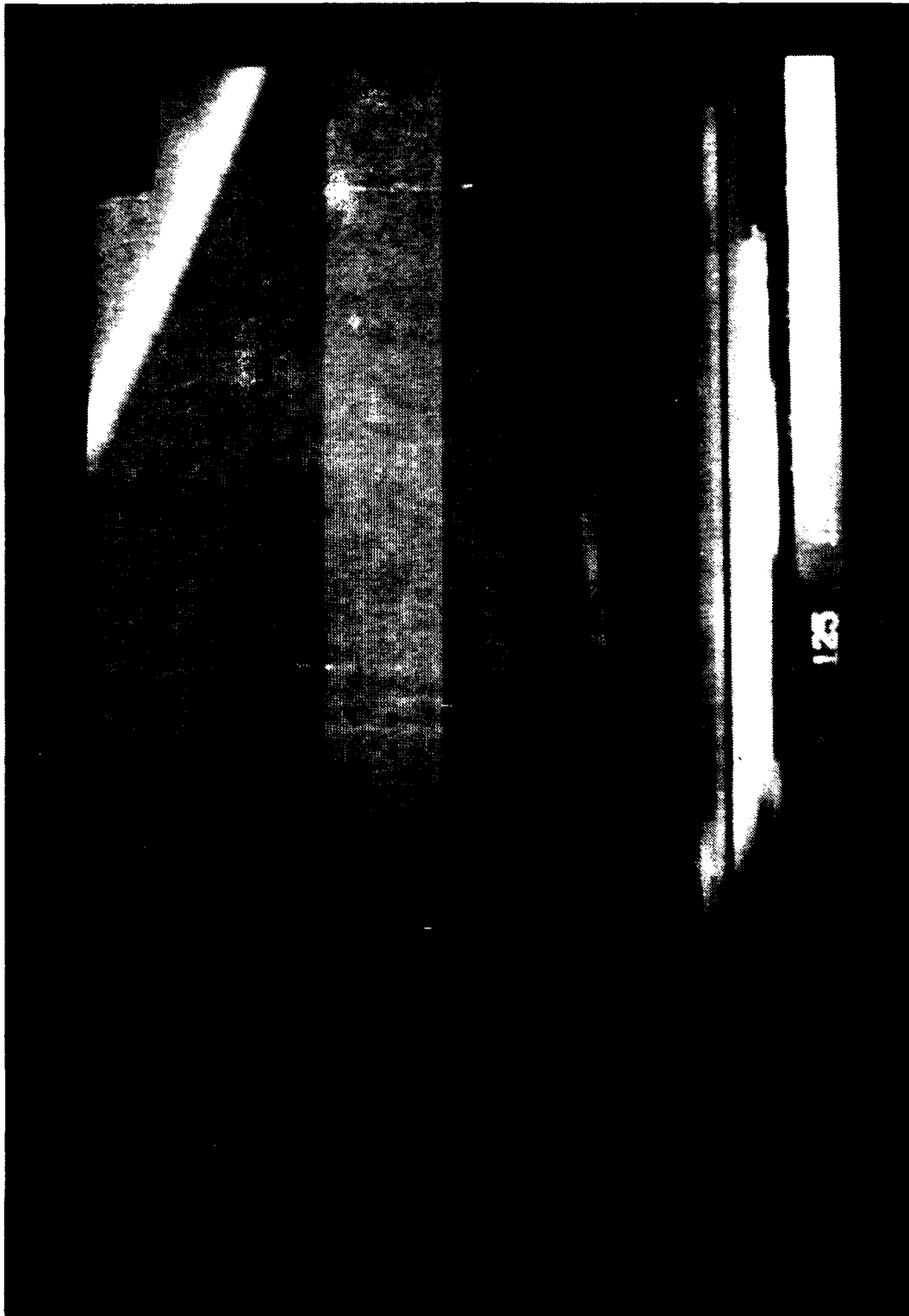


Figure 26 NPS-IRSTD Image (6° Wide) of the Bay Visible to the Right of Hermann Hall

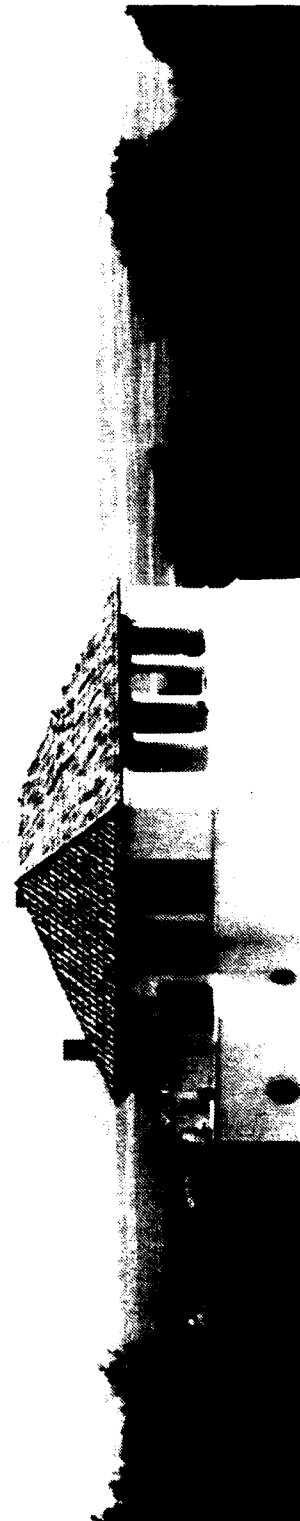


Figure 27 Photograph of the Roof of Hermann Hall

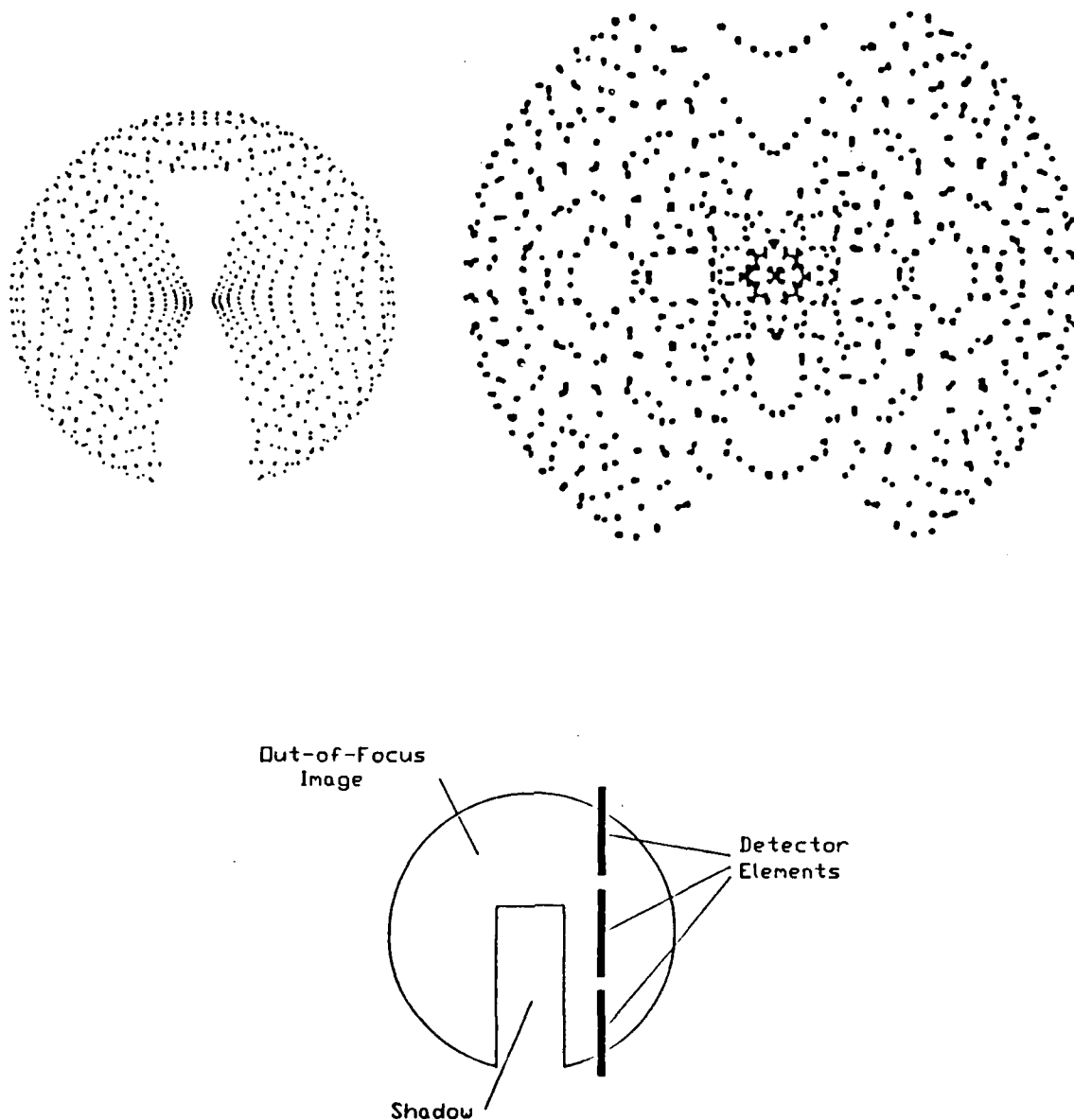


Figure 28 Diagrams Representing a Point Source Imaged on the Focal Plane.
 (Upper Left) Original AN/SAR-8, Spot Diameter is 0.0009".
 (Upper Right) NPS-IRSTD, Spot Diameter is 0.0016".
 (Bottom) Out Of Focus Condition, Detector Size is 0.02" by 0.003".

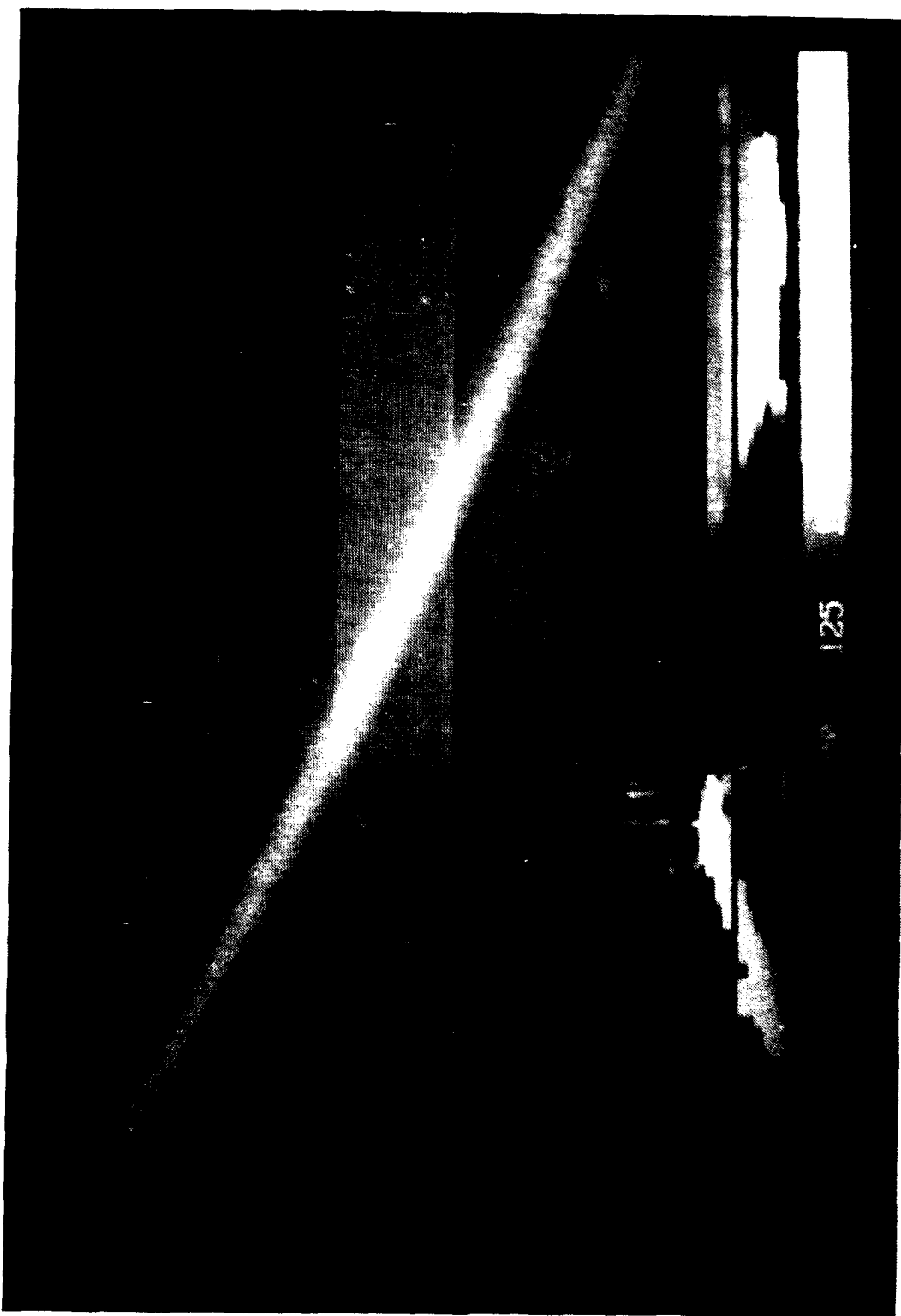


Figure 29 NPS-IRSTD Image (12° Wide) Showing the Roof of Hermann Hall



Figure 30 NPS-IRSTD Image (3° Wide) with the Monotonically Increasing Lookup Table Active



Figure 31 NPS-IRSTD Image (3' Wide) with the Monotonically Decreasing
Lookup Table Active



Figure 32 NPS-IRSTD Image (3° Wide) Corrected for Detector Response Differences



Figure 33 NPS-IRSTD Image (3° Wide) with Rows for Bad Detectors Filled

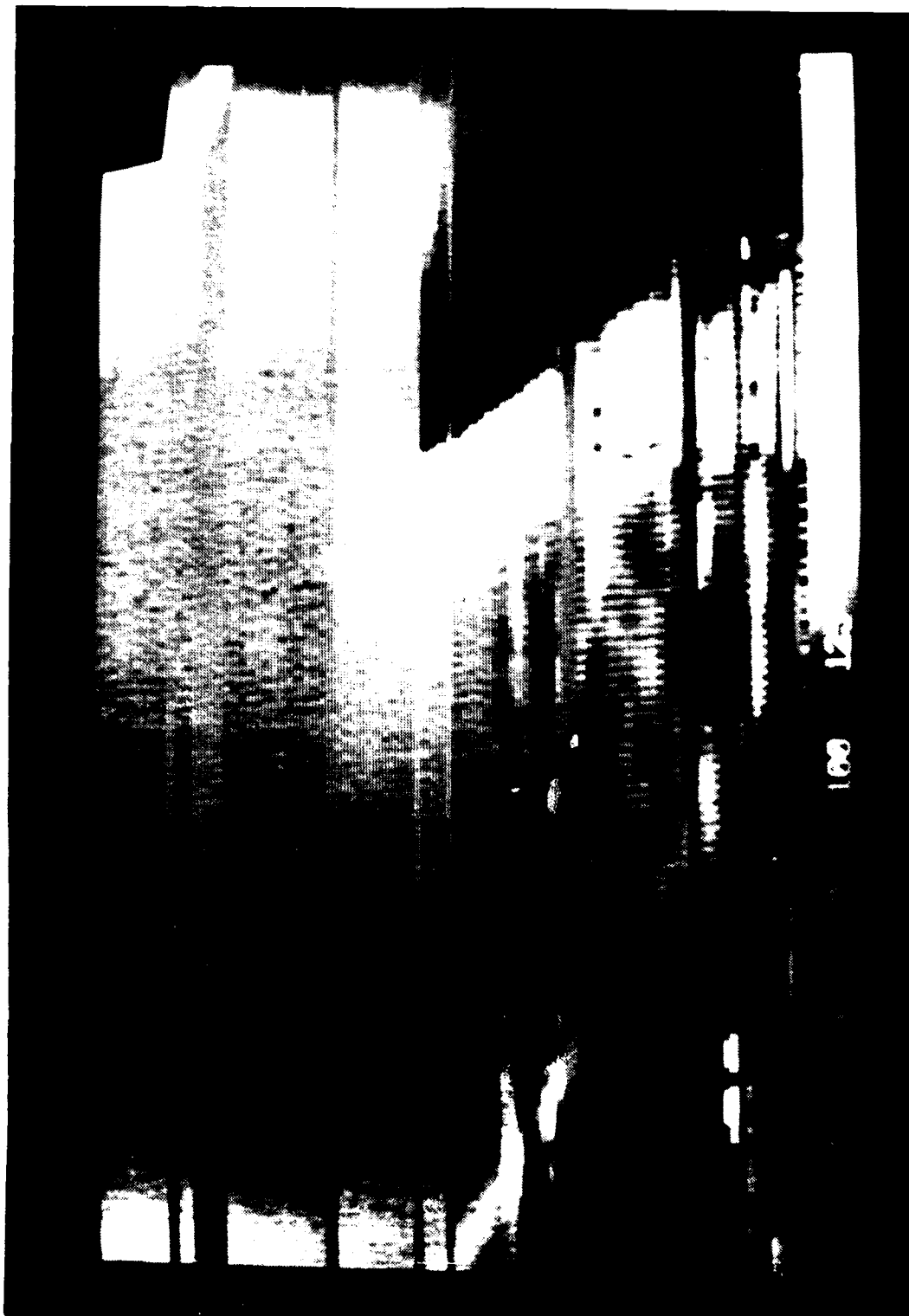


Figure 34 NPS-IRSTD Image (3° Wide) Corrected for X-direction Detector Shape MTF



Figure 35 NPS-IRSTD Image (3" Wide) Corrected for X-direction Optical MTF



Figure 36 NPS-IRSTD Image (3° Wide) with One-Detector-To-Five-Row
Expansion Smoothing Employed



Figure 37 NPS-IRSTD Image (3° Wide) with all Available Corrections Applied

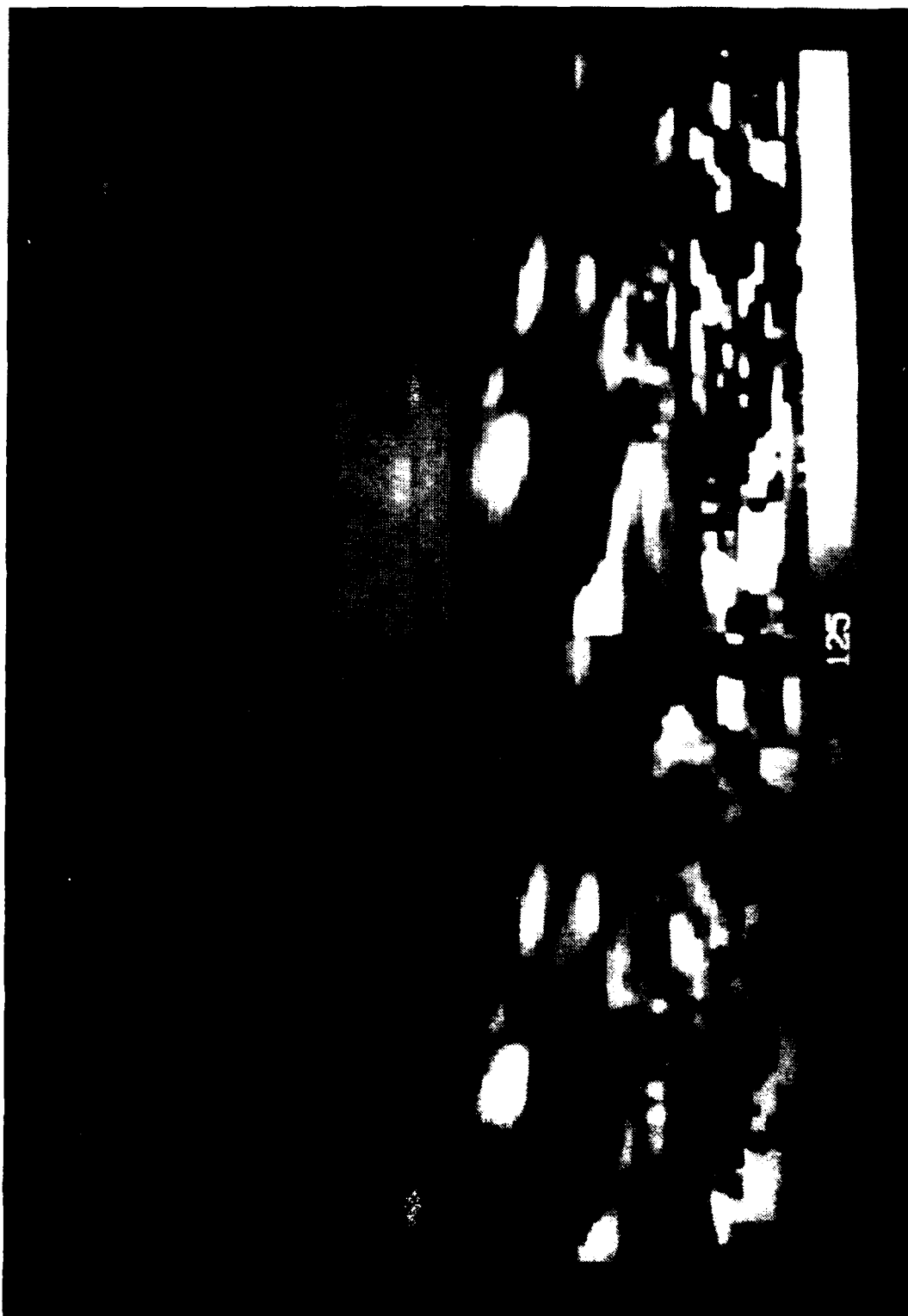


Figure 38 NPS-IRSTD Image Comparing a Corrected to an Uncorrected Image.
(Left) Corrected. (Right) Uncorrected.

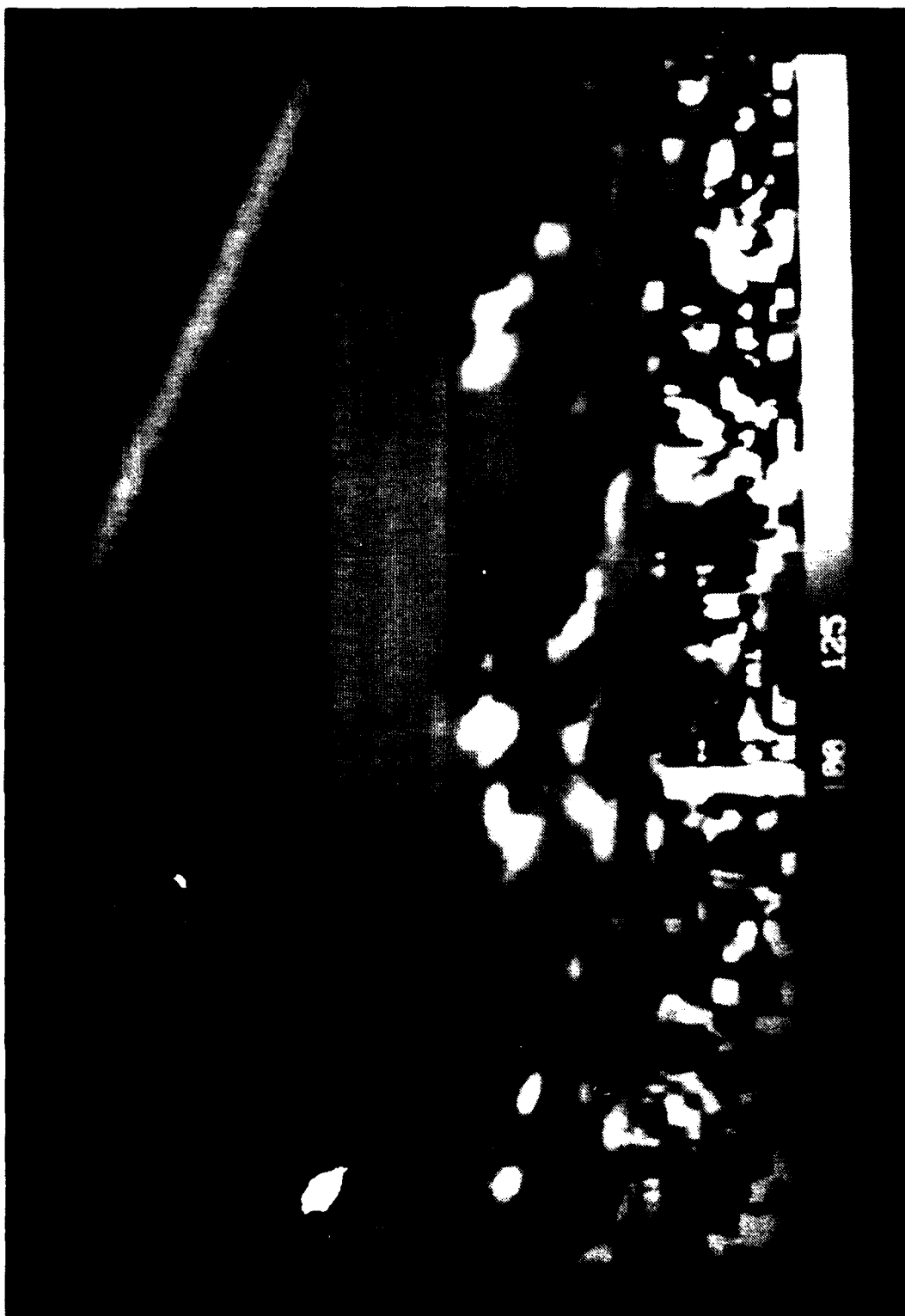


Figure 39 NPS-IRSTD Image (12° Wide) of the Monterey Hillside with all Corrections Applied



Figure 40 Photograph of the Monterey Hillside

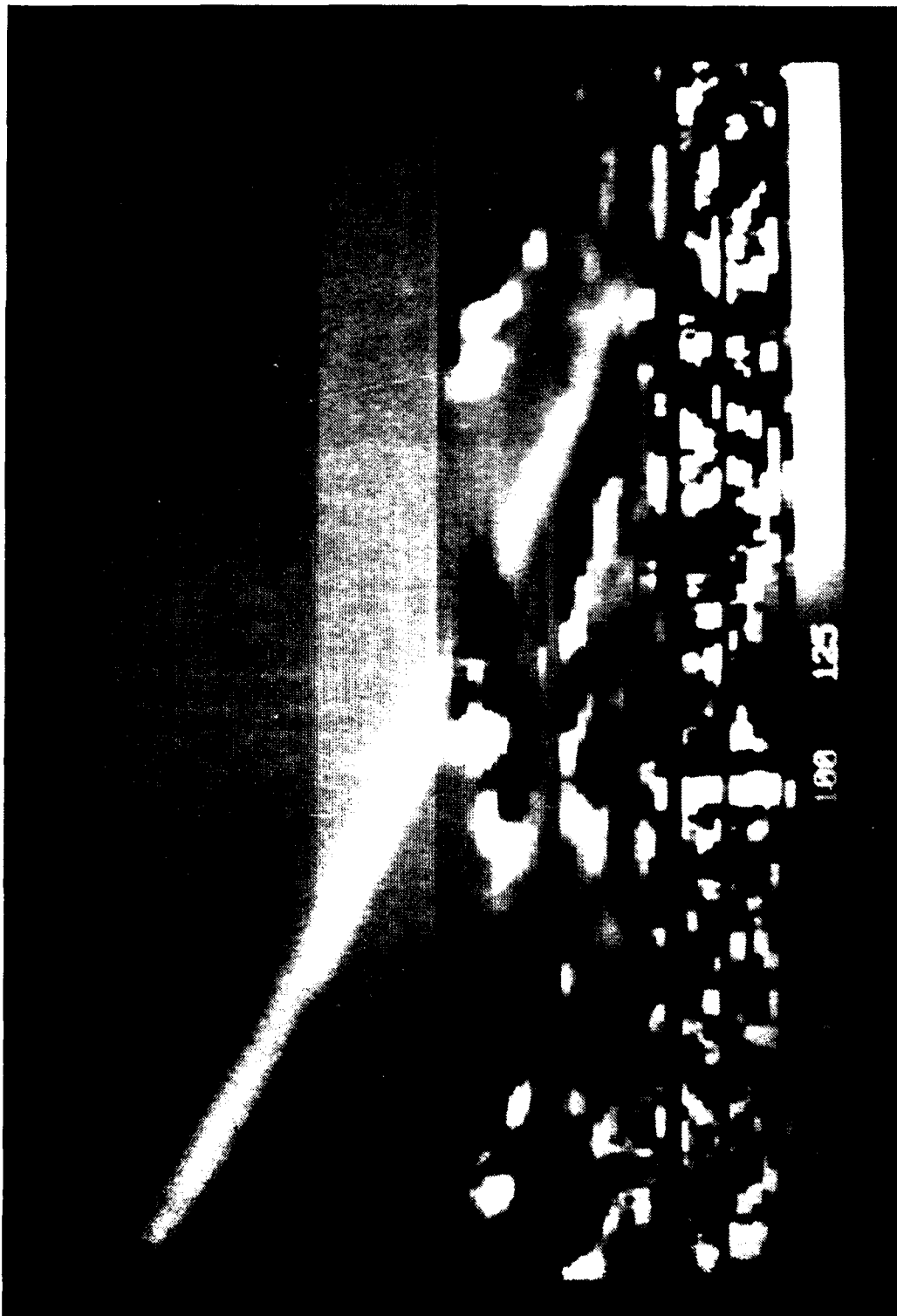


Figure 41 NPS-IRSTD Image (12° Wide) of the Monterey Hillside with no Corrections Applied

V. CONCLUSIONS AND RECOMMENDATIONS

A. CONCLUSIONS

In the process of sorting out what types of concluding comments are appropriate for a project such as this, and how they might best be presented, it became apparent that there are three distinct topics to be addressed:

- The utility of the imaging system in its present academic environment.
- The potential for generalizing the application of framegrabber technology to provide real time imaging capabilities for future IRSTD systems.
- The value of the project to me personally.

Within the context of the academic applications, the development of the capability to display the NPS-IRSTD data in image format using a PC based system that is efficient and easy to use adds a valuable asset to the overall NPS-IRSTD project. This opinion is supported by consideration of the few uses already envisioned:

- It allows the data to be searched rapidly by anyone interested in finding (or avoiding) certain features in the system's total field of view.
- The image processing capabilities support the study of linear filter systems theory as it applies to this combined optical and electronic system. This may be done in the context of thesis research or as a demonstration/laboratory for related courses.
- The results of the studies on system effects could be used to restore the data, which has passed through this series of optical and electronic filters, to a state which more closely resembles the actual irradiance distribution of the scene under investigation.
- The ability to visually present data which has been processed with a background clutter algorithm in the form of an image may provide additional insight into the algorithm's overall performance and effect.
- Finally, but certainly not least in importance, is the imaging systems potential as a tool to evaluate the performance of the NPS-IRSTD system. Simply presenting the data in image form has highlighted the fact that there are significantly more bad detector channels present than at the time Ayers was working on system calibration. The image display of the scanned scenes also

exposed the surprising image doubling effect, which will only be fully understood after further investigation.

On the topic of the potential for employing framegrabber technology to display images from future IRSTD systems, it seems appropriate to be somewhat more guarded in making an appraisal. This reservation stems from the basic fact that many of the problems noticed while using the present system will require solutions based on areas of technological expertise beyond the scope of this study.

Now, having said that, I believe it to be a reasonable assessment that framegrabber technology deserves additional study and consideration as a potential source of imaging capabilities for operational IRSTD systems. It seems reasonable to envision a framegrabber system, connected to an IRSTD through an appropriately engineered interface, filling a dual role in a shipboard system. The principal function in this environment would be real time display of a selected portion of the scan. Such a display could be used by bridge watch personnel as an additional aid in nighttime and low visibility navigation, and by CIC personnel in validating the position of targets detected by the system. Real time display does not seem possible without a significant effort being made to engineer an interface directly between the framegrabber and the IRSTD.

The second role aboard ship, similar to the final item listed for academic uses, would be as a tool to evaluate system performance. In addition to highlighting obvious items such as bad detectors and unusual imaging behavior, diagnostic routines could be developed based on standard infrared system performance measures to make checks on system performance. Properly designed and implemented, these diagnostics would fill a role similar to sonar calibrations where they provide periodic tests of system performance as well as educate the users on the real capabilities (and limitations) of the system.

Finally, I would like to make a few comments about the value of this project to my education, if for no other reason than to remind myself in future years of some very important points. At the outset I had the naive impression that it would be a straightforward task to bring together the necessary pieces of hardware according to the methods prescribed by the available documentation. The system

would then, operating as designed, receive and display data only modified by filters which match the classical descriptions offered in course lectures and notes; filters such as the optical system, detectors and electronics. The task would have been to determine experimentally the system MTF.

It has been an invaluable lesson to see all that can be involved in making a complex system such as an IRSTD produce reliable data, and how this can impact peripheral projects dependant on the system. In general it now seems much more appropriate to approach real world tasks with something less than total optimism and also to question, but not dampen, such optimism in others.

B. RECOMMENDATIONS

It is believed that framegrabber technology does have a valuable role to play in the continuing work of the research with the NPS-IRSTD and the potential for a role in operational IRSTD systems. Based on this premise, attention given to the following items can only improve system performance and usefulness:

- The DMA transfer process needs to be made faster and more reliable.
- The source of the image doubling effect should be determined, and if possible the problem corrected.
- The problems relating to the application of the FFT routines needs to be studied to determine optimal methods for scaling and otherwise handling data.
- The problem with the destination of DMA transfers getting redirected by the changing address bus of the DT2861 needs to be addressed. The solution may be accomplished best by writing directly to the appropriate DT2861 register.
- Development of a scheme whereby more than 6° of data can be received with any one set of DMA transfers would potentially increase the overall usefulness of the imaging system. This could be done by making use of the 8 MB of expanded RAM. Six or seven 64 KB transfers could be written to standard RAM, and then all data moved to expanded RAM. Then, frame by frame, the data could be returned to standard RAM for unscrambling prior to the final move to a frame buffer.
- The behavior of the DT-IRIS subroutine ISPUTP needs to be investigated to remove its adverse behavior in the smoothing routine.
- The total system transfer function should be experimentally determined, and as an additional step it may prove valuable to make a comparison to theoretical predictions.

- After the system transfer function has been determined, it should be used to deconvolve system effects from the data. The significance of the effect of the system on the data should then be determined by comparing the raw and deconvolved data sets.
- The bad detector channels should be checked for the possibility of restoring at least some of them to full operation. Also, the gain on the multiplexer outputs should be balanced to remove the horizontal band structure noticeable on all images.

APPENDIX A

I. INDIUM ANTIMONIDE INFRARED DETECTORS

A. DETECTOR PERFORMANCE

The detectors used by the NPS-IRSTD are made of the semiconductor compound Indium Antimonide (InSb), and are connected for photovoltaic operation. Each detector is 0.02" high and 0.003" wide and has an instantaneous field of view of 2 milliradians by 0.3 milliradians. The system contains 180 detectors arranged into two arrays, each with 90 detectors in a vertical column. These arrays are horizontally separated by approximately $1/2^\circ$. The full field of view of 360° by 10.5° is achieved by scanning the optical sub-assembly in a full circle about the horizon.

Infrared detector performance is generally characterized by certain figures of merit which have gained acceptance in the scientific and industrial communities. Responsivity, Noise Equivalent Power (NEP), and Detectivity are among the most commonly used figures of merit. Figure 42, extracted from *The Infrared Newsletter*, Vol 19, No. 4 [Ref. 10] gives definitions for these terms. Figure 43 is taken from *The Infrared Handbook* [Ref. 11] to show example performance data for InSb detectors, while Figure 44 was taken from *The Electro-Optics Handbook* [Ref. 12] to give a comparison between InSb and several other detector types. The values for typical InSb photovoltaic detector specifications in Table 5 are extracted from *Photonics Design and Applications Handbook* [Ref. 13].

TABLE 5
TYPICAL InSb PHOTOVOLTAIC DETECTOR SPECIFICATIONS

FORD AEROSPACE COMM. CORP.					
SPECTRAL	D^*	RESPONSIVITY	OPERATING	RISE	ACTIVE
RANGE (m)	$(\text{cmHz})^{1/2}/\text{W}$	(A/W)	TEMPERATURE	TIME (nsec)	AREA (mm^2)
3-5.5	10^{11}	3.5 (at 5 m)	77 K	500	6×10^{-3} to 16
SANTA BARBERA RESEARCH CTR.					
SPECTRAL	D^*	RESPONSIVITY	OPERATING	RISE	ACTIVE
RANGE (m)	$(\text{cmHz})^{1/2}/\text{W}$	(A/W)	TEMPERATURE	TIME (nsec)	AREA (mm^2)
1-5	$> 8 \times 10^{11}$	1.6	77 K	< 1	0.25, 0.50 1.0, 2.0

Responsivity $R(\lambda)$

The responsivity of a detector is defined as the ratio of the output signal in volts or amps to the incident optical power in watts. $R(\lambda)$ is measured in volts/watt or amps/watt.

$$R(\lambda) = \frac{v}{\Phi_\lambda \Delta\lambda}$$

where v = electrical signal
 Φ_λ = incident spectral power at wavelength λ , $W \mu m^{-1}$
 $\Delta\lambda$ = small wavelength interval that includes the wavelength λ

Detectivity D^*

D^* is the principle figure of merit for single-element detectors. It is defined as the signal-to-noise ratio of the detector when 1 W of radiant power is incident on a detector area of 1 cm^2 with a bandwidth of 1 Hz. D^* is measured in $cm Hz^{1/2} W^{-1}$.

$$D^* = \frac{S/N}{\Phi_i} \sqrt{A_d \Delta f} = \frac{\sqrt{A_d \Delta f}}{NEP} = \frac{R}{N} \sqrt{A_d \Delta f}$$

where S = rms signal voltage or current
 N = rms noise voltage or current
 Φ_i = rms incident optical power, W
 A_d = detector area, cm^2
 Δf = electrical bandwidth, Hz
 NEP = noise equivalent power, W
 R = responsivity, VW^{-1} or $amp W^{-1}$

Noise Equivalent Power NEP

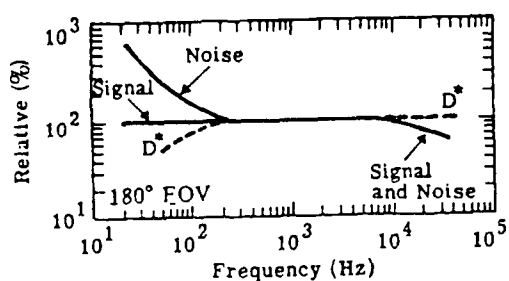
The noise equivalent power is the required power incident on the detector to produce a signal output equal to the rms noise output. NEP is measured in watts.

$$NEP = \frac{i_{rms}}{R_i}$$

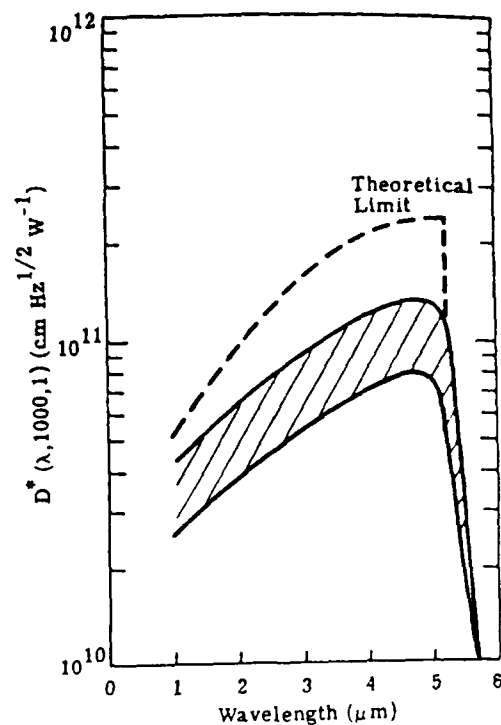
where i_{rms} = rms noise current, amps
 R_i = current responsivity, amp/W

Figure 42 Figures of Merit for Single Element Detector (Extracted from *The Infrared Newsletter*, Vol. 10, No. 1)

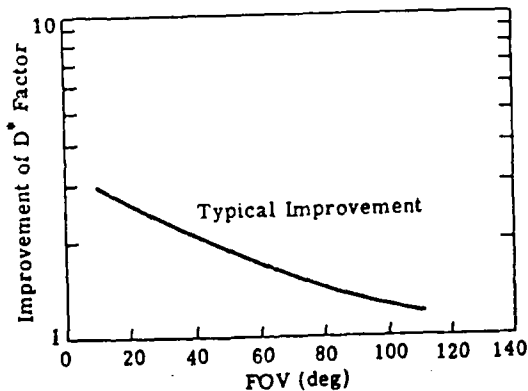
$T_d = 77 \text{ K}$
 $A_d = 10^{-4} \text{ to } 10^{-1} \text{ cm}^2$
 $R_d = 1 \text{ to } 100 \text{ megohms}$
 $\tau < 1 \mu\text{sec}$
 $\text{FOV} = 60^\circ$
 $\text{Background temperature} = 300 \text{ K}$
 $\mathcal{R}_\lambda \approx 10^5 \text{ V W}^{-1}$
 $\mathcal{R}_\lambda^p / \mathcal{R}_{bb} \approx 5.0$



(a) Frequency response of detector signal and noise.



(b) Spectral response of detector D^* (λ , 1000, 1).



(c) Improvement in D^* versus FOV for typical detectors.

Note

- (1) Resistance is area and bias voltage dependent.
- (2) D^* will increase when the FOV is restricted with cold shields or when the spectral extent is restricted with cold spectral filters.

Figure 43 InSb Detector Performance Data at 77 K (Extracted from *The Infrared Handbook*)

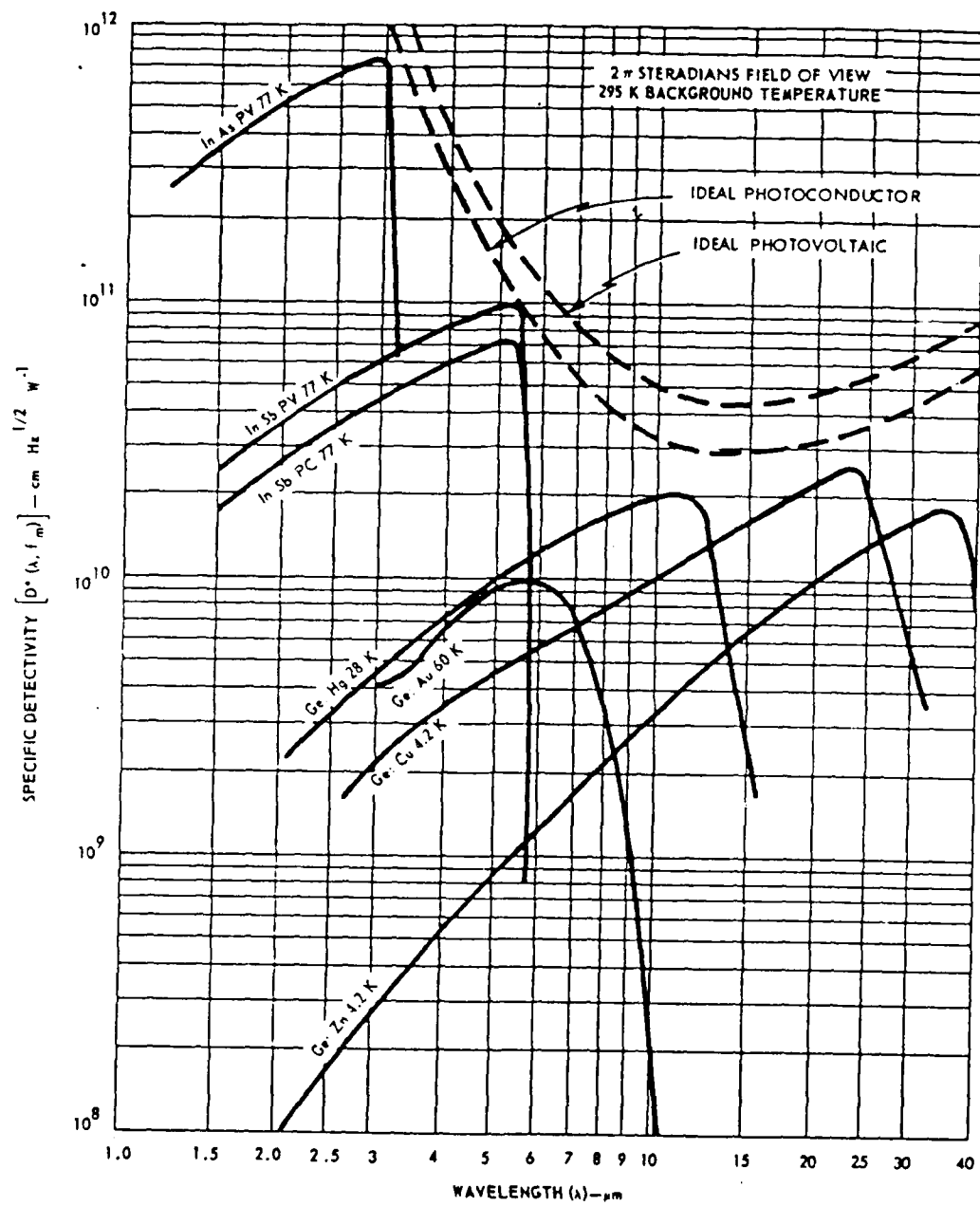


Figure 44 Spectral Detectivities for Above Average Crystal Detectors at Frequency f_m (Extracted from *The Electro-Optics Handbook*)

B. AC-COUPLING

Infrared imaging often requires detecting small fluctuations in a large background signal. The detectors simply register the arrival of all photons within their instantaneous field of view. To extract more information from the data generated by the detectors, the average value of the background can be subtracted out. A common method of implementing background subtraction in IR systems is to couple the detector output to a circuit which blocks the low frequency components of the signal. This practice is known as DC-blocking or AC-coupling. AC-coupling increases the IR apparent thermal contrast and blocks the $1/f$ noise, improving the signal-to-noise ratio. The NPS-IRSTD detector output is AC-coupled, with a low frequency cut-on at approximately 100 Hz, to increase its detection capabilities. Lloyd [Ref. 6] gives the circuit shown in Figure 45 as an example of a circuit which can be used for this purpose.

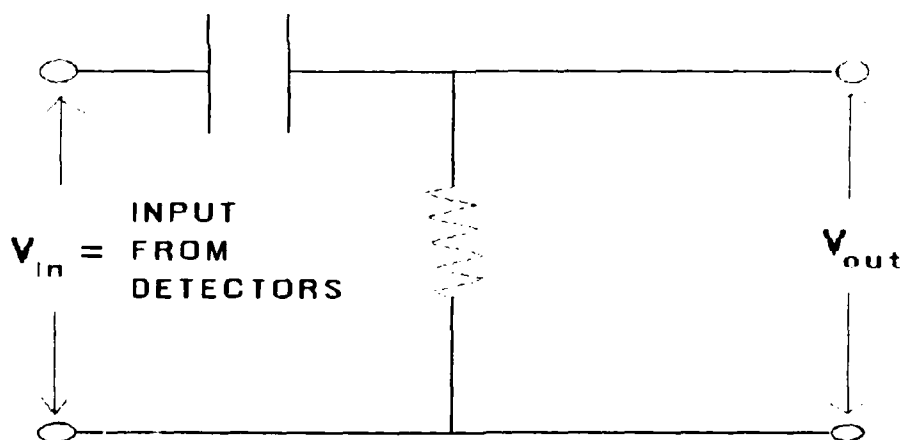


Figure 45 Simple AC-coupling Circuit

AC-coupling does have some drawbacks. One is an inability to calibrate the system for determining the actual temperature of objects present in the scene. Additional drawbacks include droop and undershoot response characteristics. Droop occurs as the detector passes from an extended region of low temperature to an

extended region of high temperature. Undershoot occurs as the detector passes from a high temperature region to a low temperature region. Both effects are demonstrated by the curves in Figure 46. The top set of curves shows signal droop while the center set shows undershoot and the bottom curves give an example of both.

Undershoot is evident in nearly all of the NPS-IRSTD images. The scan direction is from left to right across the scene, and the dark region to the right of the bright objects can be attributed to undershoot caused by the AC-coupling of the detector outputs. Comparing the prominence of the dark regions caused by AC-coupling effects to the influence of the optics and the detectors as demonstrated by the deconvolution routines points out the significant impact AC-coupling has on system operation.

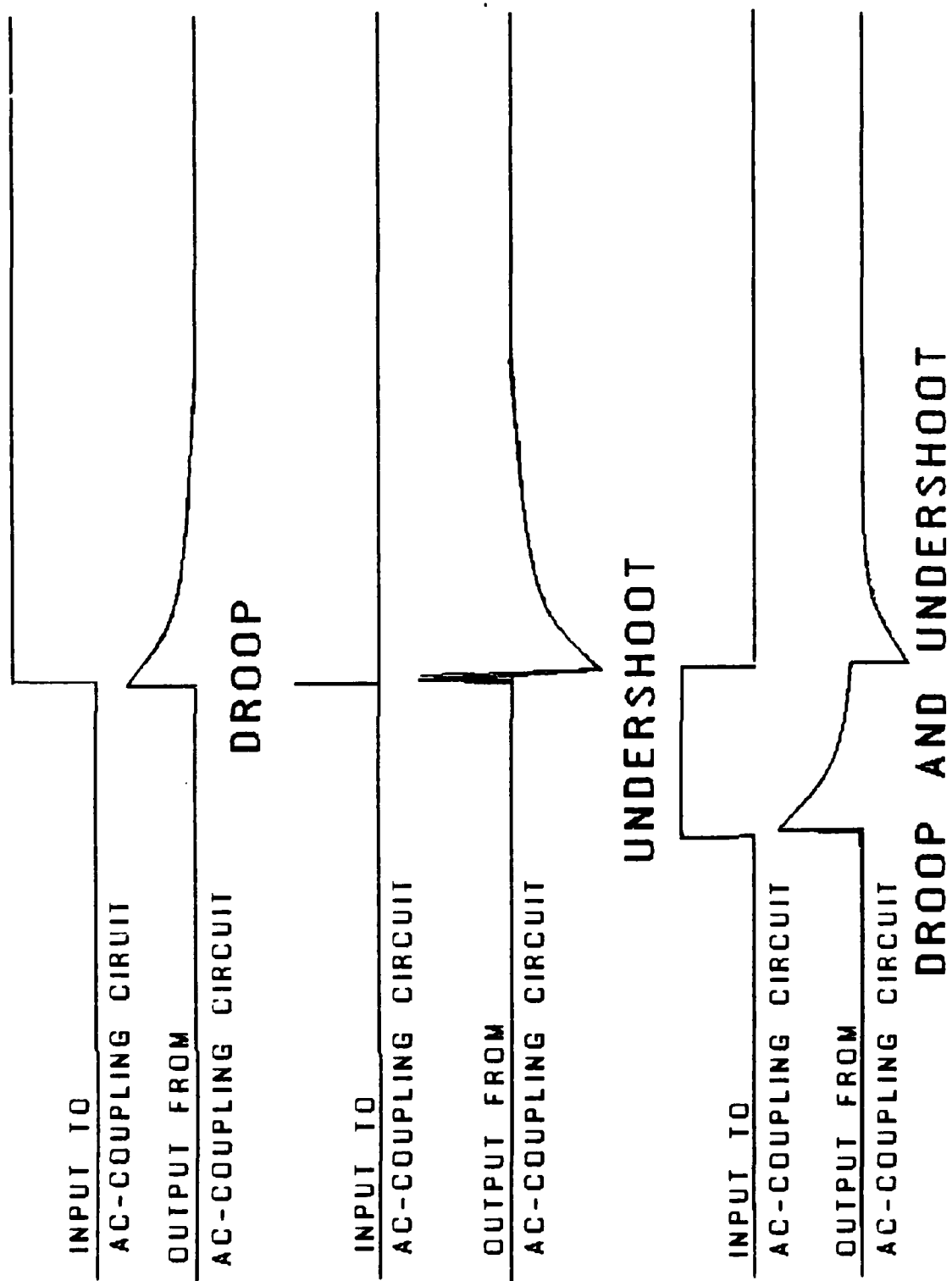


Figure 46 AC-coupling Effects on Detector Output Signals

APPENDIX B

IMAGING PRINCIPLES EXPRESSED THROUGH LINEAR SYSTEM THEORY

This appendix is provided for the reader unfamiliar with the linear systems approach to image processing. The treatment of linear system theory here will be conceptual, and most general concepts will be simply stated without proof or argument. For a mathematical formulation of the topic the reader is referred to Lloyd [Ref. 9]. A mathematical treatment specifically directed toward the Fast Fourier Transform which was implemented in the image processing program can be found in Brigham [Ref. 14]. As in most situations where an assumption regarding the linearity of a process is made, there are circumstances in which non-linear effects will cause observations to deviate from predicted results. Lloyd [Ref. 9] points out the following situations in thermal imaging when linearity may be violated:

- application of certain signal processing methods
- given a spatially variant imaging process
- when noisy conditions exist (system mapping is not single valued)

The degree to which these non-linearities impact the imaging process varies widely between differing systems.

A good starting point in the discussion of linear system theory is to introduce the concept of the Fourier function pair. Any periodic single valued function can be equivalently expressed as a weighted sum of a set of sine and/or cosine functions. A common example is a square wave, defined as a function of time and having a period T, which can be expressed as

$$\text{Square Wave} = \sum_{n=1}^{\infty} \frac{1}{n} \cos\left(\frac{2\pi n t}{T}\right) \quad (\text{for } n \text{ odd}).$$

In this form each term in the sum represents the magnitude of a cosine wave with a frequency $\omega=2\pi n/T$.

The functions $f(\omega)$ and $f(t)$ form a unique pair. When $f(t)$ is non-periodic, this relationship can often be expressed with Fourier integrals such that

$$f(\omega) = \frac{1}{2\pi} \int_{-\infty}^{\infty} f(t) e^{-i\omega t} dt$$

$$f(t) = \int_{-\infty}^{\infty} f(\omega) e^{i\omega t} d\omega$$

In shorthand notation $\mathcal{F} [f(t)]$ defines the Fourier transform of $f(t)$, then the Fourier pair can be expressed

$$F(\omega) = \mathcal{F} [f(t)]$$

$$f(t) = \mathcal{F} [F(\omega)]$$

This is important because filters affect the various frequency components of a signal differently. If $g(\omega)$ contains the information on the filter's effect on the frequency components of the signal, then the output from the filter is

$$h(\omega) = f(\omega) \cdot g(\omega)$$

In spatial coordinates $f(x)$ and $f(k)$ form the Fourier pair where k is related to spatial frequency as ω is to temporal frequency.

In imaging systems the filters are the various parts of the system through which the signal must pass before it is seen by the observer; lenses, mirrors, obstructions, windows, detectors, electronics, and the display. One strength of the linear system approach is that each component can be treated as an independent filter. The final image is obtained by multiplying together the effects of all the components.

Most of the fundamental ideas imbedded in linear filter theory can be illustrated using the imaging process for a simple lens as an example. The treatment for this discussion was taken from unpublished course notes written by A. W. Cooper and E. C. Crittenden, Jr. [Ref. 15]. Consider the scene to consist of a single point source located on the z -axis an infinite distance to the left of the x - y plane in Figure 47. The radiation from this source will arrive as plane waves parallel to the x - y plane. If the x - y plane contained a perfect lens of infinite extent, the light would be focussed to a point in the X - Y plane.

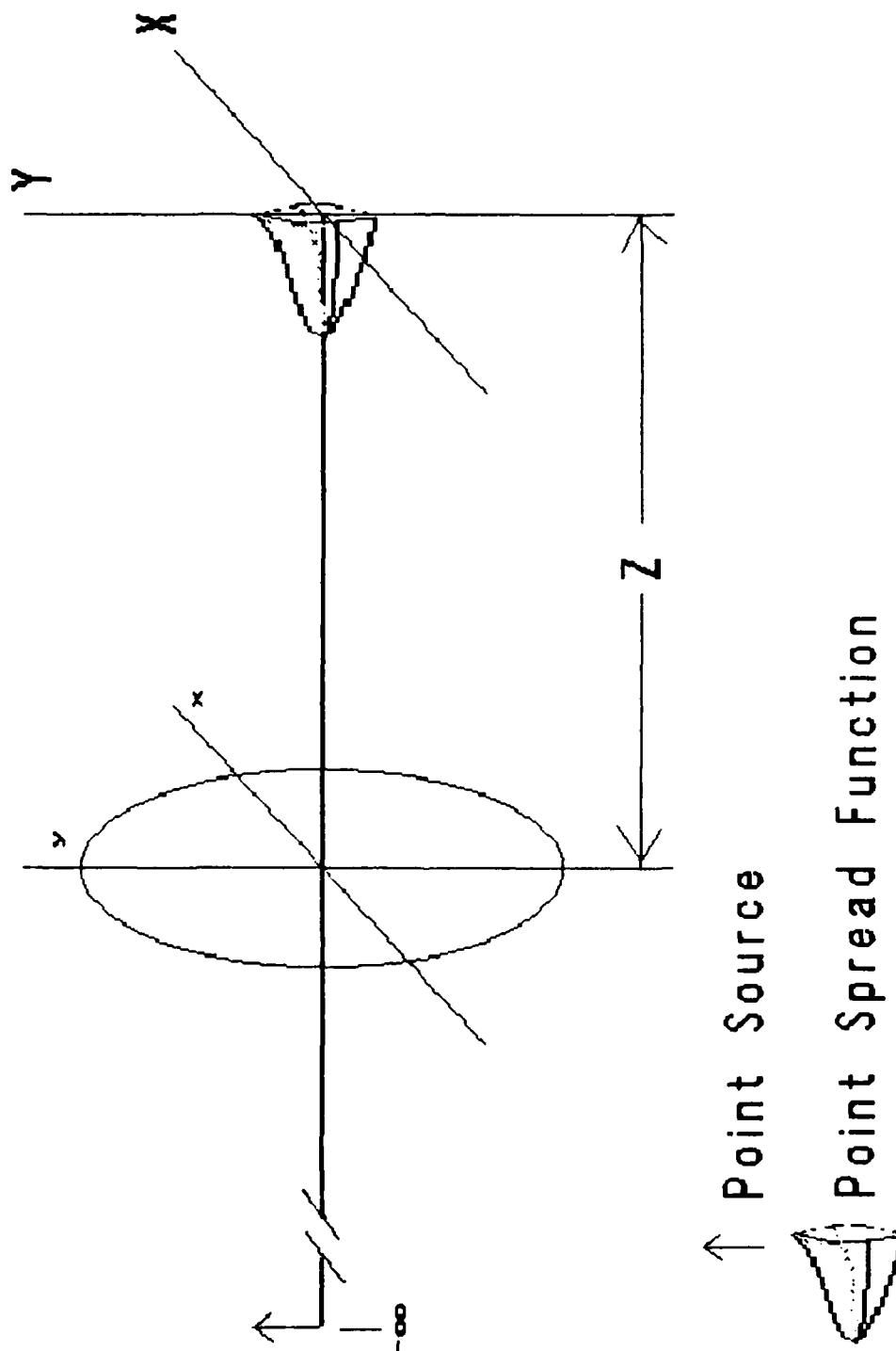


Figure 47 Imaging of a Point Source at Infinity with a Circular Lens

However, since all lenses are of finite size, a point source will not be focussed to a point. Instead, the light will be distributed in a manner similar to that shown in Figure 48, which was taken from Hecht [Ref. 16]. The distribution represented by the curve in Figure 48 is referred to as the point spread function.

The point spread function can be analytically determined by integrating the electric field incident on the x - y plane to find the resulting diffraction pattern in the X - Y plane,

$$E(X,Y) = \int_{-\infty}^{\infty} \int_{-\infty}^{\infty} A(x,y) e^{(ik/R)(Xx + Yy)} dx dy$$

In this expression $A(x,y)$ contains the electric field amplitude and phase information at the lens, $k=2\pi/\lambda$ where λ represents the wavelength of the light, R is the distance from the x - y plane origin, and $E(X,Y)$ is the electric field amplitude at the image plane. This expression can be put in the form of a standard Fourier integral by defining the radian spatial frequencies $K_x=(kX/R)=(2\pi X/\lambda R)$ and $(K_y=kY/R=2\pi Y/\lambda R)$ so that

$$E(K_x, K_y) = \int_{-\infty}^{\infty} \int_{-\infty}^{\infty} A(x,y) e^{i(K_x x + K_y y)} dx dy$$

It can be seen that E and A are a Fourier transform pair. For the case of a point source on the optic axis an infinite distance from the optical system, the amplitude and phase function $A(x,y)$ can be treated as a constant. Thus the distribution in the X - Y plane for a point source becomes just the Fourier transform of the shape of the optical component's aperture. Figure 49, from Lloyd [Ref. 9], shows the two dimensional Fourier transform for several simple geometric shapes.

A system for which the form of the point-spread function is the same for all points in the image is called spatially invariant. A linear system is described by behavior such that the scene can be decomposed into a sum of all its components. Therefore, for a linear, spatially invariant system the image projected onto the image plane is the result of convolving the point-spread function with each point in the scene. Using shorthand notation, a convolution is defined by the symbol $*$ so that

$$h(x)=f(x)*g(x)$$

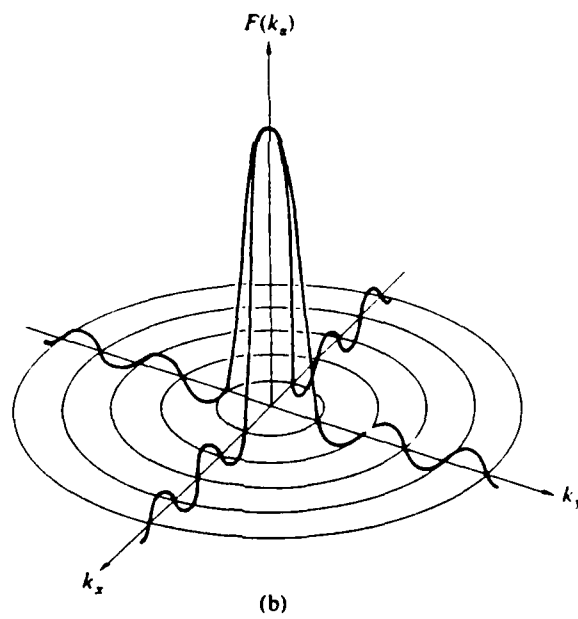
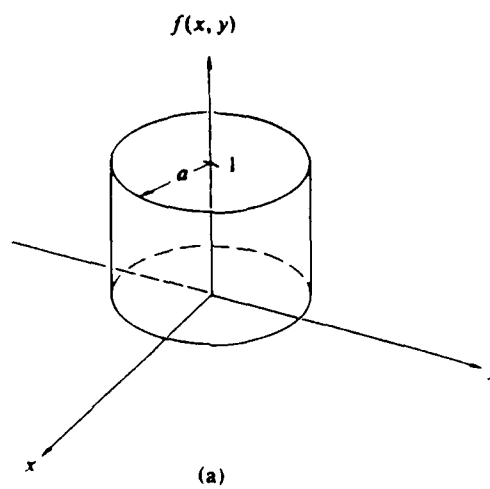


Figure 48 Point Spread Function for a Circular Aperture


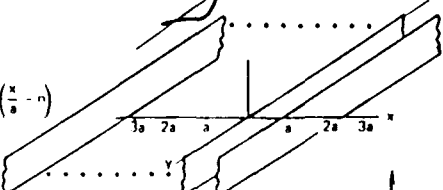
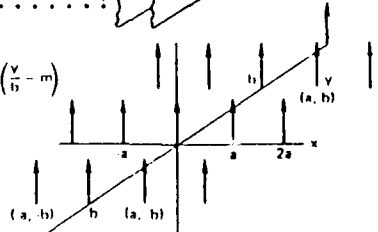
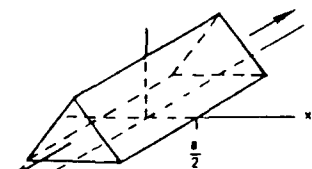
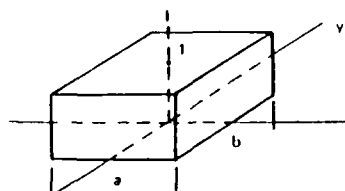
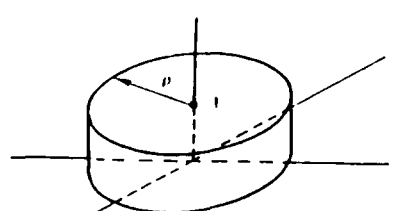
FUNCTION	DEFINITION	GRAPHICAL REPRESENTATION	FOURIER TRANSFORM
$\text{Bessinc} \left(\frac{R}{\rho} \right)$	$= \frac{2J_1 \left(\frac{\pi R}{\rho} \right)}{\left(\frac{\pi R}{\rho} \right)}$		$\text{Sinc}(\pi R)$
$\text{Comb} \left(\frac{x}{a} \right)$	$= \sum_{n=-\infty}^{\infty} \delta \left(\frac{x}{a} - n \right)$		$\text{Comb}(af_x) \delta(f_y)$
$\text{Comb} \left(\frac{x}{a} \right) \text{Comb} \left(\frac{y}{b} \right) = \sum_{n=-\infty}^{\infty} \sum_{m=-\infty}^{\infty} \delta \left(\frac{x}{a} - n \right) \delta \left(\frac{y}{b} - m \right)$			$\text{Comb}(af_x) \text{Comb}(bf_y)$
$\text{Lambda} \left(\frac{x}{a} \right)$	$= 1 - 2 \left(\frac{x}{a} \right) \left(\frac{x}{a} \right) \leq \frac{1}{2}$ $= 0, \left(\frac{x}{a} \right) > \frac{1}{2}$ FOR ALL y		$\text{Sinc}^2(af_x) \delta(f_y)$
$\text{Rect} \left(\frac{x}{a} \right) \text{Rect} \left(\frac{y}{b} \right)$	$-1, \left \frac{x}{a} \right \leq 1 \text{ AND } \left \frac{y}{b} \right \leq 1$ $0, \left \frac{x}{a} \right > 1 \text{ AND } \left \frac{y}{b} \right > 1$		$\text{Sinc}(af_x) \text{Sinc}(bf_y)$
$\text{Circ} \left(\frac{R}{\rho} \right)$	$1, \frac{R}{\rho} \leq \frac{1}{2}$ $0, \frac{R}{\rho} > \frac{1}{2}$		$\text{Bessinc}(\pi R)$

Figure 49 Two Dimensional Fourier Pairs

While computation of a convolution to evaluate the imaging characteristics of a system seems somewhat imposing, linear system analysis provides the mechanism for simplifying the problem. A fundamental theorem states that the Fourier transform of the convolution of two functions can be expressed as the product of the Fourier transforms of the functions.

$$\mathcal{F}[h(x)] = \mathcal{F}[f(x) * g(x)] = \mathcal{F}[f(x)] \cdot \mathcal{F}[g(x)] = F(k) \cdot G(k)$$

Application of this theorem involves moving the problem at hand back to the x-y plane where the functions are expressed in terms of frequencies. In other words, the convolution can be computed from the product of the Fourier transform of the scene distribution with the Fourier transform of the point spread function (which is the lens aperture shape).

Extending the concept from one filter to many involves using the output from the last filter as the input to the next filter. Computation of the effect of the current filter is most easily accomplished in the frequency domain. Therefore, leaving the results from the previous filter in terms of frequency allows the effect of both filters to be computed as a product of the two. It can now be seen that removing the effect of a filter can be accomplished by dividing by its function in the frequency domain. This is known as deconvolution, and it is the process applied to remove the systems influence from image data.

In practice the spatial fluctuations of scene brightness are described as a modulation. Modulation is sometimes defined as

$$M = (I_{\max} - I_{\min}) / (I_{\max} + I_{\min}) .$$

for both M_i , the modulation of the image and M_o , the modulation of the object, where I is the irradiance. From this it is straightforward to show that for a circular lens, higher spatial frequencies will have a much smaller modulation in the image than in the scene. This effect will be less noticeable for lower spatial frequencies. Figure 50 diagrams this concept.

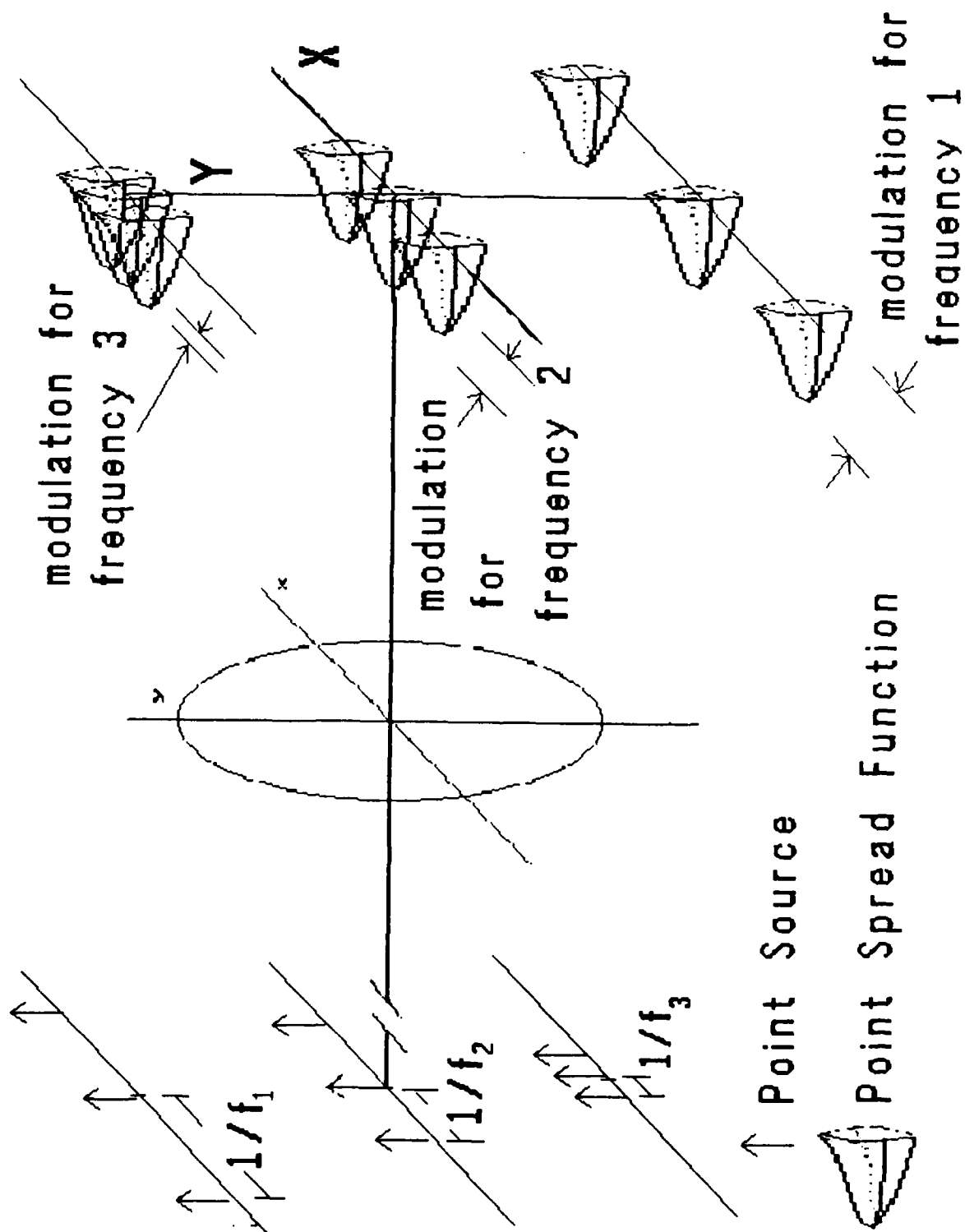


Figure 50 Modulation of Point Source Distributions at Infinity Imaged onto the Image Plane

The relationship of spatial frequencies and their corresponding degree of modulation is expressed in functional form by the modulation transfer function (MTF), where

$$\text{MTF} = M_i / M_o$$

Thus it is the MTF which is used to define the effect a system component will have on a signal passing through it.

Application of Fourier optics theory provides a vehicle for showing that the MTF of an optical system can be theoretically derived to be the autocorrelation of the pupil function (described by the physical shape of the optical component) for a system imaging non-coherent light. This derivation is contained in Cooper and Crittenden's Ph3252 course notes [Ref. 15]. Parker [Ref. 2] used ray tracing software as an analytical method to calculate the MTF of the NPS-IRSTD's optical system, for both modified and unmodified versions. The results of these calculations [Ref. 2] are presented as Figure 51.

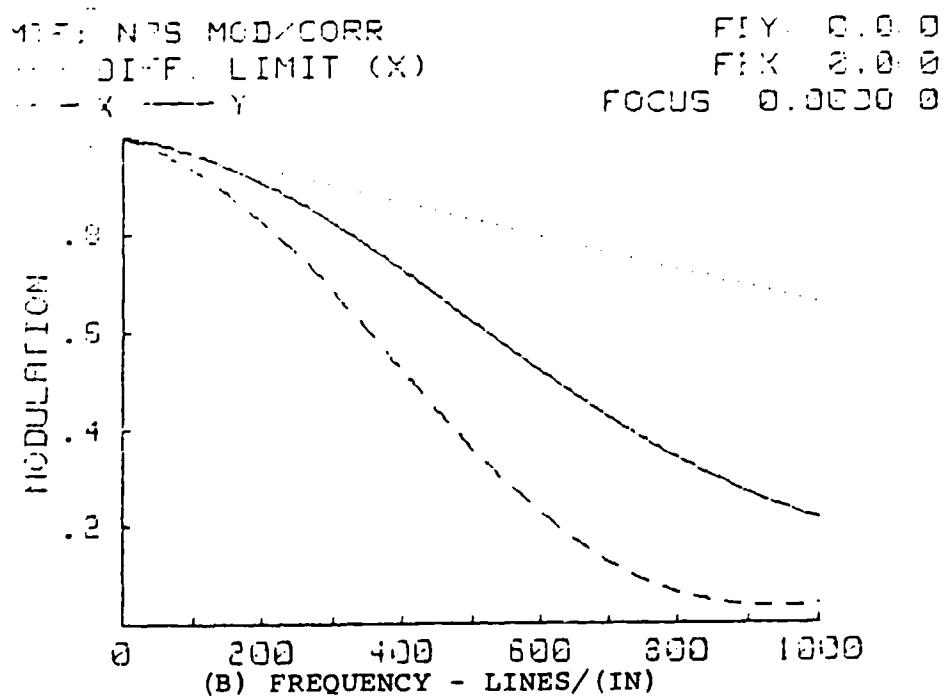
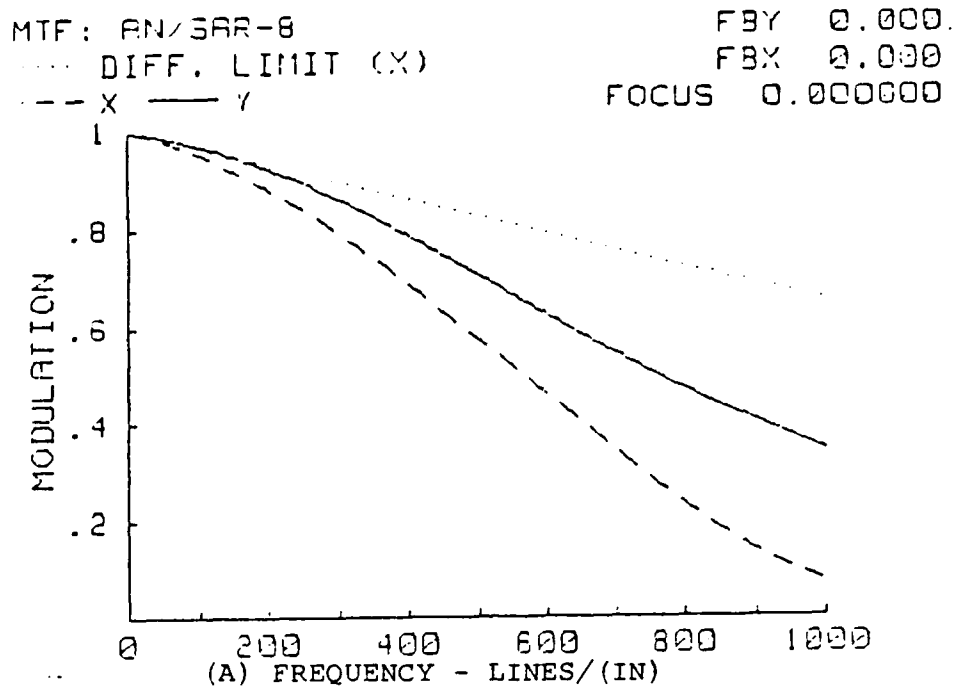


Figure 51 MTFs for the ADM and the NPS-IRSTD. (Top) AN/SAR-8 ADM
 (Bottom) NPS-IRSTD

APPENDIX C

I. COMPUTER PROGRAM LISTINGS

A. BEGIN.FOR

```
C
C PROGRAM BEGIN.FOR                WRITTEN BY: R. C. ENGEL
C                                  LAST REVISED: 13 AUGUST 1989
C                                  BY: R. C. ENGEL
C
C      INTEGER*2 IBACK(15360), NUM(2), NUM1(3)
C      REAL      XRES(90)
C      DIMENSION IRED(0:255), RED(0:255), IGREEN(0:255)
C      DIMENSION IBLUE(0:255), BLUE(0:255), GREEN(0:255)
C
C      FORMAT STATEMENTS
C
C      2 FORMAT (//)
C
C      THESE ARE DT-IRIS CALLS TO INITIALIZE THE DRIVERS AND TO
C      DISPLAY THE CONTENTS OF FRAME BUFFER 0 ON THE SCREEN.
C
C      CALL ISINIT
C      CALL ISOTFR(0)
C      CALL ISDISP(1)
C
C      MENU SECTION.
C
30 WRITE (*,2)
   WRITE (*,*) '1=CREATE COLOR SCALES FOR FRAMES 0 AND 1'
   WRITE (*,*) '2=CHANGE OUPUT LOOKUP TABLES 2-7
   *      (GAUSSIAN)'
   WRITE (*,*) '3=CHANGE OUPUT LOOKUP TABLES 2-7
   *      (LINEAR)'
   WRITE (*,*) '4=CLEAR A DESIGNATED BUFFER'
   WRITE (*,*) '5=VIEW A DESIGNATED BUFFER'
   WRITE (*,*) '6=EXIT THE PROGRAM'
   READ (*,*) NOPS
   IF (NOPS .LT. 1 .OR. NOPS .GT. 6) GO TO 30
   GOTO (99,198,201,399,449,500),NOPS
```

C THIS SECTION ADDS LABELS AND A COLOR SCALE ACROSS THE
 C BOTTOM OF THE DISPLAY SCREEN FOR BUFFERS 0 AND 1.
 C

```

99 DO 100 IFR=0,1
    DO 110 I=0,29
        DO 120 J=0,510,2
            IBACK(I*512+J+1)=J/2
            IBACK(I*512+J+2)=J/2
120     CONTINUE
110     CONTINUE
    CALL ISPU1P (IFR,450,0,15360,IBACK)
    CALL ISSFNT (0)
    NUM(1)=50
    NUM(2)=53
    CALL ISGPOS (460,45)
    CALL ITEXT (IFR,2,NUM)
    NUM(1)=53
    NUM(2)=48
    CALL ISGPOS (460,95)
    CALL ITEXT (IFR,2,NUM)
    NUM(1)=55
    NUM(2)=53
    CALL ISGPOS (460,145)
    CALL ITEXT (IFR,2,NUM)
    NUM1(1)=49
    NUM1(2)=48
    NUM1(3)=48
    CALL ISGPOS (460,192)
    CALL ITEXT (IFR,3,NUM1)
    NUM1(1)=49
    NUM1(2)=50
    NUM1(3)=53
    CALL ISGPOS (460,242)
    CALL ITEXT (IFR,3,NUM1)
    NUM1(1)=49
    NUM1(2)=53
    NUM1(3)=48
    CALL ISGPOS (460,292)
    CALL ITEXT (IFR,3,NUM1)
    NUM1(1)=49
    NUM1(2)=55
    NUM1(3)=53
    CALL ISGPOS (460,342)
    CALL ITEXT (IFR,3,NUM1)
    NUM1(1)=50
    NUM1(2)=48
  
```

```

        NUM1(3)=48
        CALL ISGPOS (460,392)
        CALL ISTEKT (IFR,3,NUM1)
        NUM1(1)=50
        NUM1(2)=50
        NUM1(3)=53
        CALL ISGPOS (460,442)
        CALL ISTEKT (IFR,3,NUM1)
100 CONTINUE
    GO TO 30

C
C   THIS SECTION BUILDS OUTPUT TABLES (GAUSSIAN)
C
198 WRITE (*,2)
    WRITE (*,*) 'ENTER THE NUMBER OF THE OUTPUT TABLE TO
    *      MODIFY'
    WRITE (*,*) '2-5 INCLUSIVE ALLOWED'
    READ (*,*) KTAB
    WRITE (*,*) 'ENTER THE MEAN VALUE FOR RED'
    READ (*,*) RMEAN
    WRITE (*,*) 'ENTER THE STD DEVIATION FOR THE RED'
    READ (*,*) RDEV
    WRITE (*,*) 'ENTER THE MEAN VALUE FOR GREEN'
    READ (*,*) GMEAN
    WRITE (*,*) 'ENTER THE STD DEVIATION FOR THE GREEN,'
    READ (*,*) GDEV
    WRITE (*,*) 'ENTER THE MEAN VALUE FOR BLUE'
    READ (*,*) BMEAN
    WRITE (*,*) 'ENTER THE STD DEVIATION FOR THE BLUE'
    READ (*,*) BDEV

C
C   CALCULATE THE VALUES FOR THE TABLE
C
    DO 199 I=0,255
        IRD=INT(255*(EXP(-0.5*((I-RMEAN)**2)/((RDEV)**2))))
        IGR=INT(255*(EXP(-0.5*((I-GMEAN)**2)/((GDEV)**2))))
        IBL=INT(255*(EXP(-0.5*((I-BMEAN)**2)/((BDEV)**2))))
        CALL ISLDOV(KTAB,I,IRD,IGR,IBL)
199 CONTINUE
    CALL ISOUTS(KTAB)
    GO TO 30

C   BUILD A COLOR TABLE USING THREE POINTS TO DEFINE TWO
C   LINES REPRESENTING THE VALUE FOR THE GIVEN INDEX.
C
201 WRITE (*,*) 'WHICH TABLE DO YOU WANT TO CHANGE 2-5'
    READ (*,*) NTAB

```

```

        IF (NTAB .LT. 2 .OR. NTAB .GT. 5) GO TO 99
        WRITE (*,*) 'ENTRIES MUST ALL BE INTEGERS FROM 0 TO
*           255'
C
C   CALCULATE THE RED LUT VALUES
C
200 WRITE (*,*) 'ENTER THE LOW RED VALUE      INDEX,
*           MAGNITUDE'
    READ (*,*) LWRDIDX, LWRDVAL
    IF (LWRDIDX .GT. 255 .OR. LWRDVAL .GT. 255) GO TO 200
205 WRITE (*,*) 'ENTER THE MIDDLE RED VALUE    INDEX,
*           MAGNITUDE'
    READ (*,*) MDRDIDX, MDRDVAL
    IF (MDRDIDX .GT. 255 .OR. MDRDVAL .GT. 255) GO TO 200
    IF (MDRDIDX .LE. LWRDIDX) THEN
        WRITE (*,*) 'INDEX TOO LOW'
        GO TO 205
    ENDIF
210 WRITE (*,*) 'ENTER THE HIGH RED VALUE      INDEX,
*           MAGNITUDE'
    READ (*,*) IHRDIDX, IHRDVAL
    IF (IHRDIDX .GT. 255 .OR. IHRDVAL .GT. 255) GO TO 200
    IF (IHRDIDX .LT. MDRDIDX) THEN
        WRITE (*,*) 'INDEX TOO LOW'
        GO TO 210
    ENDIF
    IRED(LWRDIDX) = LWRDVAL
    IRED(MDRDIDX) = MDRDVAL
    IRED(IHRDIDX) = IHRDVAL
    IF (LWRDIDX .EQ. 0) GO TO 216
    DO 215 I=0, LWRDIDX-1
        IRED(I)=0
215 CONTINUE
216 SLP=1.0*(MDRDVAL-LWRDVAL)/(MDRDIDX-LWRDIDX)
    DO 220 I=LWRDIDX+1, (MDRDIDX-1)
        RED(I)=LWRDVAL+SLP*(I-LWRDIDX)
        IRED(I)=INT(RED(I))
220 CONTINUE
    IF (IHRDIDX .EQ. MDRDIDX) GO TO 230
    SLP=1.0*(IHRDVAL-MDRDVAL)/(IHRDIDX-MDRDIDX)
    DO 225 I=MDRDIDX+1, (IHRDIDX-1)
        RED(I)=MDRDVAL+SLP*(I-MDRDIDX)
        IRED(I)=INT(RED(I))
225 CONTINUE

```

C CALCULATE THE GREEN LUT VALUES

C

```
230 WRITE (*,*) 'ENTER THE LOW GREEN VALUE    INDEX,
*           MAGNITUDE'
    READ (*,*)  LWGRIDX, LWGRVAL
    IF (LWGRIDX .GT. 255 .OR. LWGRVAL .GT. 255) GO TO 230
235 WRITE (*,*) 'ENTER THE MIDDLE GREEN VALUE    INDEX,
*           MAGNITUDE'
    READ (*,*)  MDGRIDX, MDGRVAL
    IF (MDGRIDX .GT. 255 .OR. MDGRVAL .GT. 255) GO TO 235
    IF (MDGRIDX .LE. LWGRIDX) THEN
        WRITE (*,*) 'INDEX TOO LOW'
        GO TO 235
    ENDIF
240 WRITE (*,*) 'ENTER THE HIGH GREEN VALUE    INDEX,
*           MAGNITUDE'
    READ (*,*)  IHGRIDX, IHGRVAL
    IF (IHGRIDX .GT. 255 .OR. IHGRVAL .GT. 255) GO TO 240
    IF (IHGRIDX .LT. MDGRIDX) THEN
        WRITE (*,*) 'INDEX TOO LOW'
        GO TO 240
    ENDIF
    IGREEN(LWGRIDX) = LWGRVAL
    IGREEN(MDGRIDX) = MDGRVAL
    IGREEN(IHGRIDX) = IHGRVAL
    IF (LWGRIDX .EQ. 0) GO TO 246
    DO 245 I=0, LWGRIDX-1
        IGREEN(I)=0
245 CONTINUE
246 SLP=1.0*(MDGRVAL-LWGRVAL)/(MDGRIDX-LWGRIDX)
    DO 250 I=LWGRIDX+1, (MDGRIDX-1)
        GREEN(I)=LWGRVAL+SLP*(I-LWGRIDX)
        IGREEN(I)=INT(GREEN(I))
250 CONTINUE
    IF (IHGRIDX .EQ. MDGRIDX) GO TO 260
    SLP=1.0*(IHGRVAL-MDGRVAL)/(IHGRIDX-MDGRIDX)
    DO 255 I=MDGRIDX+1, IHGRIDX-1
        GREEN(I)=MDGRVAL+SLP*(I-MDGRIDX)
        IGREEN(I)=INT(GREEN(I))
255 CONTINUE
```

C CALCULATE THE BLUE LUT VALUES

C

```
260 WRITE (*,*) 'ENTER THE LOW BLUE VALUE    INDEX,
*           MAGNITUDE'
    READ (*,*)  LWBLIDX, LWBLVAL
```

```

        IF (LWBLIDX .GT. 255 .OR. LWBLVAL .GT. 255) GO TO 260
265 WRITE (*,*) 'ENTER THE MIDDLE BLUE VALUE    INDEX,
*           MAGNITUDE'
        READ (*,*)   MDBLIDX, MDBLVAL
        IF (MDBLIDX .GT. 255 .OR. MDBLVAL .GT. 255) GO TO 265
        IF (MDBLIDX .LE. LWBLIDX) THEN
            WRITE (*,*) 'INDEX TOO LOW'
            GO TO 265
        ENDIF
270 WRITE (*,*) 'ENTER THE HIGH BLUE VALUE    INDEX,
*           MAGNITUDE '
        READ (*,*)   IHBLIDX, IHBLVAL
        IF (IHBLIDX .GT. 255 .OR. IHBLVAL .GT. 255) GO TO 270
        IF (IHBLIDX .LT. MDBLIDX) THEN
            WRITE (*,*) 'INDEX TOO LOW'
            GO TO 270
        ENDIF
        IBLUE(LWBLIDX) = LWBLVAL
        IBLUE(MDBLIDX) = MDBLVAL
        IBLUE(IHBLIDX) = IHBLVAL
        IF (LWBLIDX .EQ. 0) GO TO 276
        DO 275 I=0, LWBLIDX-1
            IBLUE(I)=0
275 CONTINUE
276 SLP=1.0*(MDBLVAL-LWBLVAL)/(MDBLIDX-LWBLIDX)
        DO 280 I=LWBLIDX+1, (MDBLIDX-1)
            BLUE(I)=LWBLVAL+(SLP*(I-LWBLIDX))
            IBLUE(I)=INT(BLUE(I))
280 CONTINUE
        IF (IHBLIDX .EQ. MDBLIDX) GO TO 290
        SLP=1.0*(IHBLVAL-MDBLVAL)/(IHBLIDX-MDBLIDX)
        DO 285 I=MDBLIDX+1, IHBLIDX-1
            BLUE(I)=MDBLVAL+SLP*(I-MDBLIDX)
            IBLUE(I)=INT(BLUE(I))
285 CONTINUE
C
C   DT-IRIS CALLS TO PUT THE CALCULATED VALUES IN THE TABLE.
C
290 CALL ISDISP(1)
        DO 296 I=0, 255
            CALL ISLDOV(NTAB, I, IRED(I), IGREEN(I), IBLUE(I))
296 CONTINUE
        CALL ISOUTS(NTAB)
        GO TO 30

```

C THIS SECTION CLEARS A DESIGNATED FRAME BUFFER.

C

```
399 WRITE (*,*) 'WHICH FRAME BUFFER WOULD YOU LIKE TO
      *          CLEAR?'
      READ (*,*) MFRAM
      CALL ISFCLR (MFRAM)
      GOTO 30
```

C

C THIS SECTION DISPLAYS A DESIGNATED FRAME BUFFER.

C

```
449 WRITE (*,*) 'WHICH FRAME BUFFER WOULD YOU LIKE TO
      *          VIEW?'
      READ (*,*) MFRAM
      CALL ISOTFR (MFRAM)
      GOTO 30
```

C

C PROGRAM ENDS. ISEND MUST BE USED TO PREVENT POSSIBLE
C CONFLICTS IN MEMORY.

C

```
500 CALL ISEND
      STOP
      END
```

B. DMA.FOR

C

C PROGRAM: DMA.FOR

C

WRITTEN BY: R. C. ENGEL

C

LAST REVISED: 07 AUGUST 1989

C

BY: RAY ENGEL

C

C THIS PROGRAM IS FOR CONTROLLING DMA INPUT TO RAM FROM
C 70000H TO A0000H. DATA RECEIVED BY DMA TRANSFER IS THEN
C SORTED TO RAM FROM 37C00H TO 70000H BEFORE BEING WRITTEN
C IN BLOCKS TO FRAME BUFFER MEMORY AT A00000H.

C

```
INTEGER*4 ISADRZ, IDADR, ISADR, IRADD1
INTEGER*4 IRADD2, IRADD3, IDADRX
INTEGER*2 NADDR(90), GDT1(24)
```

C

C FORMAT STATEMENTS.

C

2 FORMAT (//)

C

C MENU SECTION.

C

```
50 WRITE (*,2)
      WRITE (*,2)
```

```

WRITE (*,*) ' 1 = SINGLE DMA SET AFTER SECTOR FIND'
WRITE (*,*) ' 2 = IMMEDIATE SINGLE DMA SET'
WRITE (*,*) ' 3 = EXIT THE PROGRAM'
WRITE (*,2)
WRITE (*,*) ' ENTER VALUE 1-3 '
READ (*,*) IMODE
IF (IMODE .LT. 1 .OR. IMODE .GT. 3) GO TO 50
IF (IMODE .EQ. 2) GO TO 120
IF (IMODE .EQ. 3) GO TO 500

C
C THIS SECTION FINDS THE END OF ROTATION PULSE AND THEN
C COUNTS 2.66 SECONDS PER SECTOR TO FIND THE DESIRED AREA
C OF OBSERVATION. THE FIRST STEP IS TO PUT PORTS A AND B
C IN INPUT MODE. SEE PAGES 22 AND 24 OF THE PDMA-16
C MANUAL [REF. 4].
C
C SET PORT B FOR INPUT.
C
CALL OPORTB(754,0)
C
C INPUT FROM KEYBOARD THE SECTOR DESIRED TO DISPLAY
C
60 WRITE (*,*) 'ENTER THE SECTOR TO DISPLAY, (0.2-59.5
* ALLOWED)'
READ (*,*) SCTR
IF (SCTR .LT. 0.2 .OR. SCTR .GT. 59.5) GO TO 60
TIME = 2.66*SCTR

C
C NEXT THE END OF ROTATION SIGNAL MUST BE FOUND. THIS IS
C ON THE D0 BIT OF PORT B AND IS MUCH LONGER THAN THE
C SECTOR SIGNAL, WHICH IS ALSO ON D0. WHEN D0 GOES LOW,
C THE 30 KHZ ROTATION SIGNAL IS WATCHED FOR SIX CYCLES,
C THEN D0 IS CHECKED AGAIN. IF D0 IS STILL LOW, END-OF
C ROTATION HAS BEEN FOUND.
C
70 CALL IPORTB(753,ICLKS)
IEOR = IAND(ICLKS,1)
IF (IEOR.EQ.1) GO TO 70
DO 80 I=1,6
81 CALL IPORTB(753,ICLKS)
IEOR = IAND(ICLKS,2)
IF (IEOR.EQ.0) GO TO 81
82 CALL IPORTB(753,ICLKS)
IEOR = IAND(ICLKS,2)
IF (IEOR.EQ.2) GO TO 82
80 CONTINUE

```

```

C   D0 WENT LOW AND D1 HAS CYCLED SIX TIMES, IF D0 IS STILL
C   LOW THEN EOR HAS BEEN FOUND.
C
C       CALL IPORTB(753,ICLKS)
C       IEOR = IAND(ICLKS,1)
C       IF (IEOR.EQ.1) GO TO 70
C       CALL GETTIM(IHR,IMIN,ISEC,IHN)
C       CLKTIM=IHR*3600+IMIN*60+ISEC+IHN*0.01
C       WRITE (*,*) 'EOR FOUND, LOOKING FOR SECTOR ',SCTR
C
C   THE SECTOR IS FOUND BY COUNTING 2.66 SEC/SECTOR FROM THE
C   PC'S SYSTEM CLOCK. THIS PROCEDURE WAS NECESSARY BECAUSE
C   JITTER IN THE SECTOR CLOCK WOULD INADVERTENTLY TRIGGER
C   CYCLES WHICH DISRUPT THE COUNTING PROCESS.
C
C   90 CALL GETTIM(IHR,IMIN,ISEC,IHN)
C       CLKTIM1=IHR*3600+IMIN*60+ISEC+IHN*0.01
C       IF ((CLKTIM1-CLKTIM) .GT. TIME) GO TO 120
C       GO TO 90
C
C   HAVING COMPLETED THE PREVIOUS LOOP, THE CORRECT SECTOR
C   HAS BEEN LOCATED. THE NEXT THING TO DO IS FIND THE
C   STATUS OF THE 30 KHZ SCAN CLOCK. SINCE IT WILL HAVE
C   JUST GONE HIGH AT THE END OF A DMA TRANSFER, I NEED TO
C   ENTER THE DMA LOOP JUST AFTER A LOW TO HIGH TRANSITION.
C
C   120 CALL IPORTB(753,ICLKS)
C       ISCAN = IAND(ICLKS,4)
C       IF (ISCAN.EQ.4) GO TO 120
C   125 CALL IPORTB(753,ICLKS)
C       ISCAN = IAND(ICLKS,4)
C       IF (ISCAN.EQ.0) GO TO 125
C
C   THE NEXT SECTION SETS UP AND EXECUTES 3 CONSECUTIVE DMA
C   TRANSFERS FOR 65528 BYTES EACH TO STARTING ADDRESSES
C   H7000 TO H9000.
C
C       DO 150 I=7,9
C           CALL OPORTB(754,0)
C
C   DISABLE ANY DMA OPERATION IN PROGRESS.
C
C       CALL OPORTB(10,5)
C
C   SET THE PAGE (64 KB REGION) FOR THE TRANSFER
C

```

```

        CALL OPORTB(131,I)
C
C   LOAD TRANSFER OFFSET = 0, ALL TRANSFERS START ON
C   A BOUNDARY.
C
        CALL OPORTB(2,0)
        CALL OPORTB(2,0)
C
C   LOAD THE BYTE COUNT REGISTERS, LOW BYTE THEN HIGH BYTE
C   PDMA 16 ALWAYS DOES 1 EXTRA TRANSFER.
C   NUMBER = 256*HB + LB + 1 WHERE HB AND LB ARE 2ND
C   ARGUMENTS.
C
        CALL OPORTB(3,247)
        CALL OPORTB(3,255)
C
C   SET TRANSFER DIRECTION AND MODE (PAGE 13 OF I/O MANUAL).
C
        CALL OPORTB(11,69)
C
C   SCAN BIT SHOULD STILL BE HIGH, LOOK FOR IT TO GO LOW.
C   WHEN IT GOES HIGH AFTER THAT, START THE DMA.
C
151 CALL IPORTB(753,ICLKS)
    ISCAN = IAND(ICLKS,4)
    IF (ISCAN.EQ.4) GO TO 151
152 CALL IPORTB(753,ICLKS)
    ISCAN = IAND(ICLKS,4)
    IF (ISCAN.EQ.0) GO TO 152
C
C   START THE DMA. BIT D7 OF DMA REG, SEE PAGE 24 OF MANUAL.
C
        CALL OPORTB(754,128)
C
C   ENABLE 8237 MASK BIT
C
        CALL OPORTB(10,1)
        PRINT *, 'DMA TRANSFER RUNNING'
C
C   THIS SECTION CHECKS FOR COMPLETION OF DMA TRANSFER
C
155 CALL IPORTB(3,IL)
    CALL IPORTB(3,IH)
    NLEFT = 256*IH + IL
    IF (NLEFT.NE.65535) GO TO 155
150 CONTINUE

```

```

C
C THIS PROGRAM MOVES DATA FROM STANDARD RAM TO
C FRAMEGRABBER MEMORY FOR DISPLAY.
C
C THE DATA SEQUENCE IS THE PHYSICAL LOCATION OF THE NEXT
C CONSECUTIVE DETECTOR DATA IN RAM. (ie. DETECTOR 1 IS IN
C BASE + 0 WHILE DETECTOR 2 IS BASE + 6.)
    DATA NADDR/24,36,48,60,72,84,96,108,120,132,144,156,
    *168,0,12,25,37,49,61,73,85,97,109,121,133,145,157,
    *169,1,13,26,38,50,62,74,86,98,110,122,134,146,158,
    *170,2,14,27,39,51,63,75,87,99,111,123,135,147,159,
    *171,3,15,28,40,52,64,76,88,100,112,124,136,148,160,
    *172,4,16,29,41,53,65,77,89,101,113,125,137,149,161,
    *173,5,17/
C
C SCREEN MESSAGE.
C
    WRITE (*,2)
    WRITE (*,*) ' DMA TRANSFERS COMPLETE.  UNSCRAMBLING
    *          DATA AND '
    WRITE (*,*) ' WRITING TO FRAMEGRABBER MEMORY '
    WRITE (*,2)
C
C UNSCRAMBLING FROM DMA TRANSFERS TO 70000H AND 80000H FOR
C IMAGE DESTINED FOR FRAME BUFFER 0.
C ISADR* IS REFERRING TO SOURCE ADDRESSES.
C IDADR* REFERS TO DESTINATION ADDRESSES.
C
    ISADRZ=458752
    I=0
205 CALL PEEK(IOFST,ISADRZ+I,1)
    I=I+1
    IF (IOFST.NE.0) GO TO 205
    ISADRZ=458757+I
    IDADR=228352
    DO 210 I=1,90
        N=NADDR(I)
        DO 220 J=0,363
            ISADR=ISADRZ+(180*J+N)
            DO 230 L=0,4
                IDADRX=IDADR+L*512
                CALL BLKMOV(ISADR,IDADRX,1)
230         CONTINUE
            IDADR=IDADR+1
220     CONTINUE
        IDADR=IDADR+2196

```

```

210 CONTINUE
    ISADRZ=524288
    I=0
245 CALL PEEK(IOFST,ISADRZ+I,1)
    I=I+1
    IF (IOFST.NE.0) GO TO 245
    ISADRZ=524293+I
    IDADR=228352+364
    DO 250 I=1,90
        N=NADDR(I)
        DO 260 J=0,147
            ISADR=ISADRZ+(180*J+N)
            DO 270 L=0,4
                IDADRX=IDADR+L*512
                CALL BLKMOV(ISADR,IDADRX,1)
270         CONTINUE
            IDADR=IDADR+1
260     CONTINUE
        IDADR=IDADR+2412
250 CONTINUE
C
C   BLOCK TRANSFERS TO FRAME BUFFER 0.
C
    DO 290 I=0,3
        IRADD=10485760+I*57600
        ISADR=228352+I*57600
        IER = BLKMAT(GDT,ISADR,IRADD,28800)
290 CONTINUE
C
C   SORTING FROM 2ND AND 3RD DMA TRANSFERS FOR IMAGE
C   DESTINED TO FRAME BUFFER 1.
C
    ISADRZ=524288
    I=0
305 CALL PEEK(IOFST,ISADRZ+I,1)
    I=I+1
    IF (IOFST.NE.0) GO TO 305
    ISADRZ=524293+I
    IDADR=228352
    DO 310 I=1,90
        N=NADDR(I)
        DO 320 J=148,363
            ISADR=ISADRZ+(180*J+N)
            DO 330 L=0,4
                IDADRX=IDADR+L*512
                CALL BLKMOV(ISADR,IDADRX,1)

```



```

C
  IMPLICIT INTEGER*2  (I-N)
  IMPLICIT COMPLEX    (C)
  DIMENSION          CG(512),RELINE(512),REI(512),XRES(90)
  DIMENSION          AMAG(512),S8(512)
  INTEGER*2          IROW1(0:511),IROW2(0:511),IROW3(0:511)
  INTEGER*2          IROW4(0:511),IROW5(0:511),LINE(512)
  INTEGER*2          IBACK(15360),NUM(2),NUM1(3),IBTTM(9)
  INTEGER*2          ISIXA(0:255),ISIXB(0:255),NFRAME,ITOP(9)
  CHARACTER*30       FILE$, ANS$*1

C
C  FORMAT STATEMENTS.
C
  2 FORMAT (/)

C
C  ISINIT MUST BEGIN ALL DT-IRIS PROGRAMS.  ISDISP(1) PUTS
C  THE FRAMEGRABBER IN DISPLAY MODE.
C
  CALL ISINIT
  CALL ISDISP(1)

C
C  MENU SECTION.
C
  50 WRITE (*,2)
  WRITE (*,*) ' 1 = select the frame buffer to display '
  WRITE (*,*) ' 2 = select/change output look-up table '
  WRITE (*,*) ' 3 = make 6 degree image in buf 2 '
  WRITE (*,*) ' 4 = correct for detector responsivity
*          differences '
  WRITE (*,*) ' 5 = fill in lines for bad detectors '
  WRITE (*,*) ' 6 = apply MTF correction '
  WRITE (*,*) ' 7 = smooth out 1 detector to 5 row
*          expansion
  WRITE (*,*) ' 8 = store a frame to a file '
  WRITE (*,*) ' 9 = retrieve a file to a buffer '
  WRITE (*,*) '10 = copy one buffer to another '
  WRITE (*,*) '11 = subtract one buffer from another '
  WRITE (*,*) '12 = exit this program '
  READ (*,*) KSELCT
  IF (KSELCT .LT. 1 .OR. KSELCT .GT. 12) GO TO 50
  GO TO (100,200,300,400,500,600,700,800,900,
*1000,1100,1500),KSELCT

C
C  THIS SECTION SELECTS THE FRAME BUFFER TO DISPLAY
C
  100 WRITE (*,*) 'WHICH FRAME BUFFER WOULD YOU LIKE TO

```

```

      *              VIEW?'
      READ (*,'(I2)') NFRAME
      CALL ISOTFR (NFRAME)
      GO TO 50

C
C   THIS SECTION SELECTS THE ACTIVE OUTPUT LOOK-UP TABLE.
C
200 WRITE (*,*) ' SELECT LUT BY NUMBER 0-5'
      READ (*,*) ITAB
      CALL ISOUTS(ITAB)
      GO TO 50

C
C   THIS SECTION BUILDS A 6 DEGREE HORIZONTAL IMAGE IN FRAME
C   BUFFER 2 FROM THE 3 DEGREE IMAGES IN BUFFERS 0 AND 1.
C
300 CALL ISDIVC(0,2,2)
      CALL ISDIVC(1,2,3)
      DO 310 J=0,449,5
          CALL ISGETP(2,J,0,512,IROW1)
          CALL ISGETP(3,J,0,512,IROW2)
          DO 320 K=0,511,2
              ISIXA(K/2)=IROW1(K)+IROW1(K+1)
              ISIXB(K/2)=IROW2(K)+IROW2(K+1)
320      CONTINUE
          DO 321 K=0,4
              L=J+K
              CALL ISPUTP(2,L,0,256,ISIXA)
              CALL ISPUTP(2,L,256,256,ISIXB)
321      CONTINUE
310 CONTINUE

C
C   THIS SECTION ADDS LABELS AND A COLOR SCALE ACROSS THE
C   BOTTOM OF THE DISPLAY SCREEN FOR FRAME BUFFER 2.
C
      NFRAME=2
      DO 330 I=0,29
          DO 340 J=0,510,2
              IBACK(I*512+J+1)=J/2
              IBACK(I*512+J+2)=J/2
340      CONTINUE
330 CONTINUE
      CALL ISPUTP (NFRAME,450,0,15360,IBACK)
      CALL ISSFNT (0)
      NUM(1)=50
      NUM(2)=53
      CALL ISGPOS (460,45)

```

```

CALL ITEXT (NFRAME, 2, NUM)
NUM(1)=53
NUM(2)=48
CALL ISGPOS (460, 95)
CALL ITEXT (NFRAME, 2, NUM)
NUM(1)=55
NUM(2)=53
CALL ISGPOS (460, 145)
CALL ITEXT (NFRAME, 2, NUM)
NUM1(1)=49
NUM1(2)=48
NUM1(3)=48
CALL ISGPOS (460, 192)
CALL ITEXT (NFRAME, 3, NUM1)
NUM1(1)=49
NUM1(2)=50
NUM1(3)=53
CALL ISGPOS (460, 242)
CALL ITEXT (NFRAME, 3, NUM1)
NUM1(1)=49
NUM1(2)=53
NUM1(3)=48
CALL ISGPOS (460, 292)
CALL ITEXT (NFRAME, 3, NUM1)
NUM1(1)=49
NUM1(2)=55
NUM1(3)=53
CALL ISGPOS (460, 342)
CALL ITEXT (NFRAME, 3, NUM1)
NUM1(1)=50
NUM1(2)=48
NUM1(3)=48
CALL ISGPOS (460, 392)
CALL ITEXT (NFRAME, 3, NUM1)
NUM1(1)=50
NUM1(2)=50
NUM1(3)=53
CALL ISGPOS (460, 442)
CALL ITEXT (NFRAME, 3, NUM1)
CALL ISOTFR(NFRAME)
GO TO 50

```

```

C
C THIS SECTION CORRECTS FOR THE DIFFERENT RESPONSES OF THE
C DETECTORS IN THE ARRAY.
C
C THIS DATA SET CONTAINS THE VALUES OF RESPONSIVITY FOR

```

C THE LEAD ARRAY AS MEASURED BY AYERS IN HIS EVALUATION OF
C THE NPS-IRSTD.
C

```
DATA XRES/1.522,1.350,1.580,1.904,1.900,1.747,1.681,
*0.071,1.651,1.622,1.762,1.631,1.583,1.790,0.400,
*1.751,1.838,1.782,1.702,1.691,1.750,1.763,1.612,
*1.791,1.643,1.592,1.642,1.661,1.581,0.050,1.611,
*1.692,1.702,1.722,1.800,1.830,1.650,1.381,1.680,
*1.740,1.604,1.730,1.756,1.712,1.693,1.831,1.840,
*1.811,1.811,0.030,1.665,1.699,1.794,1.835,1.791,
*1.712,1.729,1.702,1.791,1.729,1.690,1.679,1.673,
*1.790,1.742,1.819,1.668,1.733,1.820,1.720,1.770,
*1.592,1.824,1.833,0.035,0.030,1.829,0.030,1.902,
*1.870,1.876,1.854,1.704,1.621,1.711,1.751,1.662,
*1.662,1.640,1.681/
```

C
C SELECT FRAME TO CORRECT.
C

```
400 WRITE (*,*) ' ENTER NUMBER OF FRAME TO CORRECT '
READ (*, '(I2)') NFRAME
```

C
C COMPUTE THE AVERAGE OF THE RESPONSIVITY VALUES.
C

```
AVGRES=0
DO 410 I=1,90
IF (XRES(I) .LT. 0.7*AVGRES/I) XRES(I)=AVGRES/(I-1)
* AVGRES=AVGRES+XRES(I)
410 CONTINUE
AVGRES=AVGRES/90
```

C
C CORRECT EACH ROW OF VALUES BASED ON THE RELATIVE
C REPSONSIVITY.
C

```
DO 420 I=0,445,5
CALL ISGETP(NFRAME,I,0,512,IROW1)
DO 430 J=0,511
IROW2(J)=INT((IROW1(J)-128)*AVGRES/
* XRES((I/5)+1)+128)
IF (IROW2(J) .GT. 255) IROW2(J)=255
430 CONTINUE
DO 440 K=0,4
CALL ISPUTP(NFRAME,I+K,0,512,IROW2)
440 CONTINUE
420 CONTINUE
CALL ISOTFR(NFRAME)
CALL ISDISP(1)
```

```

      GO TO 50
C
C   THIS PROGRAM FILLS THE ROWS FROM BAD DETECTORS IN THE
C   SCENE BY A LINEAR APPROXIMATION BETWEEN THE VALUES OF
C   THE ROWS ABOVE AND BELOW THE BAD DETECTOR.
C
C   ROWS BOUNDING BAD DETECTORS.
C
      DATA ITOP/44,59,144,199,219,294,369,404,439/
      DATA IBTTM/50,80,150,205,225,305,380,410,445/
C
C   SELECT THE FRAME TO BE CORRECTED.
C
500  WRITE (*,*) ' ENTER THE NUMBER OF THE FRAME FILL IN '
      READ (*,'(I2)') NFRAME
C
C   DISPLAY THE FRAME BEING CHANGED.
C
      CALL ISDISP(1)
      CALL ISOTFR(NFRAME)
C
C   CALCULATE THE APPROPRIATE PIXEL VALUES AND WRITE THEM TO
C   MEMORY.
C
      DO 505 I=1,9
        CALL ISGETP(NFRAME,ITOP(I),0,512,IROW1)
        CALL ISGETP(NFRAME,IBTTM(I),0,512,IROW3)
        NDIF=IBTTM(I)-ITOP(I)
        DO 510 J=ITOP(I)+1,IBTTM(I)-1
          DO 515 K=0,511
            IROW2(K)=INT(1.0*((IROW3(K)-IROW1(K))/NDIF)*
*              (J-ITOP(I)))+IROW1(K)
515      CONTINUE
          CALL ISPUTP(NFRAME,J,0,512,IROW2)
510      CONTINUE
505  CONTINUE
      GO TO 50
C
C   THIS SECTION ALLOWS CORRECTIONS FOR THE DEGRADATIONS IN
C   THE IMAGE CAUSED BY THE MTF OF THE LENS IN THE X AND Y
C   DIRECTION, THE CONVOLUTION OF THE DETECTOR SCAN IN THE X
C   DIRECTION, AND THE DETECTOR MTF IN THE Y DIRECTION.
C
C   SELECT THE DESIRED FRAME TO CORRECT.
C
600  WRITE (*,*) 'WHICH FRAME TO MTF CORRECT '

```

```

        READ (*,'(I2)') NFRAME
        IF (NFRAME .LT. 0 .OR. NFRAME .GT. 15) GO TO 600
        CALL ISDISP(1)
        CALL ISOTFR(NFRAME)
C
C      CHOOSE THE PARTICULAR ASPECT TO MANIPULATE.
C
601 WRITE (*,*) ' 1 = X-DIRECTION SCAN DECONVOLUTION '
    WRITE (*,*) ' 2 = X-DIRECTION OPTICS '
    WRITE (*,*) ' 3 = Y-DIRECTION OPTICS '
    WRITE (*,*) ' 4 = RETURN TO MAIN MENU '
    READ (*,*) ISELCT
    IF (ISELCT .LT. 1 .OR. ISELCT .GT. 5) GO TO 605
    GO TO (602,605,650,50),ISELCT
C
C      MTF OF THE DETECTOR IS THE FOURIER TRANSFORM OF ITS
C      SHAPE, A SINC FUNCTION.
C
602 WRITE (*,2)
    WRITE (*,2)
    WRITE (*,*) ' THIS TAKES TIME, SO BE PATIENT '
    S8(1)=1
    DO 603 I=1,257
        S8(I)=SIN(3.14159*0.0003*18.65*I)/
        *      (3.14159*0.0003*18.65*I)
        IF (S8(I) .LT. 0.2) S8(I)=0
        S8(514-I)=S8(I)
603 CONTINUE
    GO TO 609
C
C      THIS SECTION BUILDS A GAUSSIAN APPROXIMATION TO THE MTF
C      CURVE FOR THE NPS-IRSTD X-DIRECTION OPTICS.
C
605 WRITE (*,2)
    WRITE (*,2)
    WRITE (*,*) ' THIS TAKES TIME, SO BE PATIENT '
    S8(1)=1

    DO 606 I=2,257
        S8(I)=EXP(-1.0*(I**2)/72000)
        IF (S8(I) .LT. 0.2) S8(I)=0
        S8(514-I)=S8(I)
606 CONTINUE
C
C      WITH THE MTFs CALCULATED, EACH ROW IS REMOVED FROM THE
C      ARRAY AND PROCESSED USING THE CONVOLUTION THEOREM BEFORE

```

```

C   BEING PUT BACK INTO THE IMAGE.
C
609 DO 610 J=0,449,5
      CALL ISGETP(NFRAME,J,0,512,LINE)
      DO 620 K=1,512
        RELINE(K)=LINE(K)-128.0
620   CONTINUE
      N=512
      ID=1
      N1=9
      CALL PREPRO(RELINE,CG,N)
      CALL FFT(CG,ID,N1)

      DO 625 L=1,512
        IF (S8(L) .LT. 0.3) THEN
          CG(L)=0
          GO TO 625
        ENDIF
        CG(L)=CG(L)/S8(L)
625   CONTINUE
      ID=0
      CALL FFT(CG,ID,N1)
      CALL POSPRO(CG,RELINE,AMAG,N)
      DO 630 M=1,512
        LINE(M)=INT(RELINE(M)+128)
        IF (LINE(M) .GT. 255) LINE(M)=255
630   CONTINUE
      DO 635 L=0,4
        CALL ISPUTP(NFRAME,J+L,0,512,LINE)
635   CONTINUE
610 CONTINUE
      CALL ISOTFR(NFRAME)
      GO TO 601

C
C   THIS SECTION BUILDS A GAUSSIAN APPROXIMATION TO THE MTF
C   CURVE FOR THE NPS-IRSTD Y-DIRECTION OPTICS.
C
650 WRITE (*,2)
      WRITE (*,2)
      WRITE (*,*) ' THIS TAKES TIME, AND LOTS OF IT '
      WRITE (*,*) ' SO SIT BACK AND RELAX '
      WRITE (*,2)
      S8(1)=1
      DO 652 I=2,257
        S8(I)=EXP(-1.0*(I**2)/3.27E+6)
        IF (S8(I) .LT. 0.2) S8(I)=0

```

```

        S8(514-I)=S8(I)
652 CONTINUE
C
C   WITH THE MTF CALCULATED, EACH ROW IS REMOVED FROM THE
C   ARRAY AND PROCESSED USING THE CONVOLUTION THEOREM BEFORE
C   BEING PUT BACK INTO THE IMAGE.
C
      DO 660 J=1,512
        WRITE (*,'(A18,2X,I3,2X,A7)') ' WORKING ON COLUMN',
*                                     J-1,' OF 255'
        DO 662 K=0,449,5
          CALL ISGETP(NFRAME,K,J-1,1,LDET)
          RELINE((K/5)+1)=LDET-128.0
662    CONTINUE
        DO 664 K=91,512
          RELINE(K)=0
664    CONTINUE
        N=512
        ID=1
        N1=9
        CALL PREPRO(RELINE,CG,N)
        CALL FFT(CG,ID,N1)
        DO 675 L=1,512
          IF (S8(L) .LT. 0.3) THEN
            CG(L)=0
            GO TO 675
          ENDIF
          CG(L)=CG(L)/S8(L)
675    CONTINUE
        ID=0
        CALL FFT(CG,ID,N1)
        CALL POSPRO(CG,RELINE,AMAG,N)
        DO 677 K=0,449,5
          LDET=INT(128+RELINE((K/5)+1))
          IF (LDET .GT. 255) LDET=255
          CALL ISPUTP(NFRAME,K,J-1,1,LDET)
          CALL ISPUTP(NFRAME,K+1,J-1,1,LDET)
          CALL ISPUTP(NFRAME,K+2,J-1,1,LDET)
          CALL ISPUTP(NFRAME,K+3,J-1,1,LDET)
          CALL ISPUTP(NFRAME,K+4,J-1,1,LDET)
677    CONTINUE
660 CONTINUE
      GO TO 601

```

```

C   THIS SECTION SMOOTHS OUT THE 1 TO 5 ROW EXPANSION USED
C   IN THE DMA PROCESS TO FILL UP THE DISPLAY.  THE ROWS ARE
C   WEIGHTED TO LIMIT THE OVERALL EFFECT.
C
      WRITE (*,*) 'ENTER THE NUMBER OF THE FRAME TO SMOOTH '
      READ (*, '(I2)') NFRAME
      WRITE (*,2)
      WRITE (*,2)
      WRITE (*,*) ' THIS TAKES TIME, SO BE PATIENT '

C
C   DISPLAY THE SELECTED FRAME
C
      CALL ISDISP(1)
      CALL ISOTFR(NFRAME)

C
C   PULL 5 ROWS OUT, AND APPLY A WEIGHTED AVERAGE TO
C   RECALCULATE THE VALUES FOR THE CENTER ROW.
C
C   SELECT FRAME TO CORRECT.
C
700  WRITE (*,*) ' ENTER NUMBER OF FRAME TO CORRECT '
      READ (*, '(I2)') NFRAME
      DO 701 I=2,447
          CALL ISGETP (NFRAME,I-2,0,512,IROW1)
          CALL ISGETP (NFRAME,I-1,0,512,IROW2)
          CALL ISGETP (NFRAME,I,0,512,IROW3)
          CALL ISGETP (NFRAME,I+1,0,512,IROW4)
          CALL ISGETP (NFRAME,I+2,0,512,IROW5)
          DO 705 J=0,511
              IROW3(J)=(IROW1(J)+2*IROW2(J)+3*IROW3(J)+
*              2*IROW4(J)+IROW5(J))/9
705      CONTINUE
          CALL ISPUTP (NFRAME,I,0,512,IROW3)
701  CONTINUE
      GO TO 50

C
C   THIS SECTION ALLOWS SAVING A FRAME BUFFER TO A FILE.
C   IT AUTOMATICALLY ENCODES DATE, TIME, AND OTHER DATA.
C   SEE APPENDIX C OF THE DT-IRIS MANUAL.
C
C
800  WRITE (*,*) ' WHICH FRAME WOULD YOU LIKE TO SAVE '
      WRITE (*,*) ' ENTER VALUE 0 TO 15 '
      READ (*, '(I2)') NFRAME
      IF (NFRAME .LT. 0 .OR. NFRAME .GT. 15) GO TO 800
      WRITE (*,*) ' TYPE THE NAME, INCLUDING EXTENSION '

```

```

WRITE (*,*) ' OF THE FILE TO WRITE THE FRAME '
READ (*,'(A30)') FILE$
CALL ISSAVE(NFRAME,0,1,0,FILE$)
GO TO 50

C
C THIS SECTION ALLOWS RESTORING DT-IRIS FILES TO A FRAME
C BUFFER.
C
900 WRITE (*,*) ' ENTER NAME OF FILE TO RETRIEVE '
READ (*,'(A30)') FILE$
WRITE (*,*) ' RESTORE TO FRAME ? (VALUE 0 TO 15) '
READ (*,'(I2)') NFRAME
IF (NFRAME .LT. 0 .OR. NFRAME .GT. 15) GO TO 900
CALL ISREST(NFRAME,0,0,FILE$)
CALL ISOTFR(NFRAME)
GO TO 50

C
C THIS SECTION ALLOWS ONE BUFFER TO BE COPIED TO A SECOND
C BUFFER.
C
1000 WRITE (*,*) ' ENTER THE NUMBER OF THE SOURCE BUFFER '
READ (*,'(I2)') NFRAME
IF (NFRAME .LT. 0 .OR. NFRAME .GT. 15) GO TO 1000
WRITE (*,*) ' ENTER THE NUMBER OF THE DESTINATION
*          BUFFER '
READ (*,*) IDEST
IF (IDEST .LT. 0 .OR. IDEST .GT. 15) GO TO 1000
CALL ISFCOP(NFRAME,IDEST)
CALL ISDISP(1)
CALL ISOTFR(IDEST)
WRITE (*,*) ' YOU ARE NOW LOOKING AT THE DESTINATION
*          BUFFER '
GO TO 50

C
C THIS SECTION ALLOWS ONE BUFFER TO BE SUBTRACTED FROM
C ANOTHER.
C
1100 WRITE (*,*) ' ENTER THE NUMBER OF THE BUFFER TO BE
*          SUBTRACTED '
READ (*,'(I2)') NFRAME
IF (NFRAME .LT. 0 .OR. NFRAME .GT. 15) GO TO 1000
WRITE (*,*) ' ENTER THE FRAME TO SUBTRACT IT FROM '
READ (*,*) IDEST
IF (IDEST .LT. 0 .OR. IDEST .GT. 15) GO TO 1000
CALL ISSUB(NFRAME,IDEST,IDEST)
CALL ISDISP(1)

```

```

        CALL ISOTFR(IDEST)
        WRITE (*,*) 'YOU ARE NOW LOOKING BUFFER ',IDEST
        GO TO 50
C
C   PROGRAM ENDS.  ISEND MUST BE USED TO PREVENT POSSIBLE
C   CONTAMINATION OF SUBSEQUENT PROGRAMS.
C
1500 CALL ISEND
      STOP
      END
C
C   SUBROUTINES IN THIS SECTION WERE WRITTEN BY PROF. E.A.
C   MILNE AND USED FOR THE LAE II CLASS (PH 2013) FOR
C   INSTRUCTION ON USE OF THE FAST FOURIER TRANSFORM.
C
      SUBROUTINE FFT(CG,ID,N1)
C   FOURIER TRANSFORM SUBROUTINE           Latest update 3/14/88
C                                           by E. A. Milne
C   PARAMETERS IN THE CALL
C   CG(*)  = COMPLEX INPUT ARRAY AND OUTPUT ARRAY
C   ID = 1  FOR FORWARD TRANSFORM AND  ID = 0 FOR INVERSE
C   TRANSFORM.
C   N1 IS A MEASURE OF THE SIZE OF THE ARRAY TO BE
C   TRANSFORMED.
C   SQ=SQRT(FLOAT(N2)) = NORMALIZING FACTOR
C
C   LOCAL VARIABLES USED
C   I, LL, M, K, L, J, AND N = INTEGERS USED AS ARRAY
C   INDICES OR OR DO LOOP INDICES OR BOTH.
C   KL AND KU ARE INTEGERS FOR THE LOWER AND UPPER LIMITS OF
C   A DO LOOP.
C   N2 = 2**N1  = THE TOTAL NUMBER OF TERMS IN THE ARRAY.
C   TH = 2*PI/N2  = PHASE ANGLE INCREMENT.
C
      TYPE DECLARATION
C
      IMPLICIT COMPLEX (C)
      IMPLICIT INTEGER*2 (I-N)
      DIMENSION CG(1)
C
C   N2 AND TH ARE CALCULATED
C
      N2=2**N1
      TH=6.283185/N2

```

```

C   THIS SECTION IS THE SUMMING SECTION -  N1 SUMS
C
2 DO 5 M=1,N1
    K=2** (N1-M)
    L=2** (M-1)
    DO 4 LL=1,L
        KC=LL-1
        CALL BITINV (KC,N,N1-1)
        CD=CEXP (CMPLX (0.,TH*FLOAT (N)))
        IF (ID.EQ.1) CD=CONJG (CD)
        KL=2*KC*K+1
        KU=KL+K-1
        DO 3 I=KL,KU
            CA=CG (I)+CG (I+K) *CD
            CG (I+K)=CG (I)-CG (I+K) *CD
            CG (I)=CA
3        CONTINUE
4    CONTINUE
5 CONTINUE

C
C   THE REORDERING AND NORMALIZATION IS DONE IN THIS SECTION
C
    IF (ID.EQ.1) THEN
        SQ=1.0
    ELSE
        SQ=FLOAT (N2)
    ENDIF
    DO 8 I=1,N2
        J=I-1
        CALL BITINV (J,N,N1)
        IF (J-N) 6,7,8
6        N=N+1
        CA=CG (I) /CMPLX (SQ,0.0)
        CG (I)=CG (N)
        CG (N)=CA
7        CG (I)=CG (I) /CMPLX (SQ,0.0)
8 CONTINUE

C
C   NOW RETURN
C
    RETURN
    END

```

```

      SUBROUTINE BITINV(K,L,M)
C   FINDS THE BIT INVERSION OF A (M) BIT NUMBER (K) TO (L)
C   THIS IS USED IN THE FOURIER TRANSFORM SUBROUTINE
      IMPLICIT INTEGER*2 (I-N)
      J=K
      L=0
      DO 1 I=1,M
        L=L*2+J-J/2*2
1    J=J/2
      RETURN
      END

C
C
      SUBROUTINE PREPRO(RE,CG,N)
C
C   THIS SUBROUTINE CONVERTS A REAL ARRAY RE TO A COMPLEX
C   ARRAY CG TO BE USED BY THE FFT ROUTINE.
C
      IMPLICIT INTEGER*2 (I-N)
      IMPLICIT COMPLEX (C)
      DIMENSION RE(N),CG(N)
      DO 1 I = 1, N
        CG(I)=CMPLX(RE(I),0.0)
1    CONTINUE
      RETURN
      END

C
C
      SUBROUTINE POSPRO(CG,RE,AMAG,N)
C
C   THIS SUBROUTINE TAKES A COMPLEX ARRAY AND FINDS THE REALS
C   RE, THE IMAGINARIES AIM, THE MAGNITUDES AMAG, THE PHASES
C   PH, AND THE POWER SPECTRUM PO SO THAT THEY CAN BE
C   SEPARATELY PLOTTED.
C
      IMPLICIT INTEGER*2 (I-N)
      IMPLICIT COMPLEX (C)
      DIMENSION CG(N),RE(N),AMAG(N)
      DO 1 I = 1, N
        RE(I)= REAL(CG(I))
        AMAG(I)=CABS(CG(I))
1    CONTINUE
      RETURN
      END

```

```

      SUBROUTINE HAMM(RS, RD, N1)
C
C   THIS SUBROUTINE PARTIALLY REMOVES THE DISCONTINUITY
C   BETWEEN THE FIRST AND LAST POINTS OF THE ARRAY RS AND
C   STORES THE RESULT IN THE ARRAY RD.  AS A NOTE TO FUTURE
C   USERS OF THIS SYSTEM WHEN THIS ROUTINE WAS INCLUDED IN
C   THE PROCESSING, IT PRODUCED SEVERE INTENSITY REDUCTIONS
C   IN THE SIDES OF THE IMAGE.
C
C   THE NUMBER OF POINTS IN THE ARRAY = N = 2**N1
C
      IMPLICIT INTEGER*2 (I-N)
      DIMENSION RS(1), RD(1)
      N=2**N1
      DO 10 I = 1, N
        RD(I)=RS(I)*(0.54-.46*COS(6.283185*FLOAT(I-1)/
          *      FLOAT(N-1)))
10 CONTINUE
      RETURN
      END
C
      SUBROUTINE HANN(RS, RD, N1)
C
C   THIS SUBROUTINE COMPLETELY REMOVES THE DISCONTINUITY
C   BETWEEN THE FIRST AND LAST POINTS OF THE ARRAY RS AND
C   STORES THE RESULT IN RD.
C
C   THE NUMBER OF POINTS IN THE ARRAY = N = 2**N1
C
      IMPLICIT INTEGER*2 (I-N)
      DIMENSION RS(1), RD(1)
      N=2**N1
      DO 10 I = 1, N
        RD(I)=RS(I)*0.5*(1.-COS(6.283185*FLOAT(I-1)/
          *      FLOAT(N-1)))
10 CONTINUE
      RETURN
      END

```

APPENDIX D

I. NPS-IRSTD DETECTOR CALIBRATION DATA

A. RELATIVE RESPONSIVITY RESULTS

<u>Side 1</u>	<u>Amplitude (volts)</u>	<u>Side 2</u>	<u>Amplitude (volts)</u>
101	1.522	* 201	0.020
102	1.350	202	3.433
103	1.580	203	3.382
104	1.904	204	3.189
105	1.900	205	3.512
106	1.747	206	3.400
107	1.681	207	3.261
* 108	0.071	208	3.321
109	1.651	209	3.302
110	1.622	210	3.163
111	1.762	211	3.132
112	1.631	212	3.320
113	1.583	213	3.251
114	1.790	214	3.189
* 115	0.400	215	3.180
116	1.751	216	3.166
117	1.838	217	3.262
118	1.782	218	3.305
119	1.702	219	3.391
120	1.691	220	3.119
121	1.750	221	2.802
122	1.763	222	3.028
123	1.612	223	3.202
124	1.791	224	3.270
125	1.643	225	3.140
126	1.592	* 226	0.020
127	1.642	* 227	0.022
128	1.661	* 228	0.600
129	1.581	* 229	0.600
* 130	0.050	* 230	0.030
131	1.611	* 231	3.050
132	1.692	232	2.475
133	1.702	233	3.050
134	1.722	234	3.000

* Denotes that the detector channel's response is irregular.

<u>Side 1</u>	<u>Amplitude (volts)</u>	<u>Side 2</u>	<u>Amplitude (volts)</u>
135	1.800	235	3.322
136	1.830	236	3.120
137	1.650	237	3.122
138	1.381	238	3.030
139	1.680	239	3.150
140	1.740	240	3.361
141	1.604	241	3.281
142	1.730	242	3.410
143	1.756	243	3.450
144	1.712	244	3.452
145	1.693	245	3.404
146	1.831	246	3.303
147	1.840	247	3.233
148	1.811	248	3.261
149	1.811	249	3.383
* 150	0.030	* 250	1.183
151	1.665	251	3.291
152	1.699	252	3.268
153	1.794	253	3.113
154	1.835	254	3.201
155	1.791	255	3.242
156	1.712	256	3.144
157	1.729	257	3.109
158	1.702	258	3.280
159	1.791	259	3.131
160	1.729	260	3.231
161	1.690	261	3.058
162	1.679	262	2.911
163	1.673	263	3.102
164	1.790	264	3.055
165	1.742	265	3.141
166	1.819	266	3.031
167	1.668	267	3.101
168	1.733	268	3.149
169	1.820	269	3.267
170	1.720	270	3.110
171	1.770	* 271	0.015
172	1.592	272	3.340
173	1.824	273	3.299
174	1.833	274	3.219
* 175	0.035	275	3.160
* 176	0.030	276	3.042
177	1.829	277	3.164
* 178	0.030	* 278	2.613
179	1.902	* 279	2.580

<u>Side 1</u>	<u>Amplitude (volts)</u>	<u>Side 2</u>	<u>Amplitude (volts)</u>
180	1.870	* 280	2.480
181	1.876	281	3.142
182	1.854	282	2.970
183	1.704	283	2.882
184	1.621	284	3.082
185	1.711	285	3.213
186	1.751	286	3.330
187	1.662	287	3.161
188	1.662	288	2.952
189	1.640	289	2.840
190	1.681	290	2.919

* Denotes that the detector channel's response is irregular

B. LIST OF DEFECTIVE DETECTOR CHANNELS

<u>Lag Array</u>	<u>Lead Array</u>
01	08
26	15
27	30
28	50
29	75
30	76
50	78
71	
* 78	
* 79	
* 80	

* Denotes that detector is operational but signal strength is significantly diminished.

LIST OF REFERENCES

1. Parker, Gary W., *Optical Performance Implications of Naval Postgraduate School Modifications to the AN/SAR-8 Infrared Search and Target Designation System*, Master's Thesis, Naval Postgraduate School, Monterey, CA, September 1986.
2. Ayers, Gary R., *Calibration and Initialization of the NPS Modified Infrared Search and Target Designation (IRSTD) System*, Master's Thesis, Naval Postgraduate School, Monterey, CA, December 1987.
3. Naval Postgraduate School Report NPS61-89-011CR, *Modification, Testing, and Calibration of Infrared Search and Target Designation Hardware Received from NSWC*, by Cooper, A. W. and Crittenden, E. C. Jr., 9 May 1987.
4. *PDMA-16 Manual*, Metrabyte Corporation, Taunton, MA, 1986.
5. *IRIS Tutor User Manual*, 3rd ed., Data Translation, Inc., Marlboro, MA, 1987.
6. *DT-IRIS User Manual*, 3rd ed., Data Translation Inc., Marlboro, MA, 1988.
7. *User Manual for DT-2861 High Speed Arithmetic Framegrabber*, 1st ed., Data Translation Inc., Marlboro, MA, 1987.
8. Telephone conversation between ONTAR Corporation Technical Support Representative and the Author, 16 May 1989.
9. Lloyd, J. M., *Thermal Imaging Systems*, Plenum Press, New York, NY, 1975.
10. *The Infrared Newsletter*, Vol. 19, No. 1, Infrared Information Analysis Center, Ann Arbor, MI, 1989.
11. *The Infrared Handbook*, Office of Naval Research, Department of the Navy, Washington, DC, 1978.
12. *The Electro-Optics Handbook*, 2nd ed., p. 162, RCA Corporation, Lancaster, PA, 1974.
13. *Photonics Design and Applications Handbook*, 33rd ed., Laurin Publishing Co., Pittsfield, MA, 1987.
14. Brigham, E. O., *The Fast Fourier Transform*, Prentice-Hall, Inc., Englewood Cliffs, NJ, 1974.

15. Cooper, A. W., and Crittenden, E. C. Jr., "Electro-Optics", course text material for NPS Electro-Optics course PH3252, Naval Postgraduate School, Monterey, CA, November 1987.
16. Hecht, E., *Optics*, Addison-Wesley Publishing Company, Menlo Park, CA, 1987.

INITIAL DISTRIBUTION LIST

- | | |
|-----------------------------------------------------------------------------------------------------------------------------------|---|
| 1. Defense Technical Information Center
Cameron Station
Alexandria, VA 22304-6145 | 2 |
| 2. Library, Code 0142
Naval Postgraduate School
Monterey, CA 93943-5002 | 2 |
| 3. Professor K.E. Woehler, Code 61Wh
Chairman, Department of Physics
Naval Postgraduate School
Monterey, CA 93943-5000 | 1 |
| 4. Professor A.W. Cooper, Code 61Cr
Naval Postgraduate School
Monterey, CA 93943-5000 | 5 |
| 5. CAPT J.A. Paine, PMS-421
Naval Sea Systems Command
Washington, DC 20362-5101 | 1 |
| 6. S.K. Petropolous, Code R42
White Oak Laboratory
Naval Surface Weapons Center Detachment
Silver Springs, MD 20903-5000 | 1 |
| 7. M.W. Zurasky, Code G74
Naval Surface Weapons Center
Dahlgren, VA 22448-5000 | 1 |
| 8. Dr. D.A. Scribner, Code 6552
Naval Research Laboratory
Washington, DC 20375 | 1 |
| 9. Director, Research Administration, Code 012
Naval Postgraduate School
Monterey, CA 93943 | 1 |

- | | | |
|-----|------------------------------------------------------------------------------------------------------------------|---|
| 10. | Dr. R. Steinberg
Applied Physics Laboratory
Johns Hopkins University
Laurel, MD 20707 | 1 |
| 11. | Mr. R. Householder, Code 4Y32
Naval Ship Weapon Systems Engineering Station
Port Hueneme, CA 93043-5007 | 1 |
| 12. | DONALD WALTERS, CODE 61WE
Naval Postgraduate School
Monterey, CA 93943-5000 | 1 |
| 13. | Dr. P.L. Walker, Code 61
Naval Postgraduate School
Monterey, Ca 93943-5000 | 1 |
| 14. | R. Bloedel
Manager, Signal Processing Technology
Boeing Company
P.O. Box 3999
Seattle, WA 98124-2499 | 1 |
| 15. | Asst. Professor D. D. Cleary, Code 61CI
Naval Postgraduate School
Monterey, CA 93943-5000 | 1 |
| 16. | Commandant (G-ECV-3)
U. S. Coast Guard
2100 2nd Street SW
Washington, DC 20593 | 1 |
| 17. | Commandant (G-ER)
U. S. Coast Guard
2100 2nd Street SW
Washington, DC 20593 | 1 |
| 18. | LT Raymond C. Engel
257 Foothill Dr.
Sutter Creek, CA 95685 | 2 |
| 19. | Department of Physics Library
Naval Postgraduate School
Monterey, CA 93943-5000 | 2 |